U.PORTO

FACULDADE DE CIÊNCIAS
UNIVERSIDADE DO PORTO

MSc

MSc

2.º
CICLO

FCUP

2021

U.PORTO

Evaluation of the microalgae *Chlorella vulgaris* for their potential beneficial effects on obesity and associated comorbidities

Rita Loewenstein Simões

FC

Evaluation of the microalgae *Chlorella vulgaris* for their potential beneficial effects on obesity and associated comorbidities

Rita Loewenstein Simões

Dissertação de Mestrado apresentada à
Faculdade de Ciências da Universidade do Porto em
Biologia

2021

U.PORTO

FACULDADE DE CIÊNCIAS
UNIVERSIDADE DO PORTO

MSc

Evaluation of the microalgae *Chlorella vulgaris* for their potential beneficial effects on obesity and associated comorbidities

Rita Loewenstein Simões

Functional Biology and Biotechnology of Plants

Biology Department

2021

Orientador

Ralph Urbatzka, Postdoctoral researcher, Interdisciplinary Centre of Marine and Environmental Research (CIIMAR)

Coorientador

Ana Regueiras, Postdoctoral researcher, Interdisciplinary Centre of Marine and Environmental Research (CIIMAR)

Todas as correções determinadas pelo júri, e só essas, foram efetuadas.

O Presidente do Júri,

Porto, _____/_____/_____

Acknowledgments

Over the course of this year, I came across several challenges, which were only possible to overcome by having the right people by my side. So, to all of you, for all the incredible strength you have given me to make this possible, I address with a feeling of deep gratitude.

First, I would like to thank my supervisor, Dr Ralph Urbatzka, for his endless knowledge that inspired and sharpened my critical thinking throughout the development of this project. For all the opportunities provided to learn and for the guidance that allowed me to complete my dissertation. Second, to my co-supervisor, Dr Ana Regueiras, for welcoming me and for always being willing to help me. Finally, to Tiago for his patient supervision and valuable advice in this research work, and to my lab partner, Rita, for all the nervous laughs, but especially for never doubting me.

To the AlgaValor project (POCI-01-0247-FEDER-035234), for financing this work by the European Regional Development Fund (ERDF) through COMPETE2020-Operational Programme for Competitiveness and Internationalisation (POCI) and PORTUGAL2020, and national funds through FCT UIDB/004423/2020 and UIDP/04423/2020.

To all my dearest friends, for always and unconditionally being my rock. For keeping me going and for never leaving me alone in my battles. A special thanks to Beatriz César for the long nights and the inexhaustible source of motivation, and to Martins and Freitas for everything that cannot even be put into words.

To my parents, Jorge e Helena, for all the support, for always being there and especially for being the reason why it is possible for me to dream big.

To Frederico, not for believing in me, but for making me believe in myself. Thank you, from day zero until this day, for everything.

To all of you.

Cofinanciado por:

Resumo

A prevalência da obesidade na sociedade tem vindo a crescer dramaticamente, tendo já sido estabelecida como uma epidemia global desde o final do século 20. Os pacientes que sofrem desta doença metabólica têm ainda um risco acrescido de desenvolver comorbidades associadas, como as diabetes ou a doença do fígado gordo não alcoólico, que estão entre as principais causas de morte em todo o mundo. Os medicamentos aprovados para a obesidade apresentam baixa eficácia na perda de peso, muitos efeitos secundários e observam-se frequentemente recaídas no ganho de peso. Desta forma, é urgente encontrar novos compostos que combatam esta doença. Este trabalho teve como objetivo avaliar o potencial da microalga *Chlorella vulgaris* quanto aos seus efeitos benéficos contra a obesidade e comorbidades associadas. Os extratos foram obtidos por processamento de alta pressão (HPP), sob diferentes combinações de pressão e solventes, e por tratamento óhmico, sob combinações de frequência e tempos distintas. As diferentes combinações de extração culminaram num conjunto único de metabolitos, que, por sua vez, contribuíram para uma variedade de bioatividades. Assim, as bioatividades de cada um dos extratos foram avaliadas em diferentes modelos: o ensaio anti esteatose *in vitro* com a linha de células de carcinoma de hepatócitos humanos HepG2, o ensaio anti-inflamatório *in vitro* com a linha de células de macrófagos de rato RAW264.7, o ensaio de fluorescência *Nile red* anti obesidade *in vivo* com peixes-zebra e o ensaio antidiabético *in vivo* com peixes-zebra de monitorização de captação de um análogo fluorescente da glucose. A toxicidade foi verificada através de ensaios de citotoxicidade nas células e letalidade ou malformações nas larvas dos peixes-zebra. Os extratos de acetona (CS11, CS22, CS35, CSC11 e CSC23) revelaram a combinação de bioatividades mais promissora nos quatro bioensaios realizados. CS11, CS22 e CS35, extraídos a 420, 300 e 100 MPa, respetivamente, mostraram atividades significativas no ensaio anti esteatose. Os extratos CS22 e CS35, e os controlos CSC11 e CSC23, extraídos sem pressão, demonstraram atividades significativas no ensaio anti obesidade. CS22, e também CS1 e CS13, dois extratos aquosos a 420 e 300 MPa, respetivamente, revelaram uma atividade antidiabética significativa, confirmada em ambas as quantificações, no olho e no saco embrionário. Adicionalmente, os cinco extratos de acetona e os cinco extratos de etanol 96% exibiram atividade anti-inflamatória significativa. A cromatografia líquida acoplada à espectrometria de massa em tandem (LC-MS/MS) foi aplicada para caracterizar o perfil metabólico dos extratos ativos e não ativos no ensaio de anti

esteatose, com o objetivo de identificar os compostos responsáveis da atividade promissora. Por fim, foram efetuados estudos complementares em proteínas alvo através da técnica de w*estern blot* para elucidar quanto ao mecanismo molecular de ação subjacente aos extratos ativos, e foi mostrado que o extrato CS22 atuou através da regulação do C/EBPα.

Os resultados sugerem que alguns extratos de *Chlorella vulgaris* crescida em condições heterotróficas podem representar um potencial terapêutico contra a obesidade e as suas comorbidades.

Palavras-chave

Chlorella vulgaris, microalgas, obesidade, extração por processamento de alta pressão, extração óhmica, esteatose, HepG2, diabetes, RAW264.7, modelo com peixes-zebra, adipogénese, w*estern blot*, C/EBPα

Abstract

The prevalence of obesity in society has been dramatically rising, being established as a global epidemic since the end of the 20th century. Patients who suffer from this metabolic disease have an increased risk of developing associated comorbidities, like diabetes or non-alcoholic fatty liver disease, which are among the leading causes of death worldwide. Drug therapies approved for obesity have low weight loss efficacy, many side effects, and frequent obesity relapse. Thus, it is imperative to find new compounds to fight it. The present work aimed to evaluate the potential of the microalgae *Chlorella vulgaris* (*C. vulgaris)* regarding their beneficial effects against obesity and its associated comorbidities. Extracts were obtained by high pressure processing (HPP), under various combinations of pressure using different solvents, and by ohmic treatment, under a distinct combination of frequency and time. The different extraction conditions led to a unique set of metabolites, which, in turn, contributed to a distinctive array of bioactivities. Hence, bioactivities of each extract were evaluated in different models: the anti-steatosis *in vitro* assay with HepG2 human hepatocyte carcinoma cell line, the anti-inflammation *in vitro* assay with RAW264.7 mouse macrophage cell line, the *in vivo* zebrafish Nile red fluorescence anti-obesity assay, and anti-diabetes *in vivo* assay in zebrafish monitoring uptake of a fluorescent glucose analogue. Toxicity was assessed by cytotoxicity assays in cells and lethality or malformations in zebrafish larvae. Acetone extracts (CS11, CS22, CS35, CSC11 and CSC23) revealed the most promising combination of bioactivities across all four bioassays performed. CS11, CS22 and CS35, extracted at 420, 300 and 100 MPa, respectively, showed significant activities in the anti-steatosis assay. CS22, CS35, and the controls CSC11 and CSC23, extracted without pressure, demonstrated significant activities in the anti-obesity assay. CS22, and also CS1 and CS13, two aqueous extracts at 420 and 300 MPa, respectively, displayed a significant anti-diabetic activity, confirmed in both eye and yolk sac quantification. All five acetone extracts, along with all five ethanol 96% extracts, exhibited a significant anti-inflammatory activity. The liquid chromatography-tandem mass spectrometry (LC-MS/MS) was applied to characterize the metabolic profiles of active and non-active extracts in the anti-steatosis assay, aiming to identify the responsible compounds for the promising bioactivity. Finally, complementary studies were carried out on target proteins by western blot technique to get insights into the active extracts' underlying molecular mechanisms of action; it was shown that CS22 extract acted through C/EBPα regulation.

Overall, the results suggest that some extracts of the *C. vulgaris* grown under heterotrophic conditions could represent a potential therapeutic agent against obesity and its comorbidities.

Keywords

Chlorella vulgaris, microalgae, obesity, high pressure processing extraction, ohmic extraction, steatosis, HepG2, diabetes, inflammation, RAW264.7, zebrafish model, adipogenesis, western blot, C/EBPα

Index

i.Index of tables and figures

ii. List of abbreviations

2-NBDG - 2-deoxy-2-[(7-nitro-2,1,3-benzoxadiazol-4-yl)amino]-D-glucose

ACC - enzyme Acetyl-CoA carboxylase

AMPK - 5'-AMP-activated protein kinase

ANOVA - One-way analysis of variance

BMI - Body mass index

BSA - Albumin from bovine serum

C. vulgaris - *Chlorella vulgaris*

C/EBP - CCAAT/enhancer-binding proteins

CIIMAR - Centre for Marine and Environmental Research

CPT-1 - Carnitine palmitoyltransferase-1

CRP - C-reactive protein

DMEM - Dulbecco's Modified Eagle Medium

DMSO - Dimethyl sulfoxide

DNP - The Dictionary of Natural Products

DPF – Days post fertilization

EDTA - Ethylenediaminetetraacetic acid tetrasodium salt

EMA - European Medicines Agency

Emodin - 1,3,8-Trihydroxy-6-methylanthraquinone

FAO - Food and Agriculture Organization

FBS - Fetal bovine serum

FDA - Food and Drug Administration

FTO - Fat mass and obesity-associated gene

GLUTs - Glucose transporters

GNPS - Global Natural Product Social Molecular Networking

GRAS - Generally recognised as safe

HBSS - Hank's Buffered Salt Solution

HepG2 - Human hepatocyte carcinoma cell line

HO-33342 - Bisbenzimide H 33342 trihydrochloride

HPP - High pressure processing

IGEPAL CA-630 - Octylphenoxy poly(ethyleneoxy)ethanol

IL-6 - Interleukin-6

LC-MS/MS - liquid chromatography-tandem mass spectrometry

LPS - Lipopolysaccharides from *Escherichia coli* 0111:B4

MS-222 - Ethyl 3-aminobenzoate methanesulphonic acid salt

MTT - 3-(4.5-dimethylthiazole-2-yl)-2.5-diphenyltetrazolium bromide

NAFLD - Non-alcoholic fatty liver disease

NASH - Non-alcoholic steatohepatitis

NPA - The Natural Products Atlas

PBST - Phosphate buffered saline with Tween 1x

PPAR- γ - Peroxisome proliferator activated receptor-γ

PTU - 1-phenyl-2-thiourea

PUFAs - Polyunsaturated fatty acids

RAW264.7 - Mouse macrophage cell line

REV - Resveratrol

SDS - Sodium dodecyl sulfate

SO - Sodium oleate

SRB - Sulforhodamine B

T2DM - Type 2 diabetes mellitus

TCA - Trichloroacetic acid

TNF-α - Tumour necrosis factor-alpha

Tris-HCl - Tris hydrochloride

WHO - World Health Organization

1. Introduction

1.1 Obesity

1.1.1 Adipose tissue

Adipogenesis is the process of storing energy as fat, mainly triglycerides, in specialised cells named adipocytes. This process consists of proliferation and differentiation of adipocyte precursor cells in mature adipocytes. Then the developed adipocytes accumulate as adipose tissue at many regions in the body. In its turn, the adipose tissue is capable of undergoing changes in the number or size of adipocytes in response to alterations in the energy status (Lane, 2013). This quick and dynamic response makes adipose tissue a complex organ that is able to control overall body energy by storing triglycerides in nutrient-excess conditions and, on the contrary, by supplying them through lipid mobilisation during fasting or energy expenditure (Luo and Liu, 2016; Chait and den Hartigh, 2020). The adipose tissue also has a secretory function, which turns it into a major endocrine organ, that is known to secrete factors involved in energy expenditure, glucose homeostasis, appetite control, insulin sensitivity, lipid metabolism, immune response and even reproduction (Kershaw and Flier, 2004; Karastergiou and Mohamed-Ali, 2010).

The triglyceride removal rate consists in removing the lipids from adipose stores through a hydrolysis process followed by irreversible oxidation. The balance between triglyceride removal and storage is called lipid turnover, and it determines the size of adipose tissue (Arner et al., 2011; Arner et al., 2019). However, in abnormal situations, where the adipose tissue has to compensate for the excessive increase of lipids in the body by expanding in cell size (hypertrophy) and number (hyperplasia), a limit point can be reached where adipose tissue becomes dysfunctional, incapable of expanding correctly, and consequently, unable to regulate all body functions properly. This loss of adipose tissue homeostasis potentially leads to metabolic disorders and chronic complications, in particular associated with adipocyte hypertrophy, and the main cause is obesity (Choe et al., 2016; Longo et al., 2019; Zorena et al., 2020), considering that it increases triglyceride storage, thus reducing the lipid turnover rate.

1.1.2 Molecular mechanisms in adipogenesis and fatty acid synthesis

Since adipogenesis is a crucial process in fat accumulation in the body, many molecular mechanisms involved have already been described. Adipogenesis is a process that requires a sequential activation of transcription factors, including the well-known CCAAT/enhancer-binding protein (C/EBP) gene family and peroxisome proliferator activated receptor-γ (PPAR- γ) (Tariq et al., 2013; Lee et al., 2019). As exemplified by **Figure 1**, is the C/EBPα and the PPAR-γ that together, through positive feedback, promote differentiation and induce and maintain the expression of key adipogenic genes that are essential for adipocyte function (Longo et al., 2019). Hence, the differential expression of these two transcription factors can be a way to assess the mechanisms of action for a possible therapy.

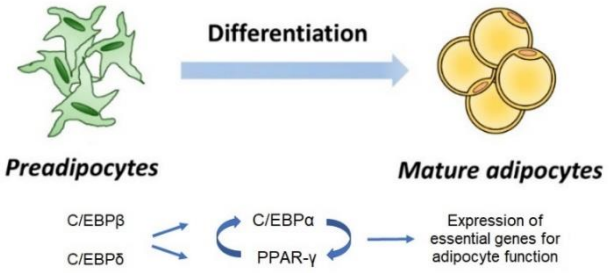

Figure 1 – Simplified vision of the mechanisms involved in adipocytes differentiation from preadipocytes. Adapted from Longo et al., 2019.

Acetyl-CoA is the precursor molecule for fatty acid synthesis and is initially originated from glucose. Acetyl-CoA is carboxylated into malonyl-CoA by the enzyme Acetyl-CoA carboxylase (ACC) in the first, and rate-limiting, step of *de novo* fatty acid biosynthesis. Malonyl-CoA is not only responsible for fatty acid synthesis, but is also an inhibitor of fatty acid oxidation by allosterically inhibiting the carnitine palmitoyltransferase-1 (CPT-1), an enzyme responsible for the transference of fatty acids from the cytosol to the mitochondria (Clarke and Nakmura, 2004). ACC appears in two different forms in humans, alpha and beta, encoded by two different genes and being ACC-alpha increased in lipogenic tissues (NCBI, 2021). *ACACA*, the gene that encodes for ACC-alpha, has even been demonstrated as a biomarker in adipose tissue associated with type 2 diabetes in obese individuals (Dharuri et al., 2014). In its turn,

ACC is regulated by 5'-AMP-activated protein kinase (AMPK) (Hardie, 2004), a heterotrimeric complex with a catalytic α subunit and regulatory β and γ subunits. The subunits differ to some degree in the structure and their expression pattern in the different tissues, and each of them has at least two isoforms encoded by distinct genes (Woods et al., 1996). AMPK regulates ACC through its phosphorylation and consequent inactivation, which drives to a lower concentration of malonyl-CoA and, consequently, to a decreased fatty acid synthesis and an increased oxidation in the mitochondria (**Figure 2**)(Kim et al., 2017; Foretz et al., 2018).

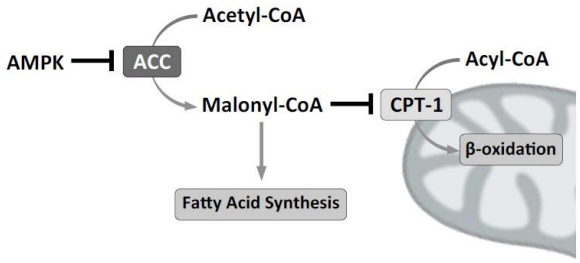

Figure 2 - Negative regulation of Acetyl-CoA carboxylase (ACC) by 5'-AMP-activated protein kinase (AMPK). When active, ACC carboxylases Acetyl-CoA into Malonyl-CoA in a rate-limiting process. Malonyl-CoA promotes fatty acid synthesis and prevents fatty acid oxidation by allosterically inhibition of carnitine palmitoyltransferase-1 (CPT-1), which catalyses fatty acids transference from the cytosol into the mitochondria. From John P Konhilas, 2015.

1.1.3 Obesity definition

According to the World Health Organization (WHO), obesity is defined as abnormal or excessive fat accumulation that presents a risk to health (WHO, 2021). This disease has grown to epidemic proportions, and in 1997 it was already recognised as such (WHO Consultation on Obesity (1999: Geneva Switzerland) & World Health Organization, 2000). In 2016, 1.9 billion people aged 18 and older were overweight, and more than 650 million were considered obese. The body mass index (BMI) is a measure of body fat based on height and weight and is commonly used for this classification. In adults aged over 18 years old, overweight is defined by a BMI ≥ 25 Kg/m^2 and obesity by a BMI ≥ 30 kg/m^2. In fact, adult obesity is actually more common globally than under-nutrition. However, this problem cuts across all ages. In the same year, 340 million

children and adolescents aged 5–19 years and 40 million children under the age of 5 years were considered overweight or obese, numbers that had almost tripled worldwide since 1975 (Bentham et al., 2017; The World Obesity Federation (World Obesity), 2019; Haththotuwa et al., 2020). But these numbers get even scariest if we look at the projections. If recent secular trends persist, by 2030 up to 57.8% of the world's adult population (3.3 billion people) could be either overweight or obese (Kelly et al., 2008).

1.1.4 Causes for obesity

Although obesity arises mainly driven by excess energy consumption relative to energy expenditure (Wright and Aronne, 2012), this disease is highly complex, since it can be triggered by many factors, such as environmental, socio-economical and genetic. First of all, it is noticeable that the food market has been changing over the last decades and now promotes highly processed and caloric, pre-packaged foods that are more accessible for families (Wright and Aronne, 2012). This economic change can be significant for individuals with low incomes, but it also leads to a rampant over-consumption and obesity (Swinburn et al., 2011). By 2019, only Sweden, Germany, Qatar and Brazil had developed dietary guidelines promoting eating patterns that ensured food security, quality and human health and well-being (Swinburn et al., 2019). Another problem is related to countries transitioning from lower to higher incomes since there is less physical activity due to the shift to motorised vehicles, with unavoidable consequences in the increased prevalence of obesity (Swinburn et al., 2019). In fact, 31% of the global population over 15 years practice insufficient physical activity, which contributes to the death of almost 3.2 million people every year (Park et al., 2020). Moreover, obesity and higher body weight are strongly associated with a sedentary lifestyle (Kearney, 1999), and it has already been shown that inactivity, or general underactivity compared to recommended guidelines, contributes to the reduction of average life expectancy (Moore et al., 2012). In terms of genetic factors, studies indicate that this is not a determining factor. On the one hand, due to the rapidity prevalence and globality of the growth of this epidemic, it does not seem likely that the gene pool has changed so much in a such short period of time (Moini et al., 2020). On the other hand, genetics of obesity is a highly researched area, and yet, most of the genetic abnormalities described are rare, accounting for only 10% of severe obesity cases around the world and still influenced by obesogenic behaviours and the environment (Bouchard, 2021). Hence, genes have an important role essentially to determine the

predisposition for an individual to gain weight while facing an unbalanced energy intake and expenditure, in other words, its susceptibility to obesity. The genetic predisposition to obesity can be polygenic, monogenic, or syndromic. Obesity originated by a rare single-gene mutation is called monogenic and causes endocrine dysregulations that affect metabolism and appetite. Syndromic obesity has overweight as a severe secondary condition associated with almost 100 syndromes and occur from discrete genetic defects or from chromosomal abnormalities. Polygenic forms of obesity occur from cumulative contribution of a large number of genes (Vidhu V. Thaker, 2017; Moini et al., 2020; Bouchard, 2021).

Considering all highly variable factors presented as possible causes or influences of obesity, the inherent complexity of the disease is quite disconcerting.

1.1.5 Obesity associated comorbidities

In addition to obesity being the result of a complex interaction of several factors, another worrying fact is that the majority of obese people develop serious associated comorbidities. As previously mentioned, the loss of adipose tissue homeostasis is caused by an unbalanced energy intake and expenditure. When this happens in the human body, it develops metabolic, cellular, and mechanical adaptations that potentially manifests as metabolic disorders and chronic complications (Schelbert, 2009). This happens because adipose tissue is under stress and becomes unable to produce or release the precursors needed for triglyceride oxidation. As a result, lipids remain in circulation, leading to lipotoxicity, or they are stored in-non adipose tissues, the entitled ectopic fat accumulation, that occurs in other organs such as the liver, heart, skeletal muscles, pancreas and intra-abdominally (Bettina Mittendorfer, 2013). In its turn, hypertrophic adipocytes release cytokines, namely interleukin-6 (IL-6), tumour necrosis factor-alpha (TNF-α), C-reactive protein (CRP) and leptin, and reduce the production of adiponectin. This response is the adipose tissue's attempt to maintain homeostasis by inducing an inflammatory process and is associated with specific metabolic dysfunctions (Daniele et al., 2014; Ellulu et al., 2017; Longo et al., 2019; Zorena et al., 2020). As a matter of fact, it is estimated that the percentage of macrophages in adipose tissue goes from less than 10% in lean humans to more than 40% in severely obese people (Weisberg et al., 2003). Macrophages operate as effectors of a complex immune program, and they generate a chronic low-grade inflammatory state in the body that, over time, leads to the development of associated comorbidities (Abdelaal et al., 2017;

Saltiel and Olefsky, 2017). As a consequence, the life expectancy in obese individuals can be reduced by an estimated 5 to 20 years (Fontaine et al., 2003).

1.1.5.1 Insulin resistance and diabetes

Blood glucose levels need to be strictly regulated in order to ensure normal body function. Insulin is a hormone secreted by the β-cells in the pancreas that induces glucose uptake (Wilcox, 2005) in insulin-sensitive tissues like skeletal muscle, adipose tissue, and liver. When insulin is no longer able to stimulate this glucose uptake, the tissues lose insulin response and their ability to capture glucose, resulting in a state of insulin resistance (Kahn and Flier, 2000). People who suffer from this resistance have a predisposition to type 2 diabetes mellitus (T2DM) (Xu et al., 2003; Kahn et al., 2006), the more common diabetes type, a chronic disease characterised by high blood glucose levels resulting from insulin resistance (DeFronzo et al., 2015).

There is an association between chronic inflammation state initiated in adipose tissue in obesity disease and the development of insulin resistance (Kahn et al., 2006; Burhans et al., 2019), and in fact, a study of 3637 diabetic patients showed that 86% of patients with type 2 diabetes were overweight or obese (Daousi et al., 2006). It is hypothesised that this association may occur due to several factors (**Figure 3**). On the one hand, the secreted pro-inflammatory cytokines listed above, like TNF-α, lead to serine phosphorylation of insulin receptor substrate-1 and blocks the insulin signalling (Aguirre et al., 2000). Alson, adiponectin is responsible for insulin sensitivity and inflammation reduction. In adipocytes with defective secretion caused by obesity, low levels of adiponectin cause the development of insulin resistance and T2DM (Weyer et al., 2001; Schelbert, 2009). On the other hand, the ectopic fat accumulation in the pancreas contributes to β-cell dysfunction and consequently defective insulin secretion (Gaborit et al., 2015). Finally, the ectopic fat accumulation in organs with an important role in glucose metabolism, such as the liver, is also linked to the development of insulin resistance by a defective suppression of glucose production (Sattar and Gill, 2014). Whatever the mechanism leading to the onset of T2DM in obese patients is, the relationship is quite evident and there is even a new term to refer to this coexistence of both diabetes and obesity, called “diabesity” (Ng et al., 2021). In its turn, this comorbidity is the main cause of blindness, kidney failure, heart attack, stroke, and lower limb amputation (WHO, 2021). Over 1 million people die every year due solely to T2DM,

making it the ninth leading cause of mortality, and still globally rising, with a worrisome higher rate in developed regions like western Europe (Khan et al., 2020).

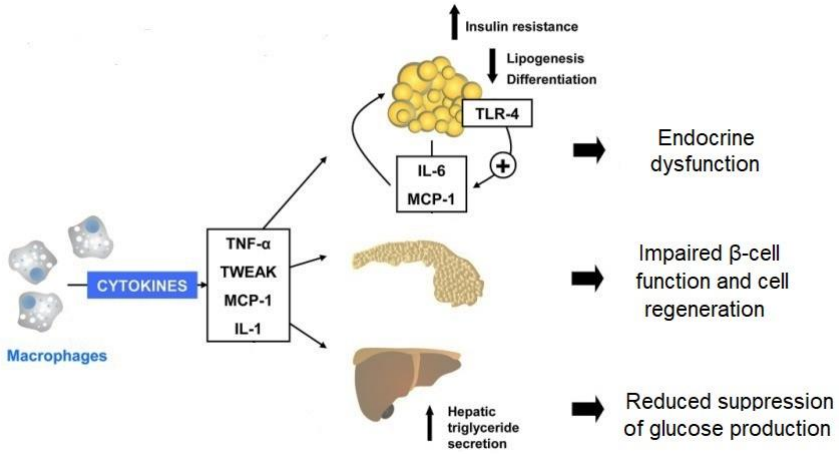

Figure 3 - Association between chronic inflammation in obesity disease and insulin resistance. Adapted from Chadt et al., 2018.

1.1.5.2 Non-alcoholic Fatty Liver Disease

The liver is the vital organ for fatty acid metabolism, and its parenchymal cells are mainly hepatocytes that have detoxification, metabolic, and secretory functions (Zhou et al., 2016). In healthy situations, the liver only stores very few triglycerides, but under obesity circumstances, there is a modification of the metabolism that leads to the storage of triglycerides in hepatocytes (Alves-Bezerra and Cohen, 2019). When the content in fatty acids exceeds 5% of liver weight, without secondary factors contributing to it, including alcohol intake, viral infection, or drug treatment, it is considered hepatic steatosis, or also called fatty liver (Nassir et al., 2015). Hepatic steatosis is the least severe state of the spectrum of a clinical condition known as non-alcoholic fatty liver disease (NAFLD) (**Figure 4**). The intermediate lesion is called non-alcoholic steatohepatitis (NASH) and is categorised by the appearance of hepatic inflammation, hepatocyte apoptosis and sometimes, fibrosis (Abdelmalek and Diehl, 2007; Satapathy et al., 2015). A more advanced liver disease follows, cirrhosis, and, at the end of the spectrum, is the hepatocellular carcinoma. The more complex stages of NAFLD usually develop within 10 to 20 years after diagnosis (Donnelly et al., 2005; Powell et al., 2021).

The world prevalence of NAFLD is 25–30%, and it has already been proven that obesity is associated with this disease and its severity (Polyzos et al., 2019). Moreover, the global prevalence of NAFLD among T2DM patients is 55.5% (Younossi et al., 2019),

so the connection between all these comorbidities seems quite evident, with obesity as the root of the problem.

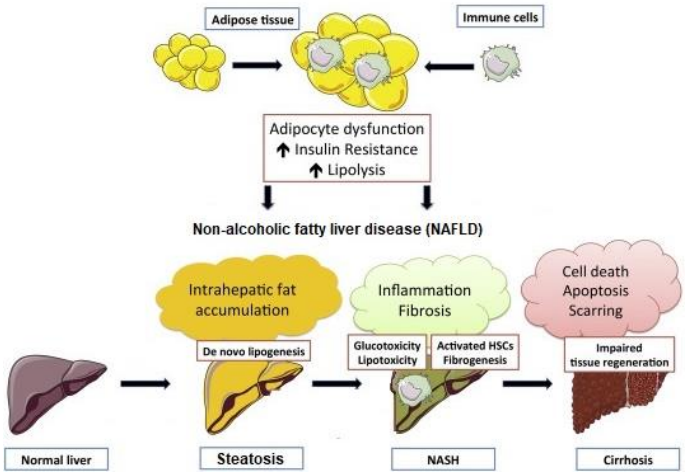

Figure 4 - Spectrum of the non-alcoholic fatty liver disease (NAFLD) obesity comorbidity, generated by fat accumulation in adipose tissue. From normal liver to cirrhosis, going through the intermediate stages of hepatic steatosis and non-alcoholic steatohepatitis. Adapted from Polyzos et al., 2019.

1.1.5.3 Other comorbidities

Besides the comorbidities already described, hypertension, cardiovascular disease (Després, 2007; Nakamura et al., 2014), sleep apnea (Reena Mehra and Redline, 2008), gallbladder disease (Boland et al., 2002), osteoarthritis (Powell et al., 2005), and certain types of cancer, like colorectal and prostate cancer in men and endometrial, and breast cancer in women, have also been associated with obesity (Freedland and Aronson, 2004; Tworoger et al., 2007; Bardou et al., 2013; Onstad et al., 2016)

The burden on national health systems caused by obesity is enormous since it is not only necessary to address the obesity problem itself, but also to have an economic and infrastructural system capable of supporting all associated comorbidities. This is actually a challenging goal to achieve, with mortality and numbers of obesity still dramatically rising. Once more, it is possible to see the urgency in finding treatments to fight obesity directly, not only because the developing mechanisms of this disease are varied, but also because its consequences are diverse with no standard solution for such a wide spectrum. The need to act is so alarming that in 2015 world leaders agreed to 17

Global Goals for Sustainable Development, in which the 3rd Goal is good health and well-being and commits to reducing by one third premature mortality attributed to cardiovascular disease, cancer, T2DM or chronic respiratory disease, through prevention and treatment, (The Global Goals for Sustainable Development, 2015), all obesity comorbidities.

1.1.6 Obesity pharmacotherapy

Regarding obesity management, the first lines in the guidelines against this disease are the therapeutic education of the patient, in which new eating habits and a more active and healthier lifestyle are recommended. This first approach is followed by the assessment of psychological factors, which are very important for the success of the treatment. Only after these attempts does the third guideline appear, in which pharmacotherapy is introduced. Regarding the existing treatments, guidelines in Europe recommend drug therapy depending on the BMI. As mentioned before, in adults aged over 18 years old, obesity is defined by BMI ≥ 30 kg/m^2, and it is precisely from this value that pharmacotherapy is recommended. It is also suggested in patients with BMI higher than 27 kg/m^2 if one or more associated comorbidities exist (Durrer Schutz et al., 2019).

At the time of writing, only three drugs to fight obesity were approved in Europe by the European Medicines Agency (EMA): orlistat, naltrexone/bupropion and liraglutide (Durrer Schutz et al., 2019), being the last approval in 2014. The US Food and Drug Administration (FDA), in addition to those approved by the EMA, has also given the green light to the drug phentermine/topiramate in 2012, and recently, in July 2021, to semaglutide (Tilinca et al., 2021). Regarding the mechanisms of action of EMA-approved anti-obesity drugs, orlistat, that is actually a synthetic derivative of lipstatin isolated from the Gram-positive bacterium *Streptomyces toxytricini*, was approved in 1998 and inhibits gastrointestinal and pancreatic lipases, so that absorption of triglycerides by the intestinal endothelium is blocked for the reason that they are not hydrolysed into fatty acids (Henness and Perry, 2006; Cowley et al., 2016). Naltrexone/bupropion is a combination of two drugs, naltrexone is an opioid receptor antagonist commonly used for alcohol addiction, and bupropion is an antidepressant that helps in smoking cessation, involving the inhibition of dopamine and reuptake of norepinephrine. The feedback that results from the association of these two drugs, through a mechanism not fully known, acts on food intake and satiety (Greenway et al., 2010; Srivastava and Apovian, 2018). Finally, liraglutide is an injectable drug that decelerates gastric emptying that induces satiety

after eating, reduces appetite and food consumption by targeting the brain (Srivastava and Apovian, 2018). Phentermine/topiramate was refused by the EMA due to concerns about long-term effects regarding the heart, psychiatric and cognitive effects like memory impairment or depression. Also, topiramate is known to be potentially harmful to fetuses (European Medicines Agency Science Medicines Health, 2013) and to have side effects like paresthesia, somnolence, constipation, insomnia and dysgeusia (Kang and Park, 2012; Tak and Lee, 2021).

In order to get approval, drugs must have a favourable risk to benefit ratio with clinically relevant weight loss compared to those treated with placebo, in association with being safe to use in the target population. However, the fact that obesity therapy is most often for life, or at least for a really long period of time, and that the obese population represents a highly diverse pool, there are many difficulties in creating safe drugs (Williams et al., 2020; Tak and Lee, 2021). The list of anti-obesity drugs withdrawal from the market by EMA or FDA is quite long and includes benfluorex, diethylpropion, sibutramine, lorcaserin, dexfenfluramine, dextroamphetamine, amphetamine, fenbutrazate, fenfluramine rimonabant, fenproporex, levamphetamine, mefenorex, methamphetamine, phenylpropanolamine, pipradrol, sibutramine, among others. Their side effects were so serious that in some cases deaths were reported. The main adverse side effects registered were pulmonary hypertension, cardiac valvulopathy, strokes, suicidal behaviour, myocardial infarction, and cancer (Kang and Park, 2012; Cheung et al., 2013; Colon-Gonzalez et al., 2013; Tak and Lee, 2021). As if this were not worrying enough, even if we consider only the three approved drugs in Europe, they have a low weight loss efficacy, with a mean of weight loss between -5.8kg and -8.4kg, dependent on the drug (Daneschvar et al., 2016; Srivastava and Apovian, 2018), with a frequent obesity relapse within 2 to 5 years (Hall and Kahan, 2018) and side effects that include insomnia, interference with absorption of vitamins, gastrointestinal problems, headache, dizziness, constipation, hypoglycemia, abdominal pain, vomiting, hepatotoxicity, kidney stones, and nausea (Daneschvar et al., 2016; Williams et al., 2020; Tak and Lee, 2021). Thus, the need to find new ways to fight this disease is imperative.

1.2 Medical products from nature

Natural products are molecules produced naturally by any living organism found in nature. Many pharmaceuticals have, in fact, their origins in nature, given that natural products were once nearly the only medicinal source available. Since prehistoric times

medical products made from plants have been successfully administered by different cultures for a broad spectrum of diseases (Halberstein, 2005). A more regulated practice was possible in the 18th century due to the work of Swedish naturalist Carolus Linnaeus, the father of taxonomy, who classified thousands of botanical species that allowed to create links between the medical plants and their effects. Now they continue to serve as a template for the creation of synthetic analogues, and even some medical products have natural products in their foundation, mainly as anticancer and antimicrobial agents (Borowitzka, 1995; Harvey et al., 2015), but also in widespread drugs like aspirin, which has the acetylsalicylic acid as its major component, or the anti-malarian drug quinine (Halberstein, 2005). Moreover, many pure natural products are able to interact with specific mammalian receptors on or within cells, and that is precisely what is wanted when developing a drug (Beutler, 2009). Thus, they are a really interesting resource for pharmaceuticals. From 1981 to September 2019, the estimated number of approved drugs in the world was 1881. Of these, 856 (45%) were natural products or synthetic variations using their novel structures, and among them, 85 (5%) were pure natural products (Newman and Cragg, 2020). Natural products have unique characteristics compared with conventional synthetic molecules, like structural complexity, distinct molecular properties, and vast scaffold diversity that confer them special advantages in the drug discovery process. Also, they are recognised as common exceptions of a set of criteria known as Lipinski's 'rule of five', which is a guideline followed for the development of oral drugs that gives a prospect of a compound to have oral bioavailability based on several properties (Shultz, 2019; Atanasov et al., 2021).

In fact, some studies have already been carried out in which the natural products were explored about their ability to reduce adipose tissue mass through inhibiting adipogenesis. And there are already some identified phytochemicals from a variety of species that act in some component of the adipocyte differentiation process (Kim et al., 2008; Drira et al., 2011; Kim et al., 2016; Lai et al., 2016; Abood et al., 2018) and even some identified PPAR- γ agonists (Mueller and Jungbauer, 2009; Park et al., 2012).

1.2.1 The aquatic environment

Historically, terrestrial plants have always been the most chosen organisms for medicinal use, for the ease of obtaining them and for the little scientific knowledge that existed, since the techniques used at the time were based on organoleptic characteristics. With microbiology advances, fungi also became organisms of interest,

starting the antibiotic era, with particular emphasis on the discovery of the natural product penicillin by Alexander Fleming in 1929 (Fleming, 1945). However, the invention of scuba diving made possible the exploration of the largest environment, the marine environment, with the oceans covering approximately 70% of the planet's surface and deep-sea biodiversity among of the highest on the planet (Ramirez-Llodra et al., 2010). Comparing with the terrestrial biota, the marine biota is more diverse, and includes 34 taxonomically identified phyla, whereas, on land, there are only 15 (Briggs, 1995). Furthermore, it is estimated that there is even a 91% gap of existing species in the ocean that are still unidentified, in particular microorganisms (Mora et al., 2011). This high biodiversity in the marine environment results in a great variety of compounds produced by the most different species, from marine microorganisms like bacteria, fungi, cyanobacteria, dinoflagellate, and microalgae, to algae, sponges, cnidarians, bryozoans, mollusc, ascidians, echinoderms (Blunt et al., 2015), that grow and live under very different conditions. In fact, over 30000 marine natural products have been discovered since the first biological active compound was described in 1950 (Lyu et al., 2021), spongothymidine, which led to the discovery of the anti-leukaemia drug cytarabine and the antiviral agent vidarabine (Altmann, 2017).

1.2.2 Aquatic organisms with lipid-reduction activity

Regarding the advances in lipid-reduction activity, aquatic organisms have already demonstrated to be a valuable natural supply of active substances and a remarkably diverse source of exploration of new bioactive compounds. *Grateloupia elliptica*, for example, is a red seaweed from Jeju Island in Korea and its extract has a proven anti-adipogenic activity in 3T3-L1 cells and mice with high-fat diet-induced obesity (Lee et al., 2020). Marine forests of *Sargassum liebmannii* from Mexican coasts of the North Pacific were studied for antiobesogenic effect, and it was shown that mice fed the *Sargassum* diet had a reduced weight gain and energy intake, and increased insulin sensitivity. Furthermore, the adipose tissue decreased 31.5% from the control at the end of treatment (Tapia-Martinez et al., 2019). Additionally, the fucoidan from the brown seaweed *Ascophyllum nodosum* has a lipid-lowering effect by enhancing reverse cholesterol transport-related genes (Yang et al., 2019), and *Kappaphycus alvarezii*, a red alga widely cultivated for carrageenan production, has shown to be effective in reverting obesity in overweight C57BL/6J mice (Chin et al., 2019). Another study demonstrated that diphlorethohydroxycarmalol, one of the most abundant bioactive

compounds in brown algae *Ishige okamurae*, has a strong effect against high-fat diet-induced obesity through regulation of multi-pathways *in vivo* in obese mice (Ding et al., 2019). Some studies in adipogenic and thermogenic gene expression in brown adipocytes, lipid metabolism and glucose uptake in hepatocytes, as well as lipid metabolism in zebrafish larvae, allowed the identification of 28 active fractions of cyanobacterial strains with interesting bioactivity concerning the fight of metabolic diseases, with no apparent toxicity (Costa et al., 2019). 18 compounds with high lipid reducing activity in the absence of toxicity were described by screening a library of 85 polyphenol derivatives and three natural polyphenols, accompanied by the zebrafish Nile red fat metabolism assay (Urbatzka et al., 2018). Moreover, chlorophyll derivatives from the marine cyanobacteria *Cyanobium* sp. showed relevant lipid-reducing activities, both on zebrafish larvae and spheroids of differentiated preadipocytes (Freitas et al., 2019). Regarding microalgae, fucoxanthin powder from microalgae *Phaeodactylum tricornutum* and used in high-fat diet-fed C57BL/6J mice and 3T3-L1 adipocytes revealed inhibited adipocytic lipogenesis, induced fat mass reduction and decreased intracellular lipid content, adipocyte size, and adipose weight (Gille et al., 2019; Koo et al., 2019). Researchers similarly found that fucoxanthin reduced body weight, body mass index, and abdominal fat in mildly obese Japanese subjects (Hitoe and Shimoda, 2017). There is also scientific evidence supporting the anti-obesity effect of *Euglena gracilis* (Sakanoi et al., 2018; Sugimoto et al., 2018), *Spirulina maxima* (Heo and Choung, 2018; Seo et al., 2018), *Spirulina platensis* (Zhao et al., 2019; Diniz et al., 2021), and *Nitzschia laevis* (Guo et al., 2019), corroborated by *in vitro*, *in vivo*, animal studies, and clinical studies with Spirulina. In fact, both *Spirulina maxima* and *Spirulina platensis* proved to have very promising results in a randomised, double-blinded, placebo-controlled clinical trial, in which anthropometric measurements such as body weight, waist circumference and BMI as well as obesity-related metabolic disorders were evaluated (Szulinska et al., 2017; Zeinalian et al., 2017; Yousefi et al., 2018).

1.2.3 Microalgae

Among the very diverse aquatic environment, algae are an important source of compounds, and they can be divided, based on size, into macro- or micro-algae. The microalgae category includes both microscopic eukaryotic algae, as well as the oxygenic photosynthetic bacteria (prokaryotes), the cyanobacteria. Hence, they can be unicellular, multicellular, or colonial with wide ranges of size and morphology. They are able to move

with the help of flagella, or they can be nonmotile. The great flexibility of microalgae allows them to grow in diverse environments, from soils, ice, lakes, rivers to hot springs and oceans. Moreover, besides the photosynthesis that produces oxygen, microalgae are also capable of fixing inorganic carbon, which supports all life on the earth. Furthermore, being a primary producer, they are a fundamental piece in aquatic food webs (Borowitzka, 2018a). Microalgae produce molecules like carbohydrates, lipids, proteins, minerals, polysaccharides, polyunsaturated fatty acids (PUFAs), antioxidants, carotenoids, sterols, and vitamins, which can be grouped into primary and secondary metabolites. Primary metabolites are generally needed for metabolic and growth processes, whereas the secondary metabolites are molecules derived from them and are not essential for those processes but provide adaptive advantages, for example, when microalgae are exposed to unfavourable environmental conditions (Rico et al., 2017; Barkia et al., 2019). Some of these microalgae metabolites are already recognised for their biotechnological value (Sathasivam et al., 2019), and the most interesting part is that the production of different combinations of bioactive compounds varies not only between specific strains but also as a physiological response to biotic and abiotic stress. This ability to adapt and respond differently to stress is a unique characteristic that makes microalgae economically appreciated. Thus, the production of a desired metabolite can be exploited by manipulating the growth conditions (Paliwal et al., 2017), which is a great advantage that is impossible to obtain by chemical synthesis. Another benefit of using microalgae compared to traditional sources is that they are renewable and can enter in a circular economy, are abundant and natural, and grow without the need for arable land, therefore they do not compete with crops or terrestrial plants (Deniz et al., 2017). Moreover, large scale bioreactors enable mass-controlled cultivation (Masojídek and Torzillo, 2008) so that it is also possible to meet the challenging demands of pharmaceutical industries.

1.2.4 *Chlorella vulgaris*

Chlorella vulgaris (*C. vulgaris)* (**Figure 5**) was discovered in 1890 as the first microalgae with a well-defined nucleus by Martinus Willem Beyerinck (Beyerinck, 1890). It is spherical, subspherical or ellipsoid microalgae, with 2 to 10 µm without flagella, able to form colonies or appear as a single cell. It has only one cup-shaped chloroplast and reproduces through the production of autospores that reproduce asexually by mitosis, usually by forming four daughter cells within the parental cell. *C. vulgaris* has a large

distribution, both in marine or freshwater and terrestrial environments, with the ability to grow under auto, mixo and heterotrophic conditions (Borowitzka, 2018a; Tiong et al., 2020), which is a feature that makes it noteworthy in terms of commercial cultivation. The ease of growing this microalgae made it the first to be sold as a health food, with the first large scale cultures in Taiwan and Japan in the late 1950s (Borowitzka, 2018b).

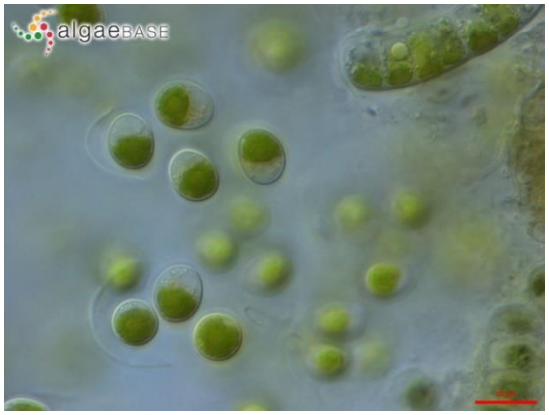

Figure 5 - Microalgae *Chlorella vulgaris* (*C. vulgaris*) from Algaebase database (Guiry, 2021).

The potential of *C. vulgaris* has already been recognised in the most diverse areas, such as for aquaculture feeding, where it dominates the market, being one of the most used species with proven antibacterial and antioxidant effects (Ahmad et al., 2020; Maliwat et al., 2021), as biofuel production (Pruvost et al., 2011; Mao et al., 2020), also in bioremediation of a variety of wastewaters like for decolourisation and removal of heavy metals from textile wastewater (Lim et al., 2010; Mubashar et al., 2020) or agro-industrial effluents (Viegas et al., 2016). It can also be used in areas as distinct as a biofertilizer for agriculture (Faheed and Fattah, 2008; Agwa et al., 2017; Bumandalai and Tserennadmid, 2019; Gitau et al., 2021) and as a stimulant for collagen synthesis for skincare cosmetic products (Mourelle et al., 2017). However, regarding obesity and obesity comorbidities, there is still very little, and sometimes contradictory, evidence about *C. vulgaris* effects (Sanayei et al., 2021b). Clinical trials were published very recently, where supplementation with the microalgae was done in association with physical exercise, however the sample studied was relatively small and gender-specific (Karbalamahdi et al., 2019; Samadi et al., 2020; Sanayei et al., 2021a). Therefore, it is still important to investigate the lipid-lowering effects of this microalgae, thus finding new sources to fight obesity epidemics.

1.3 Nutraceutical industry

Microalgae can also reach the final consumer under different forms besides drugs, namely as food supplements or nutraceuticals. The term nutraceuticals was first introduced in Japan in the 1980s as a processed food comprising ingredients that, besides the nutrition values, also have specific physiological functions (Nicoletti, 2012). Nowadays, nutraceuticals are defined somewhere between nutrients and pharmaceuticals. On the one hand, they are biologically active phytochemicals with health benefits, but on the other hand, they are less regulated by the health authorities compared to pharmaceuticals (Lachance and Das, 2007), with no explicit international consent about its regulation (Koch et al., 2014). In developed countries, they have a usage frequency of 50 to 70% with a growing trend (Télessy, 2019), and they can be sold in pharmacies, supermarkets or online as part of a normal diet.

Even though microalgae are estimated to be between 30.000 and 1.000.000 species (Rumin et al., 2020), only a very few are used in nutraceuticals applications. This is a consequence of the fact that food products must be “generally recognised as safe” (GRAS) officially by the US FDA (U.S. Food and Drug Administration, 1997), and in the European Union, microalgae must be commercialized under the “Novel Food Regulation” (EU) 2015/2283 with a strict level of safety for consumers (The European Union Parliament and the Council of the European, 2015). *C. vulgaris* have a long history of safe use, being on the market and consumed before 15 May 1997, therefore the consumption of its biomass is not subject to Novel Food Regulation (García et al., 2017; Dvir et al., 2021). Furthermore, it has also the GRAS status by the US FDA. Consequently, its use as biomass is allowed as food supplements internationally, making *C. vulgaris* one of the best-established microalgae in the market (Barkia et al., 2019) with growing consumer interest in healthier products and lifestyle.

C. vulgaris has a total protein content of 43–58% of its dry weight, depending on growth conditions (Tiong et al., 2020). This content can quantitatively and qualitatively compete with conventional protein sources. This microalgae has essential amino acids that mammals are unable to synthesize, which are well-balanced according to the WHO and The Food and Agriculture Organization (FAO) recommendations regarding human’s requirements of essential amino acids. Additionally, *C. vulgaris* amino acids are identical to high-quality protein sources, such as lactoglobulin, eggs and soy, making it a good competitor in the food market. Furthermore, this *C. vulgaris*-based proteins have lower land requirements when compared to animal-based proteins and some plant-based proteins like soy or peas. They also have slight freshwater consumption, and they can

potentially grow in seawater (Caporgno and Mathys, 2018; Barkia et al., 2019; Koyande et al., 2019), which together makes it a sustainable supplement as well.

Besides proteins, microalgae are also a source of several valuable compounds with health benefits such as carbohydrates, PUFAs, pigments, essential minerals, and vitamins (Masojídek and Torzillo, 2008; Safi et al., 2014; Barkia et al., 2019).

Currently, about 2000 tons of Chlorella dry weight are produced annually by more than 70 industrial companies, with Taiwan being the largest producer, with a production of 400 tons/year, followed by Germany with 130–150 tons/year (Spolaore et al., 2006; Koyande et al., 2019). Snacks, candies, pasta, gums, baked goods, cereals, and various drinks containing microalgae have been increasingly commercialized, although nowadays, the majority of microalgae commercialized as nutraceuticals are sold as dietary supplements in tablet, capsule, powder, or liquid forms (Fradique et al., 2010; Yasin and Shalaby, 2013; Dvir et al., 2021). These options could represent an alternative to high calorific foods that are also, coupled to modern sedentary lifestyles, causes for obesity.

1.3.1 Illegal supplements for weight loss

However, the thin layer of regulation of nutraceutical products makes room for a potentially dangerous market. Considering the low efficacy and the various side effects already mentioned regarding the approved anti-obesity drugs, it is clear why consumers are looking for new alternatives. Many of these nutraceutical products with weight loss properties have a way to attract consumers with health claims, assumed safety, with a natural label and a strong marketing technique. Nevertheless, the allegation that the use of substances that come from nature is always safe and harmless is wrong, and yet there are many misperceptions about them (Pillitteri et al., 2008; Chan, 2009). Not only, and due to lack of legislation, the products have a heterogeneous level of ingredients and variable active compounds, they also are manufactured with the addition of unauthorized or illegal ingredients to weight loss supplements in order to increase their efficacy (Colman, 2007). Moreover, even though nature is a source of natural products with a wide spectrum of beneficial activities, some species are also toxin producers, which can be quite harmful or even lethal to humans (Egmond, 2004). From here, it is possible to understand that this may be presented as a market that does not deliver results that can potentially pose a health risk (Lekehal et al., 1996; Pittler et al., 1999; Pittler and Ernst, 2001; Dwyer et al., 2005). Hence, it is crucial to validate the results through differentiated

bioassays to invest in a good nutraceutical products policy, whose laws must also be revised.

1.4 Bioassays

Bioassay refers to a biological assay that determines the potential effect of a substance on biological material that can either be conducted *in vitro*, using living cells or tissues or *in vivo*, applied to living organisms. Since obesity is an alarming and growing problem, it is important to develop assays that improve our knowledge of this problem and its associated comorbidities, with the ultimate goal of uncovering new bioactive compounds.

1.4.1 Microalgae extractions

The microalgae performance in bioassays, which leads to its categorization for potential use in the most diverse areas, depends largely on the biomass used. The most common in laboratory assays is to use microalgae in the form of extracts. Extraction is also the first step when it comes to the isolation and purification of compounds of special interest. This occurs because most microalgae metabolites are stored intracellularly, and the cellular membrane and the cell wall act as physical barriers that prevent the release of the compounds into the environment (Alhattab et al., 2019). Therefore, there is a need to disrupt these structural constituents of microalgae to have access to its valuable metabolites.

Ohmic extraction was developed based on the passage of electric current through the biomass, which increases kinetic and vibration energy, resulting in heat generation by a phenomenon called Joule's effect, resulting in electroporation of the membrane and cell wall leading to intracellular component diffusion (Knirsch et al., 2010; Rodrigues et al., 2019). Another example is high pressure processing (HPP), which consists of applying pressure at a defined period and temperature, with water or other solvents. The pressure applied is able to disrupt cell structures, including the cell wall, leading to the exit of bioactive compounds (Jun, 2013; Chemat et al., 2020).

It is important to notice that in the extraction step, all the chosen variables determine the final product obtained, namely the solvent used, the duration of the extraction, the intensity applied, the frequency, the pressure or any other force used to

disrupt the cell wall. Hence, depending on the combination of variables, extracts differ in their composition and, consequently, in their activity.

1.4.2 *In vivo* and *in vitro* models

1.4.2.1 Cells (*in vitro*)

Compounds are often screened in cell-based assays to determine its effects and eventual cytotoxicity that can lead to cell death. The *in vitro* model of choice needs to express the pathway or mechanism of interest, and the results are usually based on the quantification of a measurable response (Sarine Markossian et al., 2012). There are numerous available cell lines and protocols developed for a variety of studies, from the simplest to the most extensive and complex. Opting for an *in vitro* assay is an important, faster, and cheaper approach to analyse extracts or compounds. Obesity, for instance, can be evaluated in numerous cell culture models, like preadipocytes, adipose-derived stem cells, brown/beige adipose cells (Ruiz-Ojeda et al., 2016; Tung et al., 2017). *In vitro* models for steatosis have also been developed, where the human hepatocyte cell lines are treated in culture with fatty acids (Gómez-Lechón et al., 2007; Cui et al., 2010), which reproduce the clinical condition NAFLD.

1.4.2.2 Zebrafish model (*in vivo*)

Mouse models are the first ones that come to mind when we talk about *in vivo* models, however, it is necessary to sacrifice the animals, surgically remove and separate the organs to determine their lipid content. And that is where the advantages of using a smaller animal model arise. The zebrafish (*Danio rerio*), a small freshwater fish, is an outstanding model system to study lipid metabolism *in vivo* due to its small size, ease of care, optical transparency in the first days of development, high fecundity with a lot of egg produced, and short generation times (Dooley and Zon, 2000; Ulloa et al., 2011; Meyers, 2018). Additionally, they have a high degree of genetic and functional homology with the mammalian metabolic pathways and the same gastrointestinal organs as humans: liver, intestine, exocrine and endocrine pancreas, and gallbladder (Wallace and Pack, 2003; Carten and Farber, 2009; Oka et al., 2010; Broeder et al., 2015).

During the first days of development, zebrafish embryo and larva stages have the lipids necessary for sustaining the growth mostly circumscribed to a single organ, the

yolk sac (**Figure 6**). It is only by 5 to 6 days postfertilization that it depletes, and the larva has to start eating to obtain energy (Kimmel et al., 1995). Thus, in these early days of development, when lipids are stored in the yolk sac, and the larva is still quite transparent, there is a great window of opportunity for the study of lipid metabolism and possible determination of the bioactivity of compounds or extracts on that metabolism.

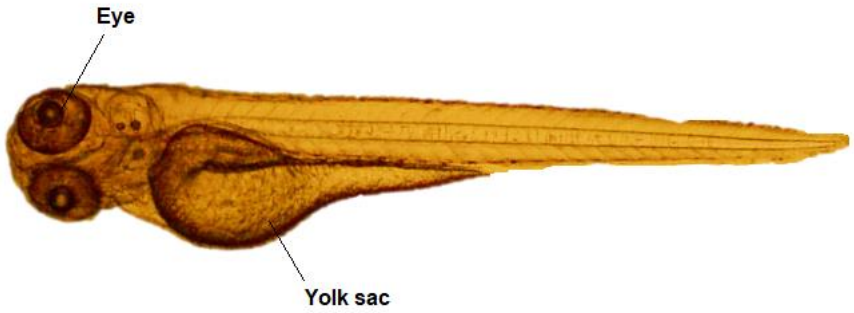

Figure 6 - 3 days post fertilization zebrafish larva with the yolk sac already developed and visible due to the body transparency.

For that, lipophilic dyes can be used to visualize lipids through live imaging or fluorescence screens. Nile red is one of the commonly used dyes for imaging and quantification of intracellular neutral lipid droplets, usually triacylglycerols or cholesteryl esters (Fowler and Greenspan, 1985; Greenspan et al., 1985). Besides this approach, induced obesity by overfeeding (Landgraf et al., 2017; Vargas and Vásquez, 2017), or the utilization of mutant or transgenic lines expressing obesogenic genes (Chu et al., 2012; Hsu et al., 2018), are additional successful strategies to study lipid metabolism in the zebrafish model.

Although the intention is to fight obesity directly and, consequently, reduce the occurrence or severity of its associated comorbidities, it is also possible to use these zebrafish *in vivo* model to assess bioactivities that may be relevant for the regulation of the comorbidities. Mammalians and zebrafish share morphological and physiological similarities of the pancreas and conserved signalling pathways and mechanisms of endocrine pancreas formation (Tehrani and Lin, 2011). Furthermore, the glucoregulation and glucose transporter's structure and tissue distribution are also conserved between zebrafish and mammals (Elo et al., 2007; Jurczyk et al., 2011). Thus, this similarity in the glucose homeostasis system makes zebrafish valuable to study diabetes (Tabassum et al., 2015; Zang et al., 2018). In fact, one way to screen for anti-diabetic agents is by measurement of cellular glucose uptake. Due to the use of fluorescent glucose analogues, like 2-NBDG or GB2-Cy3, the monitoring of glucose flux is possible (Um et

al., 2015). These fluorescent-tagged glucose probes have glucose transporters (GLUTs) as substrates, which are highly expressed at the eye level of the zebrafish larva in 3 days post fertilization (Tseng et al., 2009). Hence, the fluorescent quantification characterizes the glucose uptake and consequently the ability of a compound to operate as an anti-diabetic drug (Kim et al., 2012; Park et al., 2014). It is possible to perform this methodology in wild type zebrafish larvae, which has the advantage of being less expensive and easier to maintain than genetically modified lines used in transgenic models (van de Venter et al., 2021).

2. Aims

This work was integrated into the "ALGAVALOR" project, which has the general aim of an integrated production of microalgae and its biomass valorisation for different applications. In line with this, the present work had as main goal the evaluation of the potential beneficial effects of the microalgae *C. vulgaris*, grown under heterotrophic conditions and extracted by different methodologies, against obesity and its associated comorbidities. Several specific aims were defined. First, the assessment of the anti-steatosis, anti-inflammatory, anti-obesity, and anti-diabetes activities of *C. vulgaris* extracts by performing *in vitro* and *in vivo* screening assays. 20 extracts from high pressure processing and 6 from ohmic treatments were received from project partners and were evaluated for promising activities. Second, the putative identification of responsible metabolites by application of resolution liquid chromatography-tandem mass spectrometry (LC-MS/MS), and the comparison of the metabolic profiles of active and non-active extracts. Finally, the third aim was to get insight into the molecular mechanisms of action of those promising *C. vulgaris* extracts by the analysis of target proteins using western blot.

Overall, this work should contribute to the application of *C. vulgaris* in the pharmaceutical or nutraceutical industry for the treatment of obesity and associated comorbidities through the discrimination of the best extraction methodology, as well as some of their molecular targets.

3. Materials and methods

3.1 Microalgae extracts

The microalgae biomass used in this thesis project was provided by the partners of the ALGAVALOR project. *Chlorella vulgaris* was cultivated by the company Allmicroalgae in heterotrophic conditions, and the biomass extractions were made by University of Aveiro (Chemical Department, Professor Jorge Saraiva) and University of Minho (Centre of Biological Engineering, Professor José Teixeira).

3.1.1 High pressure processing (HPP) extraction from University of Aveiro and ohmic extraction from University of Minho

C. vulgaris biomass was extracted by high pressure processing (HPP) and ohmic extraction, following the experimental design at **Table 1** and **Table 2**, respectively**.** For the ohmic extraction ethanol 70% was used as solvent. The dry extracts were delivered to the Interdisciplinary Centre for Marine and Environmental Research (CIIMAR), where all the bioassays were carried out.

3.1.2 Samples preparation

Depending on the mass of each extract, the dry extracts were dissolved in dimethyl sulfoxide (DMSO, VWR Chemicals BDH®, USA), with correspondent volumes, to obtain stock solutions with a final concentration of 10 mg/mL (**Figures 7** and **Figure 8**). Dilutions of these solutions were made in DMSO for a final concentration of 5 mg/mL to perform cell assays. All samples were stored at -20 ºC.

Table 1 - HPP extraction conditions of pressure applied per time of extraction and solvent used (water, ethanol 48%, ethanol 96% and acetone) for each sample.

Conditions (Pressure/Time)	Sample	Solvent
420 MPa / 9 min	CS1	Water
	CS4	Ethanol 48%
	CS8	Ethanol 96%
	CS11	Acetone
300 MPa / 8 min	CS13	Water
	CS16	Ethanol 48%
	CS19	Ethanol 96%
	CS22	Acetone
100 MPa / 8 min	CS25	Water
	CS29	Ethanol 48%
	CS31	Ethanol 96%
	CS35	Acetone
0 MPa / 9 min (Control)	CSC1	Water
	CSC4	Ethanol 48%
	CSC8	Ethanol 96%
	CSC11	Acetone
0 MPa / 8 min (Control)	CSC13	Water
	CSC17	Ethanol 48%
	CSC20	Ethanol 96%
	CSC23	Acetone

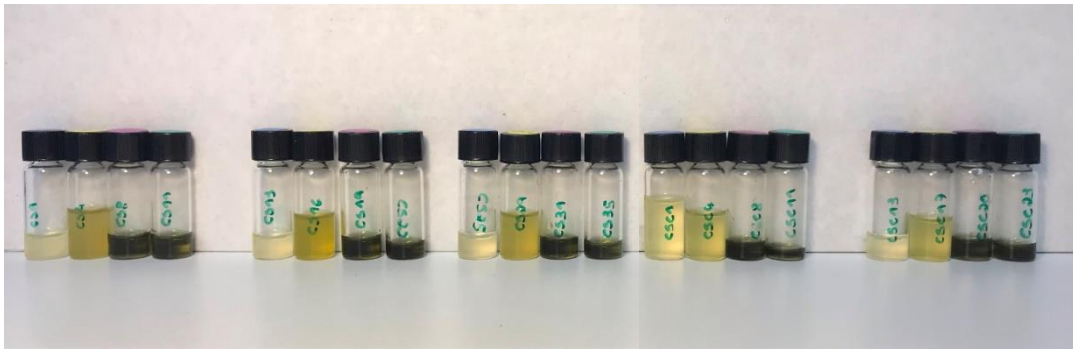

Figure 7 - Stock solutions of HPP-extracted *C. vulgaris* samples with a 10 mg/mL concentration.

Table 2 - Ohmic extraction conditions of frequency and temperature applied per time of extraction for each sample.

Sample number	Frequency (Hz)	Time (min)	Temperature (ºC)
D11	0 (control)	15	25
D21	0 (control)	15	70
D31	25000	15	70
D41	50	15	70
D102	50	30	70
D111	50	45	70

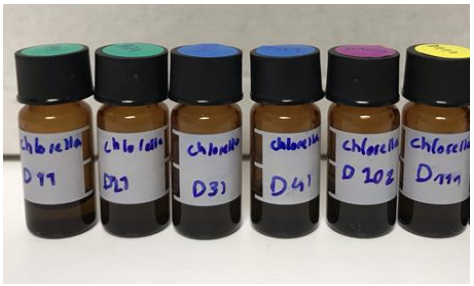

Figure 8 - Stock solution of ohmic-extracted *C. vulgaris* samples with a 10 mg/mL concentration.

3.2 Bioactivity assays

3.2.1 *In vitro* bioactivity assays

3.2.1.1 Cell culture

Cryopreserved human hepatocyte carcinoma cell line (HepG2, American Type Culture Collection, USA) and mouse macrophage cell line (RAW264.7, European Collection of Authenticated Cell Cultures, England) were defrosted and transferred to a 25 cm^2 culture flask with 5 mL of Dulbecco's Modified Eagle Medium (DMEM, Biowest, France) completed with 10% (v/v) of fetal bovine serum (FBS, Pan Biotech, Germany), 1% (v/v) of antibiotic penicillin/streptomycin (Pan Biotech, Germany) and 0.1% (v/v) of antifungal amphotericin B (Biochrom GmbH, Germany). These were left to grow in an

incubator (Thermo Fisher Scientific, USA) at 37 ºC in a humidified 5% CO_2 atmosphere. After confluency in the culture flask was reached (**Figure 9**), cell passage was performed to a new medium. This was repeated twice to ensure the robustness of the cells before starting the bioassays.

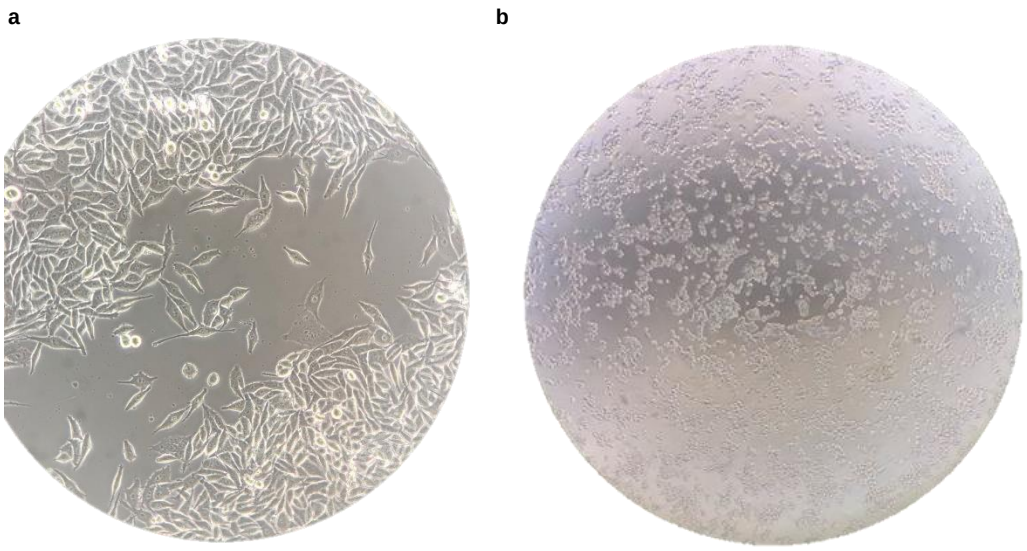

Figure 9 - Cell confluency in culture flask under Olympus CKX41 (Japan) inverted phase contrast microscope 100x amplification. (**a**) HepG2 cell line; (**b**) RAW264.7 cell line.

3.2.1.2 Anti-steatosis assay

After reaching confluency in the culture flask, HepG2 were seeded in 96-well plates at a density of $1x10^5$ cells/mL, for a total volume of 100 µL of DMEM complete per well. Cell count was performed using the Countess™ Automated Cell Counter (Thermo Fisher Scientific Invitrogen, USA), where 10 µL of cell culture was mixed to 10 µL of a solution of trypan blue (Thermo Fisher Scientific Invitrogen, USA) stain in 0.4% concentration to assess the number of live and dead cells, and to calculate their viability. Cells were left growing for 24 h in an incubator at 37 ºC in a humidified 5% CO_2 atmosphere.

After 24 h, cell growth in the wells was confirmed under a microscope before starting exposure. The entire volume of the wells was removed and 100 µL of DMEM incomplete (DMEM medium with 1% (v/v) of antibiotic penicillin/streptomycin and 0.1% (v/v) of antifungal amphotericin B) were added. A solution of sodium oleate (SO, Sigma, USA) in filtrated methanol was mixed with the medium for a final concentration of 62 µM per well to stimulate a fat-overloaded state in cells (Gómez-Lechón et al., 2007). A co-

exposure with *C. vulgaris* samples was performed in three technical replicates for a final concentration of 10 µg/mL or 25 µg/mL exposure. Each exposure concentration was repeated in two independent assays (n=6). For this experimental design, three controls were used in which the same percentage of the solvent (DMSO) was added to the medium to a final concentration of 0.2% (v/v) and 0.5% (v/v) per well, in the 10 µg/mL and 25 µg/mL assay, respectively. For the first control, nothing else was added. In the second control, filtrated methanol at a concentration of 0.5% per well was added, which corresponded to the concentration from the SO solution. In the third control, SO at 62 µM per well was added to mimic the fat-overloaded state in cells. Cells were incubated for 6 h at 37 ºC in a humidified 5% CO_2 atmosphere.

After incubation, the whole volume of the wells was replaced by 100 µL of Hank's Buffered Salt Solution (HBSS, prepared in distilled water by adding five stocks: 1:10 of stock#1: 4 g of sodium chloride (NaCl, Panreac, Spain) and 0.2 g of potassium chloride (KCl, Sigma-Aldrich, USA) in 50 mL of distilled water; 1:100 of stock#2: 0,358 g of disodium hydrogen phosphate (Na_2HPO_4, Sigma-Aldrich, USA) and 0.60 g of potassium dihydrogen phosphate (KH_2PO_4, Sigma-Aldrich, USA) in 50 mL of distilled water; 1:100 of stock#3: 0.72 g of calcium chloride ($CaCl_2$, Sigma-Aldrich, USA) in 50 mL of distilled water; 1:100 of stock#4: 1.23 g of magnesium sulphate heptahydrate ($MgSO_4$ x$7H_2O$, Honeywell, USA) in 50 mL of distilled water; 1:100 of stock#5: 0.35 g of sodium bicarbonate ($NaHCO_3$, Sigma-Aldrich, USA) in 10 ml of distilled water). Nile red (Sigma-Aldrich, USA) and bisbenzimide H 33342 trihydrochloride (HO-33342, Sigma-Aldrich, USA) dyes were added to the HBSS solution at concentrations of 1:400 and 1:100, to stain the lipids and the nucleus, respectively. Incubation took place for 15 min at 37 ºC in a humidified 5% CO_2 atmosphere in the dark. The entire volume was again discarded, and 100 µL of HBSS were added. This washing step was repeated three times, and subsequently, three different measurements were taken: point fluorescence, area scan and imaging, using a Cytation 5 Cell Imaging Multi-Mode Reader (BioTek, USA), at 530/25 nm excitation and 590/35 nm emission for the Nile red and 360/40 nm excitation and 460/40 nm emission for the HO-33342. In point fluorescence, lipid content was expressed as a percentage of the Nile Red fluorescence and cell viability as a percentage of the HO-33342 fluorescence, both considering 100% in the DMSO+SO control. In area scan fluorescence, lipid content was expressed as a percentage of the average intensity emitted by the Nile Red and cell viability as an average intensity emitted by HO-33342, both considering 100% in the DMSO+SO control. In imaging analysis, Gen5™ software (BioTek, 2021) was used to detect cells, cytoplasm, nucleus,

and lipid content. Final values represent the average lipid content per cell per well, expressed as a percentage of the quotient between the average intensity emitted by the Nile Red per cytoplasm and the average intensity emitted by the HO-33342 per nucleus.

After spectrophotometry reading, 25 µL of ice-cold trichloroacetic acid (TCA, Thermo Fisher Scientific, USA) 50% (w/v) solution in distillate water was added to the wells, and the plate was incubated for 1 h at 4 ºC in the dark to fix the cells. Then the volume was discarded, and four washes with distilled water were performed to remove TCA. The plate was air-dried at room temperature, and 100 µL of sulforhodamine B (SRB, MP Biomedicals, USA) 0,4% (w/v) solution in 1% acetic acid (Merck KGaA, Germany) were added to verify cell viability (Vichai and Kirtikara, 2006), followed by 15 min incubation in the dark at room temperature. Next, four washes with acetic acid 1% were made to remove all the unbound SRB, and the plate was air-dried at room temperature. 100 µL of Tris hydrochloride (Tris-HCl, VWR, USA) solution at 10 mmol/L and pH=10.5 in distilled water were added to solubilize bound dyes. Absorbance was read in Cytation 5 Cell Imaging Multi-Mode Reader at 554 nm. Cell viability was expressed as a percentage of SRB absorbance considering 100% viability in the control DMSO+SO.

3.2.1.3 Pro- and anti-inflammatory assays

After reaching confluency in the culture flask, RAW264.7 were seeded in 96-well plates at a density of $3.5x10^5$ cells/mL, for a total volume of 100 µL of DMEM complete with inactivated FBS per well. Cell count was performed using the Countess™ Automated Cell Counter, as previously described. Cells were left growing for 24 h in an incubator at 37 ºC in a humidified 5% CO_2 atmosphere.

The medium was renewed, and the exposure with *C. vulgaris* samples was performed in eight technical replicates for a final concentration of 10 µg/mL or 25 µg/mL exposure. Technical replicates were divided in half. Four wells were kept for a pro-inflammatory assay to evaluate the capacity of the extracts to induce inflammation by themselves. The other four technical replicates wells were co-exposed with lipopolysaccharides from *Escherichia coli* 0111:B4 (LPS, Sigma, USA) to a final concentration of 1 µg/mL to induce inflammation in cells (Stuehr and Marletta, 1985). Since LPS is a structure from the bacterial cell membrane, it triggers the inflammatory reaction in the RAW264.7 cells. These four wells were kept to perform the anti-inflammatory assay to assess the ability of the extracts to reverse the induced

inflammation. Each exposure concentration was repeated in two independent assays (n=8) for both anti and pro-inflammatory assays.

Two controls were used in both assays. DMSO was added to the medium at the same percentage as in extracts, namely 0.2% (v/v) and 0.5% (v/v) per well, in the 10 µg/mL and 25 µg/mL assay. For the first control, nothing else was added. For the second control, 1 µg/mL of LPS was added to induce inflammation. Cell incubation was done at 37ºC in a humidified 5% CO_2 atmosphere.

After 24 h, 75 µL of the supernatant was transferred to a new 96-well plate, and 75 µL of Griess Reagent (solution of 1 mg/mL of N-(1-Naphthyl)ethylenediamine dihydrochloride (Honeywell, USA) and 10 mg/mL sulfanilamide ($H_2NC_6H4SO_2NH_2$, Sigma-Aldrish, USA) in 2% orthophosphoric acid (H_3PO_4, Acros Organics, USA)) were added for nitrite quantification as an indicator of the nitric oxide production. Nitric oxide is a signalling molecule that plays a crucial role in inflammation. If the inflammation process is triggered, so is the nitric oxide production, which can be measured by nitrites quantification since they are a product of its oxidation (Stuehr and Marletta, 1985). The plate was incubated for 10 min at room temperature in the dark, and subsequently, the absorbance was read at 562 nm in Cytation 5 Cell Imaging Multi-Mode Reader. Inflammation was expressed as a percentage of nitrite content considering 100% in the control DMSO+LPS.

The residual volume of the original plate was discarded, and 100 µL of heated 3-(4.5-dimethylthiazole-2-yl)-2.5-diphenyltetrazolium bromide (MTT, Duchefa Biochemie, Netherlands) solution at a concentration of 0.5 mg/mL in DMEM complete with inactivated FBS were added. Incubation took place for 45 min at 37 ºC in a humidified 5% CO_2 atmosphere. The growth medium was discarded, and 100 µL of DMSO were added to dissolve the formazan salts, formed by the conversion of MTT by living cells (Meerloo et al., 2011). Shaking was carried out for 10 min, and absorbance was read at 510 nm in Cytation 5 Cell Imaging Multi-Mode Reader. Cell viability was expressed as a percentage of MTT absorbance considering 100% viability in the control DMSO+LPS.

In the inflammatory process, the presence of released nitrites together with the Griess reagent form a final azo dye that exhibits a more or less red colour dependent on the inflammation state (**Figure10a**). In the viability assay, the colours are based on the passage of the MTT from its yellow form to its purple form by the mitochondria (**Figure10b**). These two properties made it possible to verify the results by spectrophotometry as well as directly with the naked eye.

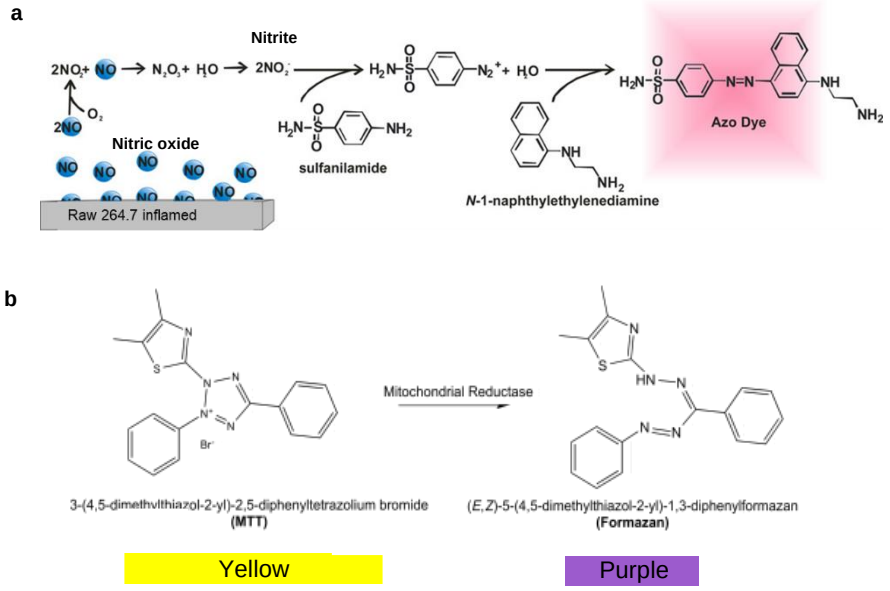

Figure 10 - Colorimetric properties of the inflammatory assay in RAW264.7 cells. (**a**) Schematic representation of the reaction of nitrite with Griess reagents to form an azo dye. Adapted from: Coneski and Schoenfisch, 2012; **(b**) schematic representation of MTT mitochondrial reduction to formazan.

3.2.2 *In vivo* bioactivity assays

3.2.2.1 Zebrafish larvae

6 female and 6 male zebrafish wild-type adults in reproductive age were placed overnight in breeding aquariums at the Animal Facility for Aquatic Organisms of CIIMAR, at 28 ºC with an air pump and marbles to stimulate spawning. Zebrafish embryos were collected and cleaned the following morning by discarding the dead and the non-viable ones and kept in egg water (60 µg/mL marine sea salt dissolved in distilled water) at 28 ºC. 1-day post-fertilization (1DPF), a maximum of 40 larvae were placed in Petri dishes with 20 mL of egg water complemented with 200 µM of 1-phenyl-2-thiourea (PTU, Acros Organics, USA) to inhibit pigmentation **(Figure 11a**).

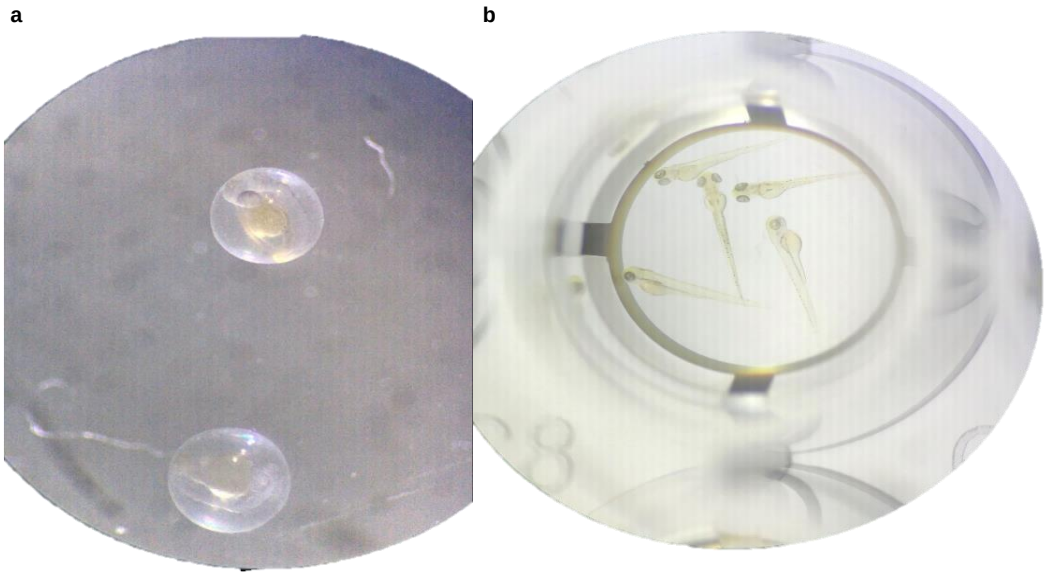

Figure 11 - Zebrafish under stereo microscope Leica EZ4. (**a**) Zebrafish embryo with 1 DPF; (**b**) Zebrafish larvae 3 DPF.

3.2.2.2 Anti-obesity assay

3 DPF zebrafish larvae at the same development stage were placed in a 48-well plate with a density of 6-8 larvae per well, in which each larva corresponded to a technical replicate. Egg water with PTU was renewed for a total volume of 750 µL per well. Zebrafish larvae were exposed to *C. vulgaris* extracts at a final concentration of 10 µg/mL. For this experimental design, resveratrol (REV, Focus biomolecules, Philadelphia) solution in DMSO was used as a positive control with a final concentration of 50 µM to inhibit lipid formation (Pardal et al., 2014), and a solvent control with 0.1% (v/v) DMSO, correspondent to the concentration of added extract. Zebrafish larvae were left for 24 h at 28 ºC. At 4 DPF, water, compounds and extracts were renewed, and Nile red solution in DMSO was also added to all wells overnight at the final concentration of 0.01 µg/mL for lipid staining. At 5 DPF, the larvae were anaesthetized with ethyl 3-aminobenzoate methanesulphonic acid salt (MS-222, Acros Organics, USA) solution in egg water at the final concentration of 0.3 µg/mL for 5 min. Fluorescence microscopy images were taken with the microscope Leica DM6000 B (Germany). Fluorescence intensity was quantified in each individual zebrafish larvae by ImageJ software (Rasband, 1997; Schneider et al., 2012). Lipid content was expressed as a percentage of Nile red fluorescence considering 100% in the DMSO control. Three independent anti-obesity assays with the same experimental design were performed (n=18-24).

3.2.2.3 Anti-diabetes assay

3 DPF zebrafish larvae at the same development stage were placed in a 96-well plate with a density of 5 larvae per well (**Figure 11b**), in which each larva corresponded to a technical replicate. Egg water with PTU was renewed for a total volume of 200 µL per well. Zebrafish larvae were exposed to *C. vulgaris* extracts at a final concentration of 10 µg/mL. For this experimental design, 1,3,8-Trihydroxy-6-methylanthraquinone (emodin, Targetmol, USA) solution at 500 µM in DMSO diluted in egg water was used as a positive control for a final exposure concentration of 10 µM. Emodin has been shown to increase glucose tolerance and insulin sensitivity, behaving as a compound with anti-diabetic properties in zebrafish (Xue et al., 2010). A solvent control was used with DMSO at a final concentration of 0.1% (v/v), corresponding to the concentration of added extract and emodin. After zebrafish larvae were left for 1 h at 28 ºC, all volume was removed from wells, and 200 µL of 2-deoxy-2-[(7-nitro-2,1,3-benzoxadiazol-4-yl)amino]-D-glucose (2-NBDG, Thermo Fisher Scientific Invitrogen, USA) were added at 200 µM. 2-NBDG is a probe that can be used to provide an expedient measurement of spatiotemporal glucose flux (Lee et al., 2013). Since 2-NBDG is highly sensitive to light, all this methodology was carried out in an environment of maximum possible darkness, followed by a 3 h incubation at 28 ºC. Next, the entire volume was removed from the wells, and three successive washes with egg water were conducted. 200 µL of egg water were left in wells, and a concentration of 0.3 µg/mL of the anaesthetic MS-222 was added for 5 min. Fluorescence microscopy images were taken under the microscope Olympus BX41 (Japan). Fluorescence intensity was quantified in individual zebrafish larvae by ImageJ software (Rasband, 1997). Glucose uptake was expressed as a percentage of 2-NBDG fluorescence considering 100% DMSO control. Two independent anti-diabetes assays with the same experimental design were performed (n=8-10).

3.3 Metabolite profiling

3.3.1 LC-MS/MS analysis

For LC-MS/MS analysis, 40 µL of each 10 mg/mL stock of *C. vulgaris* extracts were dried and then dissolved in 400 µL of UHPLC-MS grade acetonitrile (Carlo Erba, Italy) to obtain a final concentration of 1 mg/mL. 200 µL were filtrated by a syringe-filters with a diameter of 0.2 µm (Millex Syringe Filter, Merck Millipoore Millex ™, Germany) into 2 mL vials (Millex Syringe Filter, Merck Millipoore Millex ™, Germany). The LC/MS

analysis was carried out at Materials Center of the University of Porto, by Orbitrap Exploris 120 Mass Spectrometer (Thermo Scientific™) coupled with a column ACE UltraCore 2.5 SuperC18 (50x2.1 mm; 5 µm ACE® UltraCore™, Scotland), with electrospray ionisation (ESI) source, operating in positive mode and controlled by Xcalibur 4.4.16.14 (Thermo Scientific™). Each sample was injected with a volume of 5 µL.The samples were eluted with a gradient of 99.5% of the mobile phase A (95% H_2O + 5% MeOH + 0.1% formic acid), by decreasing mobile phase A to 10% and increasing mobile phase B to 90% at 9.5 min, eventually rose to 99.5% the mobile phase A and decreased to 0.5% the mobile phase B at 17 min. The gradient was established at a flow rate of 0.35 mL/min for 20 min. The separation temperature was kept at 40 ºC for the entire analysis.

3.3.2 Molecular networking

Data obtained from LC-MS/MS was converted from files .raw to .mzXML files by MSConvert software (Kessner et al., 2008). Data was then submitted to the Global Natural Product Social Molecular Networking (GNPS) platform (Wang et al., 2016) to create a molecular network, in which parameters of precursor ion mass tolerance and fragment ion mass tolerance were set to 0.02 Da. The created network was filtered so that 0.7 was the minimum cosine score that occurred between a pair of consensus MS/MS spectra to form an edge in the molecular network, and 6 was the minimum number of common fragment ions shared by two separate consensus MS/MS spectra to be connected. Consensus MS/MS spectra with a size less than 2 were not considered, and, on the other hand, the edge between two nodes was retained if each other were in their own top 10 most similar nodes. Additionally, the maximum size allowed in a single connected molecular network was selected as 100 nodes. The spectra in the network were searched against GNPS spectral libraries that were filtered with the same parameters as in the input data, and the analogues search was enabled.

Bioinformatic tools of GNPS were also used, including the Dereplicator, Dereplicator + and MolNetEnhacer. The Dereplicator, an *in silico* peptidic natural products tool, was applied to compare data to chemical structure databases. The Dereplicator +, an algorithm for *in silico* identification of metabolites, was used to annotate both peptidic or non-peptidic metabolites through database search of fragmentation data. For Dereplicator, the search for analogues of known natural products was established, and parameters were set for low-resolution instruments

(precursor ion mass tolerance 2.0 Da and fragment ion mass tolerance 0.5 Da). In the Dereplicator + tool, parameters of precursor ion mass tolerance and fragment ion mass tolerance were set for high-resolution instruments (both parameters 0.02 Da). Finally, MoINetEnhancer was used to merge the outputs from molecular networking, *in silico* annotation tools and the automated chemical classification through ClassyFire.

The output data were then imported into Cytoscape v3.8.2 (Shannon et al., 2003) to visualise the created networks. Compounds that were unique in active extracts and that had no possible identification by previous mentioned tools and databases were selected and searched by their m/z values +/- 0.002 in The Natural Products Atlas (NPA) (Santen et al., 2019) and in the Dictionary of Natural Products 30.1 (DNP) (Dictionary of Natural Products, 2021). Possible matches were only considered if the calculated mass error was lower than 5 ppm.

3.4 Western blot

3.4.1 Samples preparation

Western blots were performed with HepG2 proteins exposed to samples CS11, CS22 and DMSO control, following the previously described conditions used in the anti-steatosis assay. For that, HepG2 cell line were seeded in a 12-well plate at a density of $4x10^5$ cells/mL in 1 mL of DMEM complete per well. The exposure with CS11 and CS22 *C. vulgaris* extracts was performed at a final concentration of 25 µg/mL per well in four technical replicates.

Then, cells were transferred to a precellys eppendorf and centrifuged for 5 min at 13500 rpm in the micro star 17R centrifuge (VWR, USA) at room temperature. The supernatant was discarded, and 198 µL of RIPA buffer (150mM NaCl, 5 mM ethylenediaminetetraacetic acid tetrasodium salt (EDTA, Panreac, Spain) solution with pH 8.0, 50 mM Tris-HCl (VWR) with pH 8.0, 1% octylphenoxy poly(ethyleneoxy)ethanol (IGEPAL CA-630, Sigma, USA), 0.5% sodium deoxycholate (Sigma, USA) and 0.1% sodium dodecyl sulfate (SDS, Amresco, USA)) were added, as well as 2 µL of protease & phosphatase inhibitor cocktail 100x (Thermo Fisher Scientific, USA) and a metal sphere to aid cell lysis. The content was vortexed and placed in ice until disrupted by Precellys® Evolution (Bertin Corp., USA) in a 2x30 s cycles at 5000 rpm at 20 ºC, with a 60 s pause between cycles. After that, the samples were left to rest on ice for 1 h,

followed by a 15 min centrifugation at 13500 rpm and 4 ºC in the micro star 17R centrifuge. The supernatant was then transferred to new eppendorfs and kept at -20 ºC.

3.4.2 Protein quantification by Bradford assay

1:10 dilutions of the samples were prepared in distilled water, and 5 µL of each were added to a well with 245 µL of a Coomassie dye-binding reagent (Bradford reagent, Sigma, USA), in a 96-well plate. The plate was incubated for 15 min in the dark, and the absorbance was read at 595 nm since quantification is based on the fact that the anionic form of the dye binds to proteins, which has a maximum wavelength at 595 nm (Kruger, 1996). A standard curve was prepared for the determination of protein concentration in the same assay by using a 2-fold dilution series from 10 to 0.0781 mg/mL in 8 dilution steps using albumin from bovine serum (BSA, Sigma, USA) in RIPA buffer 1:10.

3.4.3 Electrophoresis and membrane transference

To prepare each sample for electrophoresis, a 30 µL mix was prepared with 7.5 µL of NuPAGE LDS Sample Buffer 4x (Thermo Fisher Scientific Invitrogen, USA), 3 µL of Sample Reducing Agent 10x (Thermo Fisher Scientific Invitrogen, USA), and the volume corresponding to 20 µg protein of each sample. 3 replicates were prepared for each exposure (DMSO, CS11 and CS22), and the final volume was adjusted with distilled water. The mixes were heated at 97 ºC for 10 min, followed by cooling on ice.

20µL of each sample was loaded into corresponding wells of precast polyacrylamide gels assembled in the XCell SureLock™ Novex™ Mini-Cell gel system (Thermo Fisher Scientific Invitrogen, USA). In the first well of the gel, a mix was loaded composed of 2.5 µL of SeeBlue™ Plus2 pre-stained protein standard (Thermo Fisher Scientific Invitrogen, USA), 1 µL MagicMark™ XP western protein standard (Thermo Fisher Scientific Invitrogen, USA), and 7.5 µL of NuPAGE LDS Sample Buffer 4x (Thermo Fisher Scientific Invitrogen). To obtain an optimal separation of the proteins, and depending on the molecular weight of the protein of interest, two different combinations of gels and running buffer were used: the Invitrogen NuPAGE 4-12% Bis-Tris gel (Thermo Fisher Scientific Invitrogen, USA), with a separation range from 3.5 to 260 kd, combined with MOPS-SDS running buffer (Alfa Aesar, USA) to resolve medium to large-size proteins, and the NuPAGE 3-8% Tris-Acetate gel (Thermo Fisher Scientific Invitrogen, USA), with a separation range from 40 to 500 kd, combined with Tris-Acetate

SDS running buffer (Thermo Fisher Scientific Novex™, USA) for larger proteins. After loading all 10 wells of the gel, the electrophoresis run was performed for 1 h at 170 V (**Figure 12**).

After electrophoresis, a semi-dry western blotting transfer was executed to a nitrocellulose membrane in the iBlot™ 2 Gel Transfer Device (Thermo Fisher Scientific, USA) using iBlot™ 2 NC Mini Stacks (Thermo Fisher Scientific Invitrogen, USA) and following the protocol 20 V for 2 min, 23 V for 8 min and 25 V for 3 min. Transference quality was verified by protein staining with a Ponceau S (Sigma-Aldrich, USA) solution at 0.1% (w/v) in 5% (v/v) acetic acid. A new membrane was prepared for each antibody to be tested.

The membrane was then washed with phosphate buffered saline with Tween 1x (PBST, Cell Signalling Technologies, USA) to remove staining, followed by a blocking step, in which it was immersed in 5% (w/v) non-fat dried milk (Panreac, Spain) in PBST 1x with agitation for 1h to prevent antibodies from binding to the membrane non-specifically. Differently, for phosphorylated antibodies, blocking was performed in 3% (w/v) BSA solution in PBST 1x.

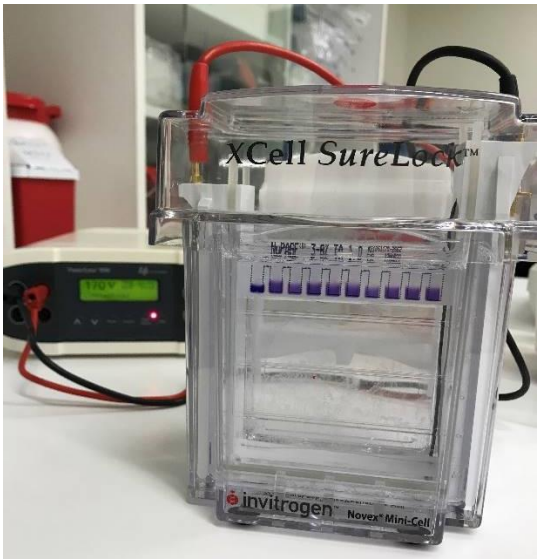

Figure 12 - Loaded protein standard and protein samples in Invitrogen NuPAGE gel assembled in the XCell SureLock™ Novex™ Mini-Cell gel system.

3.4.4 Antibodies incubation and develop

After blocking, the membrane was washed with PBST 1x with agitation for 10 min and kept overnight at 4 ºC in a rotative support with the primary antibody anti-C/EBPα, anti-PRKA-β1, anti-PRKA-β1 (p-Ser-181), anti-PPAR γ, anti-ACACα and anti-ACACα (p-Ser-80), all from Antibody Verify, USA, prepared in 5 mL of PBST 1x.

On the following day, the membrane was washed 3 times for 10 min with PBST 1x with agitation and subsequently kept for 1h at room temperature in a rotative support with the secondary antibody Goat anti-rabbit IgG (H+L) peroxidase/HRP conjugated (Elabscience, USA), prepared in 5 mL of 5% (w/v) non-fat dried milk in PBST 1x. In the case of phosphorylated antibodies, secondary antibodies were prepared in 5 mL of BSA solution at 3% (w/v) in PBST 1x. The combination of antibodies concentrations used was previously optimised in several attempts for cells of the HepG2 line and are described in **Table 3**.

Following the incubation with secondary antibody, another three washes with PBST 1x with agitation were done. Then the excess volume was discarded, and the membrane was placed in a support for chemiluminescence detection. 2 mL of a mix of Clarity™ Western ECL Substrate (Bio Rad, USA) were added on top of the membrane for a 5 min incubation exposed to air. Then, antibody chemiluminescence was visualized in the LAS-4000 imaging system (Fujifilm Life Science, USA), where sequential exposures of 10 s were done to determine the optimal exposure time. The membrane image was acquired by a precision pulse with the defined time.

The stripping was performed for 5 min with Restore™ PLUS Western Blot Stripping Buffer (Thermo Fisher Scientific, USA) to remove antibodies, and the incubation was repeated with Anti-β-actin (Sigma-Aldrich, USA) for loading control.

Chemiluminescence intensity was quantified in individual bands by ImageJ software (Rasband, 1997). The intensity was expressed as a ratio between the chemiluminescence intensity of each antibody and the chemiluminescence intensity of antibody β-actin from the same membrane.

Table 3- Combination of primary and secondary antibodies concentrations used in membrane incubation for protein detection in western blot.

Primary antibody	Primary antibody concentration	Secondary antibody	Secondary antibody concentration
Anti-C/EBPα	1:1000	Goat anti-rabbit IgG (H+L) peroxidase/HRP conjugated	1:10000
Anti-PRKA-β1	1:500	Goat anti-rabbit IgG (H+L) peroxidase/HRP conjugated	1:5000
Anti-PRKA-β1 (p-Ser-181)	1:1000	Goat anti-rabbit IgG (H+L) peroxidase/HRP conjugated	1:10000
Anti-PPAR γ	1:500	Goat anti-rabbit IgG (H+L) peroxidase/HRP conjugated	1:1000
Anti-ACACα	1:500	Goat anti-rabbit IgG (H+L) peroxidase/HRP conjugated	1:5000
Anti-ACACα (p- Ser-80)	1:2000	Goat anti-rabbit IgG (H+L) peroxidase/HRP conjugated	1:10000
Anti-β-actin	1:4000	Goat anti-mouse IgG (H+L) peroxidase/HRP conjugated	1:25000

3.5 Statistics

All statistical analysis and graph development were performed on GraphPad Prism version 8.0.2 (GraphPad Software, USA).

To determine statistically significant differences between the means of the data, a one-way analysis of variance (ANOVA) was performed. It was necessary to verify if data was distributed according to a Gaussian distribution, and for that, normality was assessed by Kolmogorov-Smirnov normality test (*p*-value<0.05). Simultaneously, all data needed to fulfil the criteria of equal variance, and for that, Bartlett's test (*p*-value<0.05) was used. Data that verified these statistical assumptions were submitted to a one-way ANOVA. If only normality was verified, Brown-Forsythe test and Welch ANOVA test was performed. If none of the statistical assumptions were confirmed, a non-parametric test was used, like Kruskal–Wallis. Analyses were followed by Dunnett's multiple comparisons test. Statistically significant differences were considered with *p*-value < 0.05, and * represented *p*-value < 0.05, ** *p*-value < 0.01, *** *p-value* < 0.001, and **** *p-value* < 0.0001.

Data from bioactivity assays were displayed as box-and-whiskers graphs and data from western blot as column charts, both with error bars representing the standard deviation of the data.

4. Results

4.1 *In vitro* screening of *C. vulgaris* extracts for anti-steatosis activity in HepG2 cell line

4.1.1 Fluorescence quantification optimisation

The intensity of the fluorescence emitted by the Nile red dye was quantified to determine the lipid content in the cells for the anti-steatosis assay, as it stains neutral lipid droplets, while the intensity of the fluorescence emitted by the HO-33342 was quantified as a measure for the cell viability, staining the nucleus. The critical point of the quantification was the optimisation of the fluorescence readings. The first methodology applied was the point fluorescence, which consists of a single beam passing through the centre point of each well, so only one fluorescent measurement was taken. In the second methodology, the area scan, a protocol optimisation was performed for the Cytation 5 Cell Imaging Multi-Mode Reader, where a certain area was scanned by multiple reads. Hence, instead of the output being a single measurement of the centre of the well (**Figure 13a**), it becomes the mean of 13 measurements spread to a larger area (**Figure 13b**). Finally, the third methodology was an imaging approach. 4 images of each well were taken with a 20x objective, stitched, and analysed as 1 image in order to have a cell-by-cell quantification (**Figure 13c**). The output consisted of the quotient between the average intensity emitted by the Nile Red per cytoplasm and the average intensity emitted by the HO-33342 per nucleus, thus giving as a final result the lipid content for each cell in each well. As a result, the total number of measurements in each well is 1 for the fluorescence point, 13 for the area scan, and in the order of hundreds in the imaging method.

a

	1	2	3	4	5	6	7	8	9	10	11	12
A		76067	79924	57042	73046	80515	81684	76669	59084	78923	58263	
B		83876	80950	82204	77667	86294	73122	86286	111367	87302	75252	
C		69401	52408	49704	45253	58397	55320	50334	45767	66724	57713	
D		57612	76814	76151	63394	55254	55387	72972	93634	77341	79335	
E		69359	89622	82200	89424	79882	72336	82352	85437	133862	119416	
F		61364	94295	89033	89900	68120	80621	78766	77432	83489	64853	
G		27441	37231	40240	41206	36937	33082	72414	76289	87536		
H												

b

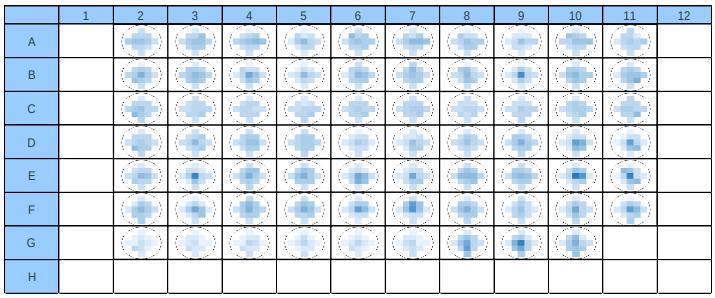

C

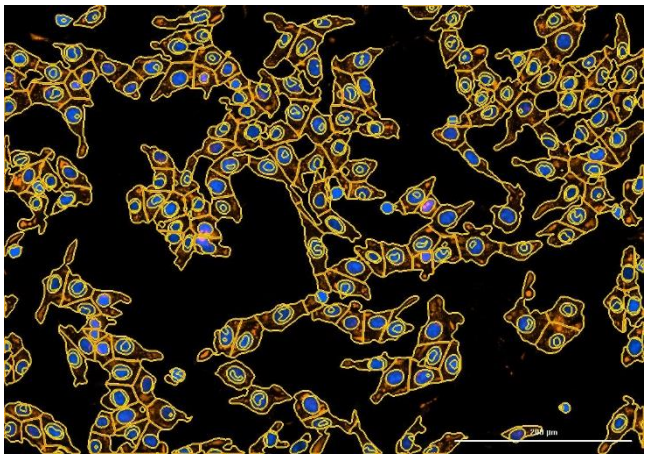

Figure 13 - Output of fluorescence measurements of a 96-well plate setup by the Cytation 5 Cell Imaging Multi-Mode Reader in Gen5™ software for (**a**) point fluorescence; (**b**) area scan; and (**c**) imaging.

4.1.2 Assessment of lipid reduction activity of HPP and ohmic extracts through point fluorescence, area scan and imaging measurements

Plots from **Figure 14** and **Figure16** represent HepG2 lipid content, quantified by the three different approaches after co-exposure with SO and *C. vulgaris* extracts from HPP extraction and ohmic extraction, respectively. It is important to note that the baseline fluorescence of lipid content of the HepG2 cells was around 50%, as it can be assessed from the percentage of Nile red fluorescence in DMSO and DMSO+MeoH controls, compared to the same percentage in DMSO+SO control, that is, fatty acid overloaded

cells to non-treated cells. Thus, the maximum detectable lipid-lowering capacity was 50% in this steatosis assay.

When looking in a generalised way at all the results of fluorescence reading of the HPP extracts (**Figure 14**), the extracts with acetone as solvent showed the most significant results.

In the point fluorescent at 10 µg/mL exposure concentration (**Figure 14a)**, a significant reduction was observed in two of the acetone extracts. Nevertheless, this activity seemed a false positive since it was not verified at the higher exposure concentration, 25 µg/mL (**Figure 14b**). In the area scan plot, this activity of the acetone extracts was confirmed, and even extracts without additional pressure showed significant activity. More interestingly, at the exposure concentration of 25 µg/mL, the pressure applied in the extraction influenced the bioactivity of the extracts (**Figure 14d**). The higher the applied pressure, the more the extracts decreased the lipid content of HepG2 cells. Finally, the most promising activity for acetone extracts was again verified in the imaging approach (**Figure 14e** and **Figure14f**). However, the bioactivity was only observed for extracts with additional pressure, while acetone extracts without it were not active.

Overall, the area scan and the imaging showed consistent results at 25 µg/mL exposure for HPP extracts, and in particular the strongest effects at higher pressures, 420 and 300 MPa. In both approaches, CS11 extracted by acetone at 420 MPa for 9 min, CS22, an extract extracted by acetone at 300 MPa for 8 min, and CS35, extracted by acetone at 100 MPa for 8 min, had the most significant bioactivity. These results are shown by the images obtained by Cytation 5 Cell Imaging Multi-Mode Reader (**Figure 15**). The lipid fluorescent intensity in DMSO+SO control (**Figure 15b**) and in the cells exposed to CS16 (**Figure 15f**), a non-active extract, was higher when compared to lipid fluorescent intensity of cells exposed to CS11 (**Figure 15c**), CS22 (**Figure 15d**) and CS35 (**Figure 15e**) extracts. This can be assessed by the accumulation of lipid droplets in cell cytoplasm noticeable in the images by the reddish orange dots stained by Nile red.

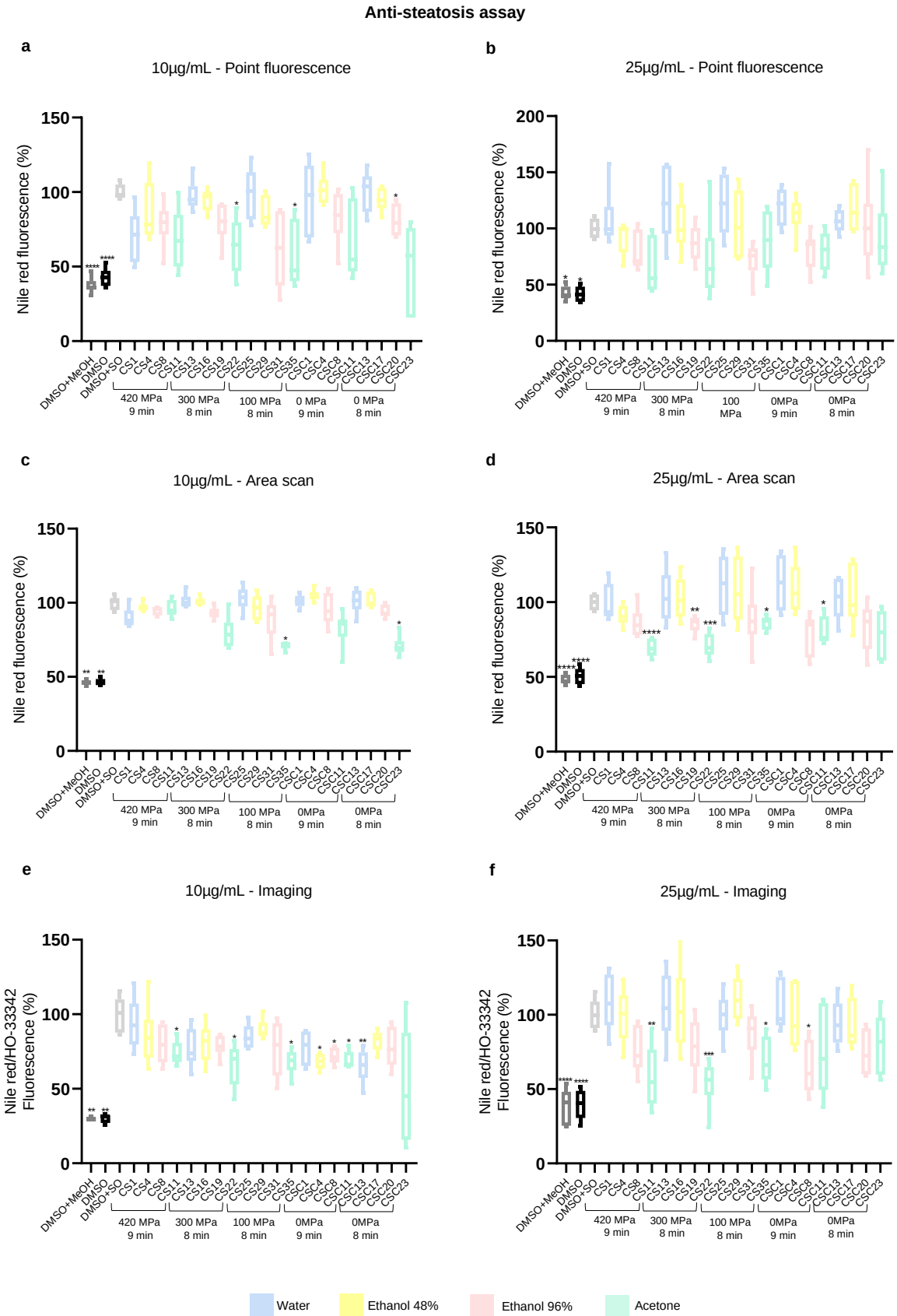

Figure 14 – Anti-steatosis activity after co-exposure with SO and *C. vulgaris* extracts from HPP extraction in HepG2 cells. Left side (**a**, **c**, **e**) refers to a 10 µg/mL exposure, and right side (**b**, **d**, **f**) refers to a 25 µg/mL exposure: (**a** and **b**) Nile red fluorescence quantification results by point fluorescence expressed as a percentage; (**c** and **d**) Nile red

fluorescence quantification results by area scan expressed as a percentage; (**e** and **f**) Nile red and HO-33342 fluorescence quantification ratio results by imaging expressed as a percentage. CS1-CS11 designates 420 MPa for 9 min extraction; CS13-CS22 designates 300 MPa for 8 min extraction; CS25-CS35 designates 100 MPa for 8 min extraction; CSC1-CSC11 designates control extraction for 9 min without pressure; CSC13-CSC23 designates control extraction for 8 min without pressure. Blue represents water as extraction solvent; yellow represents ethanol 48% as extraction solvent; pink represents ethanol 96% as extraction solvent; green represents acetone as extraction solvent. Dark grey represents DMSO+MeOH control; black represents DMSO control; light grey represents DMSO+SO control. The data have been derived from two independent assays and shown as box-and-whisker plots (5–95 percentiles). Statistical differences compared to DMSO+SO control are indicated by asterisks. Asterisks highlight significant altered fluorescence percentage, indicating lipid-reduction activity (****=*p*-value ≤ 0.0001; *** = *p-value* ≤ 0.001; ** = *p-value* ≤ 0.01; * = *p-value* ≤ 0.05).

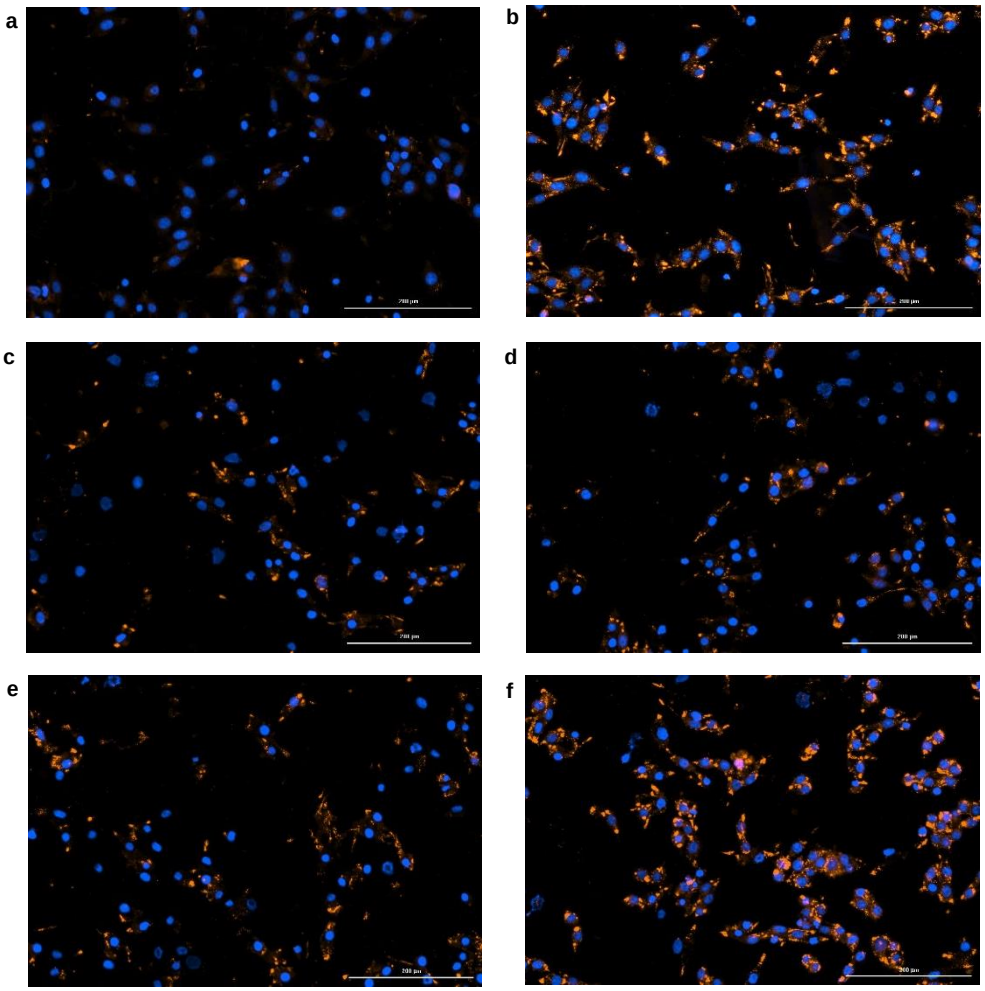

Figure 15 - Representative stitched, prepossessed, deconvoluted images of anti-steatosis assay with HepG2 cell line co-exposed to SO and 25 µg/mL of HPP extracts. Images were obtained by automated microscopy fluorescence by Cytation 5 through RFP and DAPI channels and analysed in Gen5™ software. (**a**) DMSO control; (**b**) DMSO+SO control; (**c, d, e**) Images of HepG2 cell line exposed to extracts that showed significant lipid-reduction activity in both area scan and imaging analyses; (**c**) HepG2 cell line exposed to CS11 extract; (**d**) HepG2 cell line exposed to CS22 extract; (**e**) HepG2 cell line exposed to CS35 extract; (**f**) Representative image of a HepG2 cell line expose to an extract that exerted no lipid-reduction activity (CS16).

In turn, the results of the anti-steatosis assay of ohmic extracts did not show as much bioactivity as the HPP extracts. The lipid reduction in the anti-steatosis assay was only significant for extracts D31 and D41 at 25µg/mL exposure measured by the imaging approach, however, bioactivity was low (**Figure 16f**).

4.1.3 Evaluation of cytotoxicity of HPP and ohmic extracts

The steatosis assay was followed by the assessment of cytotoxicity by two distinct approaches. The first was directly evaluated by the quantification of fluorescence emitted by HO-33342 that stained the nucleus. The second measure was the SRB assay, a widely used method for *in vitro* cytotoxicity screening. None of the extracts exhibited toxic effects on the cells, as assessed by cell viability percentage in **Figure17** and **Supplementary Figure 1**. Moreover, cell viability was verified to be around 100% for all HPP and ohmic extracts for both cytotoxicity evaluation methods and exposure concentrations.

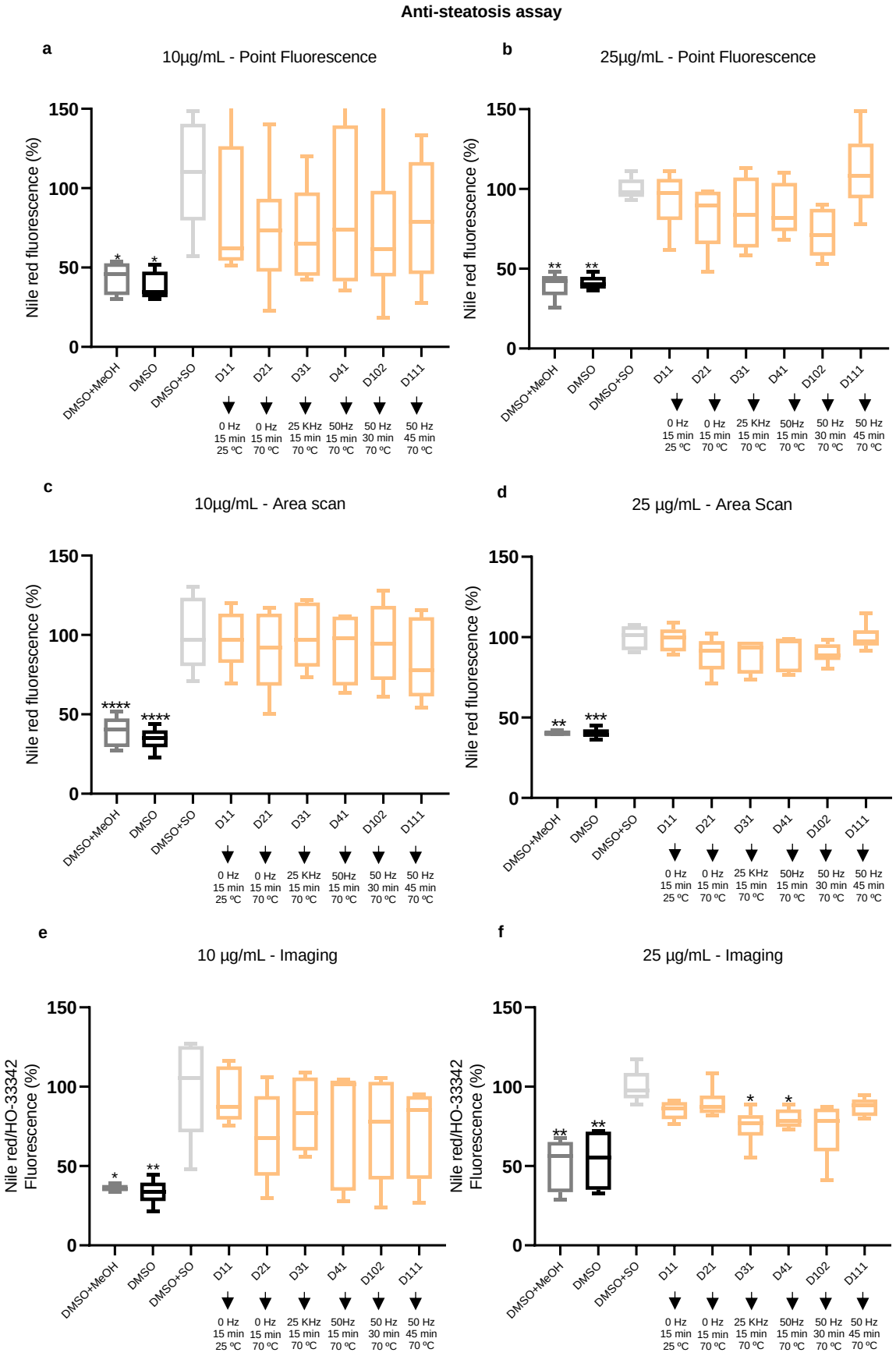

Figure 16 - Anti-steatosis activity after co-exposure with SO and *C. vulgaris* extracts from ohmic extraction in HepG2 cells. Left side (**a**, **c**, **e**) refers to a 10 µg/mL exposure and right side (**b**, **d**, **f**) refers to a 25 µg/mL exposure: (**a** and **b**) Nile red

fluorescence quantification results by point fluorescence expressed as a percentage; (**c** and **d**) Nile red fluorescence quantification results by area scan expressed as a percentage; (**e** and **f**) Nile red and HO-33342 fluorescence quantification ratio results by imaging expressed as a percentage. D11 designates control extraction for 15 min at 25 ºC without frequency; D21 designates control extraction for 15 min at 70 ºC without frequency; D31 designates 25 KHz extraction for 15 min at 70 ºC; D41 designates 50 Hz extraction for 15 min at 70 ºC; D102 designates 50 Hz extraction for 30 min at 70 ºC; D111 designates 50 Hz extraction for 45 min at 70 ºC. Dark grey represents DMSO+MeOH control; black represents DMSO control; light grey represents DMSO+SO control. The data have been derived from two independent assays and shown as box-and-whisker plots (5–95 percentiles). Statistical differences compared to DMSO+SO control are indicated by asterisks. Asterisks highlight significant altered fluorescence percentage, indicating lipid-reduction activity (****=*p-value* ≤ 0.0001; *** = *p-value* ≤ 0.001; ** = *p-value* ≤ 0.01; * = *p-value* ≤ 0.05).

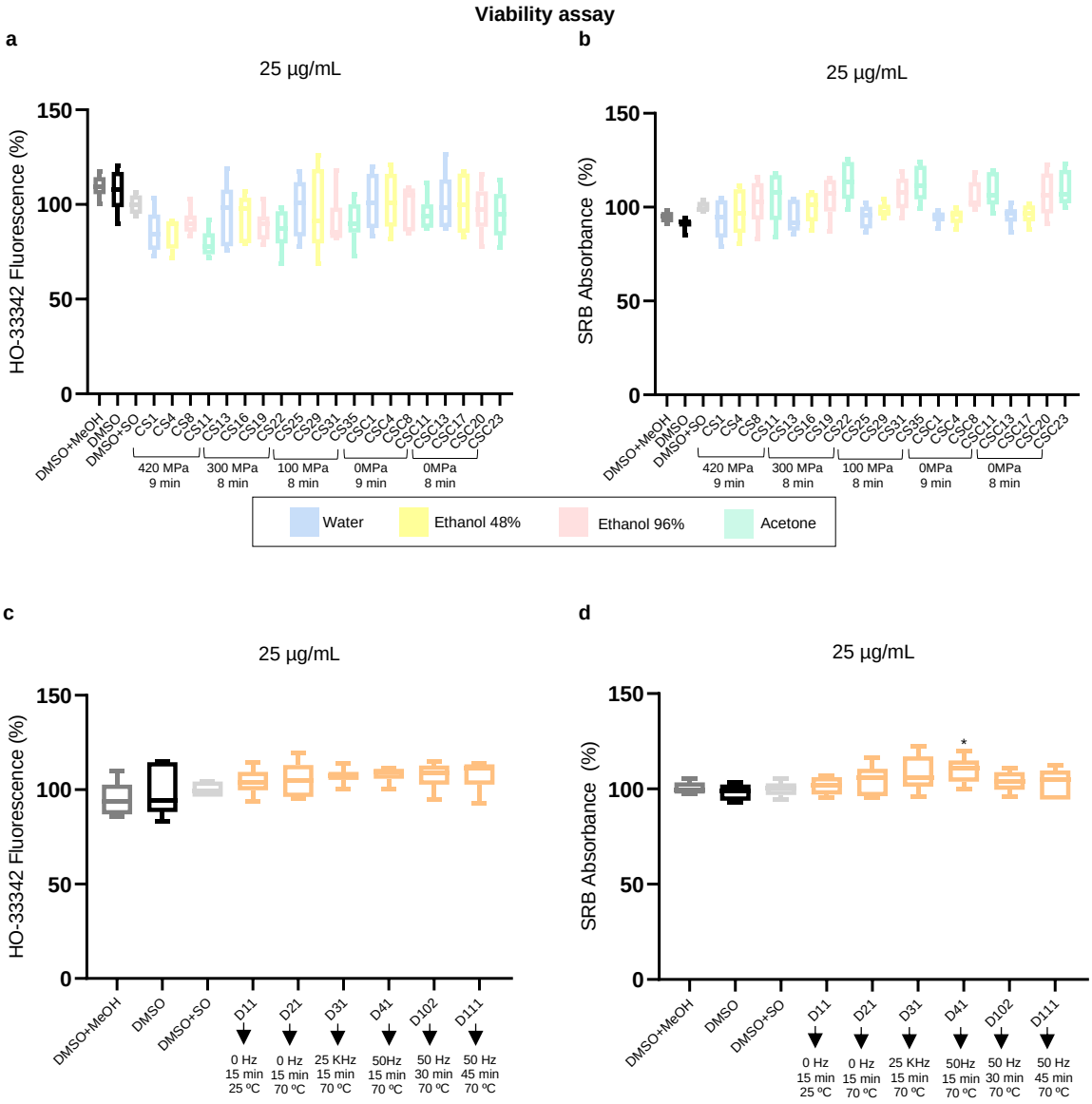

Figure 17 - HepG2 cell viability for anti-steatosis assay assessed by (**a** and **c**) HO-33342 fluorescence reading and (**b** and **d**) SRB method. (**a** and **b**) refer to 25 µg/mL exposure to HPP extracts. (**c** and **d**) refer to 25 µg/mL exposure to ohmic extracts. Dark grey represents DMSO+MeOH control; black represents DMSO control; light grey represents DMSO+SO control. The data have been derived from two independent assays and shown as box-and-whisker plots (5–95 percentiles) as percentage considering 100% the DMSO+SO control. Statistical differences compared to DMSO+SO control are indicated by asterisks (* = p-value ≤ 0.05).

4.2 *In vitro* screening of *C. vulgaris* extracts for pro- and anti-inflammatory activity in Raw464.7 cell line

4.2.1 Pro-inflammatory assay with HPP and ohmic extracts

Results from RAW264.7 exposed only to *C. vulgaris* extracts allowed to demonstrate that the extracts by themselves did not cause inflammation in the cells. This pro-inflammatory result was true for both extraction methodologies, HPP (**Figure18a** and **Figure18b**) and ohmic (**Figure18c** and **Figure18d**) extracts, and for both exposure concentration, 10 µg/mL and 25 µg/mL, since none of the extracts caused an increase in the percentage of nitrites compared to DMSO control.

4.2.2 Anti-inflammatory assay with HPP and ohmic extracts

This model consisted in evaluating the ability of *C. vulgaris* extracts to reduce the LPS-induced inflammation in RAW264.7 cells. For HPP extracts, the observed reduction pattern was quite interesting. Even at the lowest exposure concentration, at 10 µg/mL (**Figure 19a**), it was possible to notice that the extracts with water or 48% ethanol had no effect. In some cases, there was even a slight increase in induced inflammation compared to the DMSO control. In contrast, in the exposure with the extracts with 96% ethanol and acetone, a significant decrease was observed in the inflammation (*p-value* ≤ 0.01). In the higher exposure concentration of 25 µg/mL, this pattern only became even more significant (**Figure 19b**). The decrease in nitrites percentage, as an estimate of nitrite oxide production, reached values very close to the DMSO control, especially in those with 96% ethanol as solvent. It is important to note that extraction with pressure did not modulate the anti-inflammatory activity, which was observed in the ethanol and acetone extracts alone.

On the opposite, the results obtained with the ohmic extracts did not show promising anti-inflammatory results. D21, D41 and D102 only showed a significant reduction in lower exposure concentration (**Figure 19c**), but the results were not confirmed with increasing exposure to 25 µg/mL (**Figure 19d**).

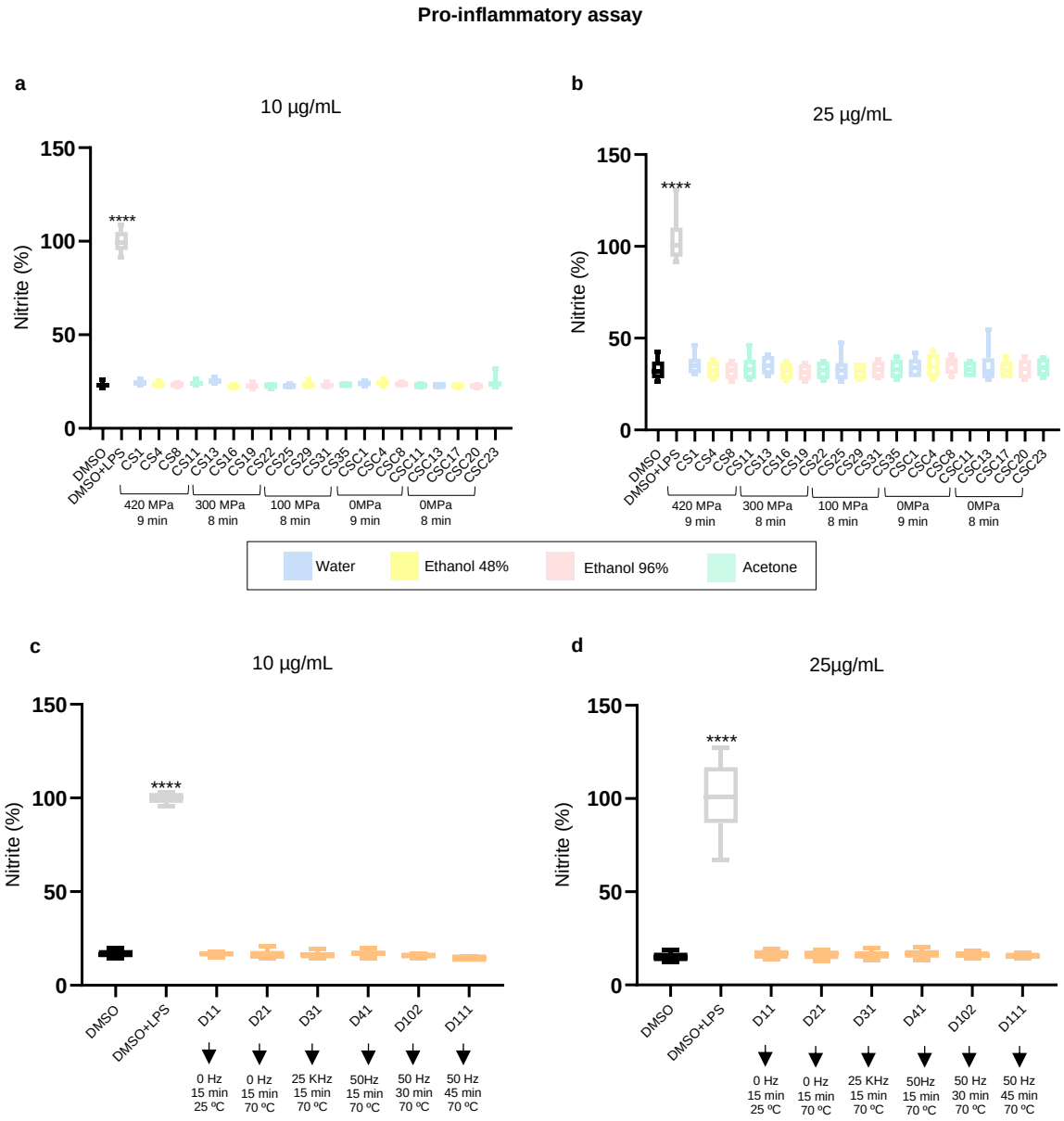

Figure 18 - Pro-inflammatory assay in RAW264.7 cell line exposed to (**a**) 10 µg/mL HPP extracts; (**b**) 25 µg/mL HPP extracts; (**c**) 10 µg/mL ohmic extracts; (**d**) 25 µg/mL ohmic extracts. Black represents DMSO control; grey represents DMSO+LPS control. The data have been derived from two independent assays and shown as box-and-whisker plots (5–95 percentiles). Statistical differences compared to DMSO control are indicated by asterisks. Asterisks highlight significant altered nitrite percentage content, indicating pro-inflammation (****=*p*-value ≤ 0.0001).

4.2.3 Evaluation of HPP and ohmic extracts cytotoxicity

Pro- and anti-inflammatory assays were followed by the MTT cell viability assay to ensure that the extracts had no cytotoxic effects in RAW264.7 cells. Cell viability results of the 25 µg/mL exposure to HPP extracts are shown in **Figure 20a** for pro-inflammatory assay and **Figure 20b** for anti-inflammatory assay. The 25 µg/mL exposure

to ohmic extracts are shown in **Figure 20c** for pro-inflammatory assay and **Figure 20d** for anti-inflammatory assay. The results of lower concentration exposure are shown in **Supplementary Figure 2**. Cell viability was not affected by exposure to any of the extracts, HPP or ohmic, in both exposure concentrations.

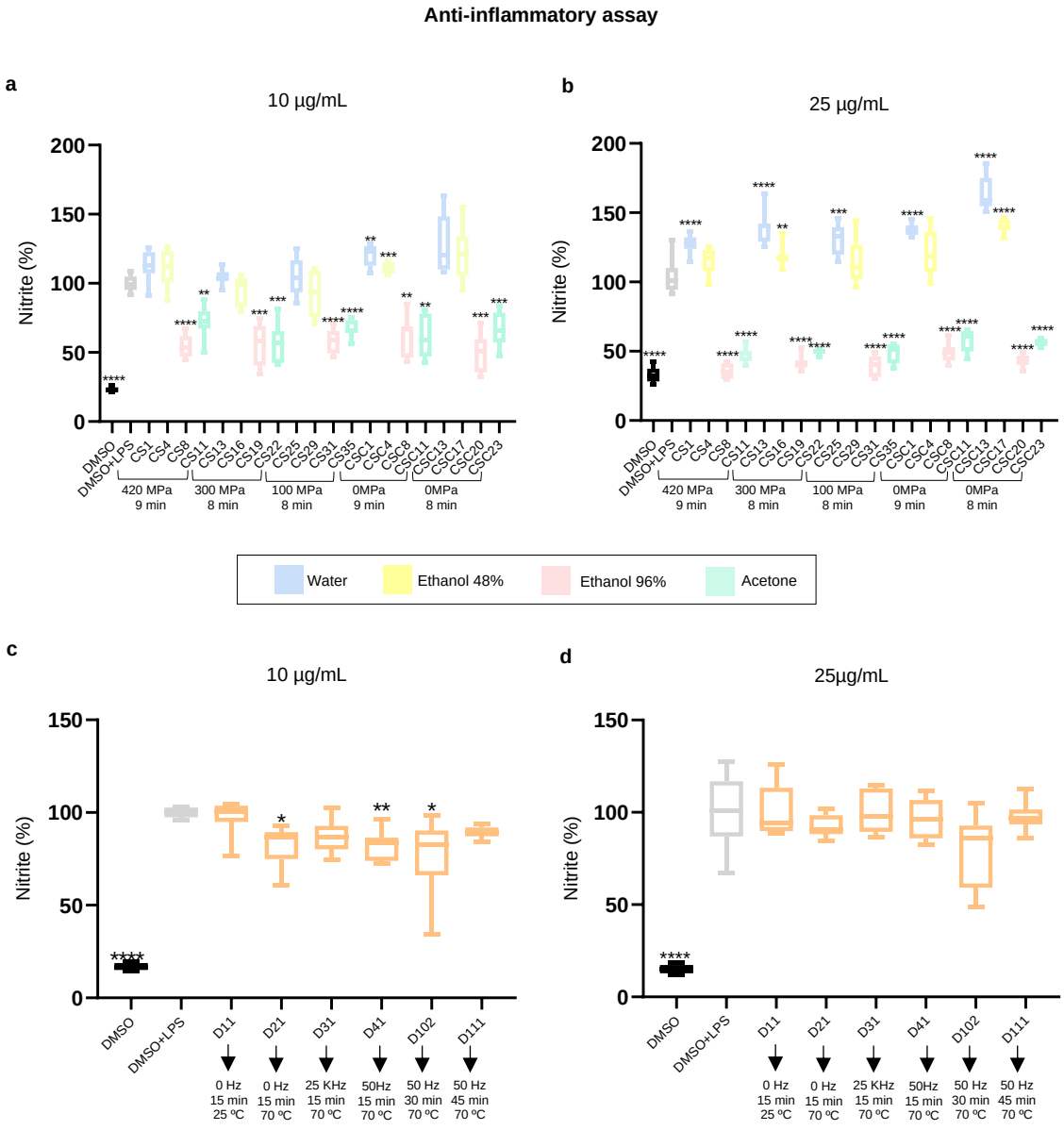

Figure 19 - Anti-inflammatory assay in RAW264.7 cell line exposed to LPS and (**a**) 10 µg/mL HPP extracts; (**b**) 25 µg/mL HPP extracts; (**c**) 10 µg/mL ohmic extracts; (**d**) 25 µg/mL ohmic extracts. Black represents DMSO control; grey represents DMSO+LPS control. The data have been derived from two independent assays and shown as box-and-whisker plots (5–95 percentiles). Statistical differences compared to DMSO+LPS control are indicated by asterisks. Asterisks highlight significant altered nitrite percentage content, indicating change in inflammation level (****=*p-value* ≤ 0.0001; *** = *p-value* ≤ 0.001; ** = *p-value* ≤ 0.01; * = *p-value* ≤ 0.05).

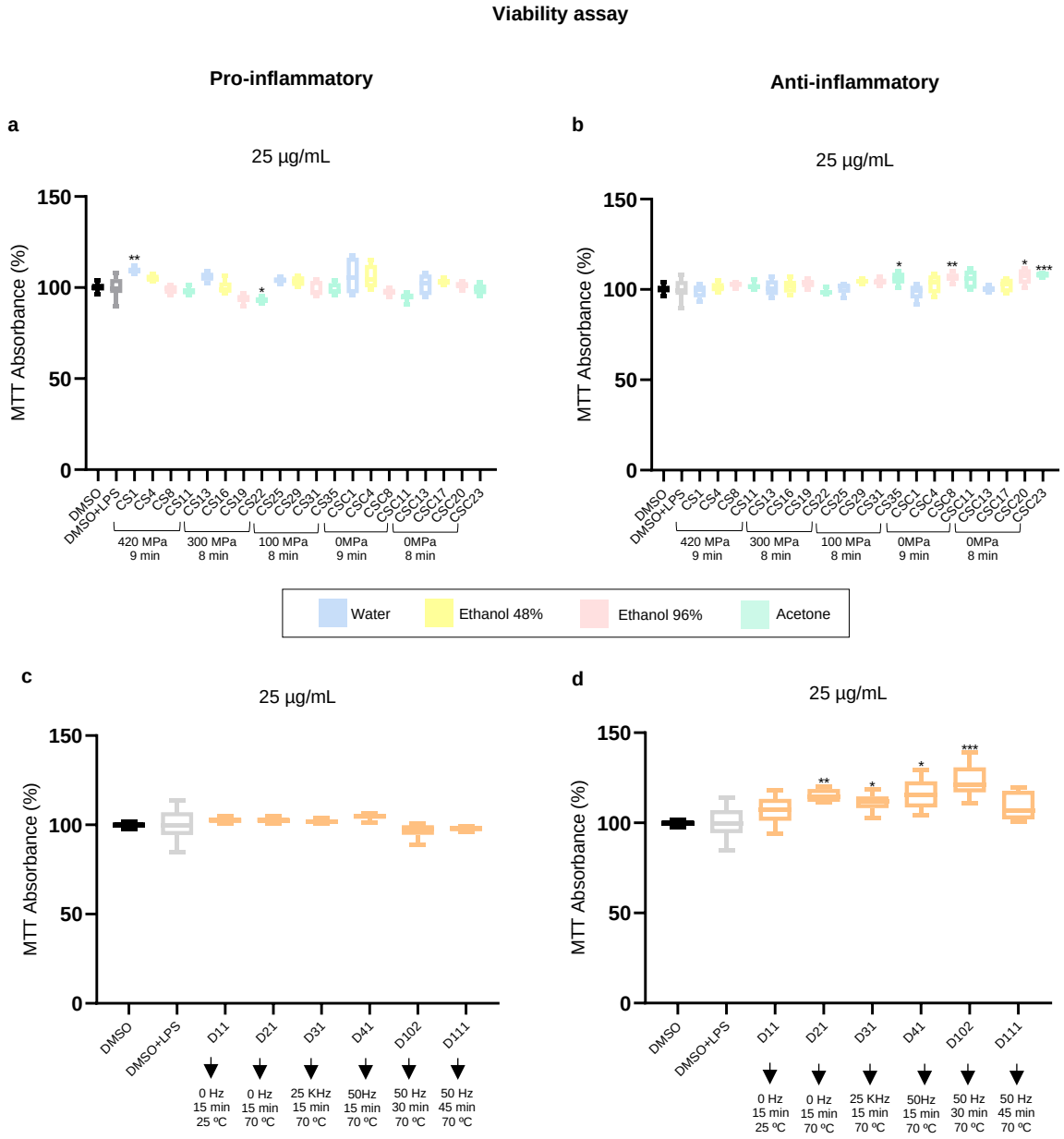

Figure 20 - Cell viability MTT assay in RAW264.7 cell line of (**a**) pro-inflammatory assay with HPP extracts 25 µg/mL exposure; (**b**) anti-inflammatory assay with HPP extracts 25 µg/mL exposure; (**c**) pro-inflammatory assay with ohmic extracts 25 µg/mL exposure; (**d**) anti-inflammatory assay with ohmic extracts 25 µg/mL exposure. Black represents DMSO control; grey represents DMSO+LPS control. The data have been derived from two independent assays and shown as box-and-whisker plots (5–95 percentiles) as percentage considering 100% the DMSO control. Statistical differences compared to DMSO+LPS control are indicated by asterisks (*** = *p-value* ≤ 0.001; ** = *p-value* ≤ 0.01; * = *p-value* ≤ 0.05).

As explained above in the materials and methods section, both inflammatory and MTT cell viability assays had colorimetric properties, shown in **Figure 21**. Released nitrites together with the Griess reagent formed a final red azo dye. A more yellowish colour reflects a lower inflammatory state (**Figure 21a)** that was visible in pro-inflammatory assay lines in the 96-well plate and also in some wells of the anti-inflammatory assay in which cells were exposed to extracts that reduced inflammation, like CS8, CS11, CS19 or CS22, for example. Moreover, MTT has a yellow colour in its original form, whereas purple represents its conversion into formazan salts by living cells, which reflects higher cell viability, verified for all extracts (**Figure 21b**).

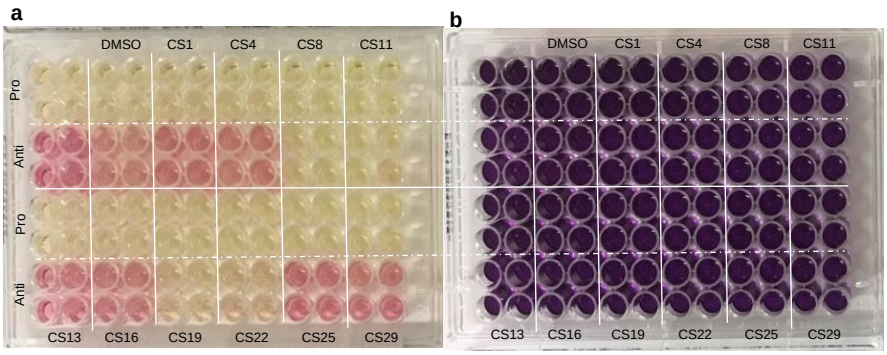

Figure 21 - Representative images of pro- and anti-inflammatory assay in a 96-well plate. (**a**) Lines A, B, E and F with RAW264.7 cell line exposed to *C. vulgaris* extracts for pro-inflammatory assay, and lines C, D, G and H exposed to *C. vulgaris* extracts and LPS for anti-inflammatory assay (**b**) MTT cell viability assay.

4.3 *In vivo* screening of *C. vulgaris* extracts for anti-obesity activity in zebrafish larvae

The anti-obesity assay in zebrafish showed more significant lipid reduction activity for extracts with lower pressures or without any pressure for the HPP extracts (**Figure 22a**). The extraction at 420 MPa, the highest pressure used, led to the absence of activity in all extracts. In contrast, extracts with 48% ethanol (CSC4 and CSC17) and acetone (CSC11 and CSC23) as a solvent without pressure, demonstrated significant lipid reduction activity. Moreover, acetone extracts proved to be the most consistent. Those extracted at 300 MPa and 100 MPa, CS22 and CS35, respectively, significantly lowered the lipid content in the zebrafish larvae, (*p-value* ≤ 0.0001). Thus, the use of acetone revealed bioactivity, which, however, seemed affected by high pressure.

These activity differences are shown by the fluorescence images of the zebrafish exposed to HPP extracts (**Figure 23**). Fluorescence emitted by the Nile Red in the zebrafish larvae exposed to CS22 (**Figure 23f**) and CSC4 (**Figure 23h**) was almost imperceptible and very similar to the REV control (**Figure 23d**) used to inhibit lipid production. In contrast, CS16 (**Figure 23j**), also extracted with 48% ethanol as a solvent like CSC4, but at 300 MPa, showed a robust fluorescence emitted by the Nile red, almost as the emitted in DMSO control (**Figure 23b**).

In contrast, the ohmic extracts did not show significant reducing activity in anti-obesity assays with zebrafish larvae (**Figure 22b**). All extracts were evaluated for toxicity by lethality or malformations in zebrafish larvae, which were not verified.

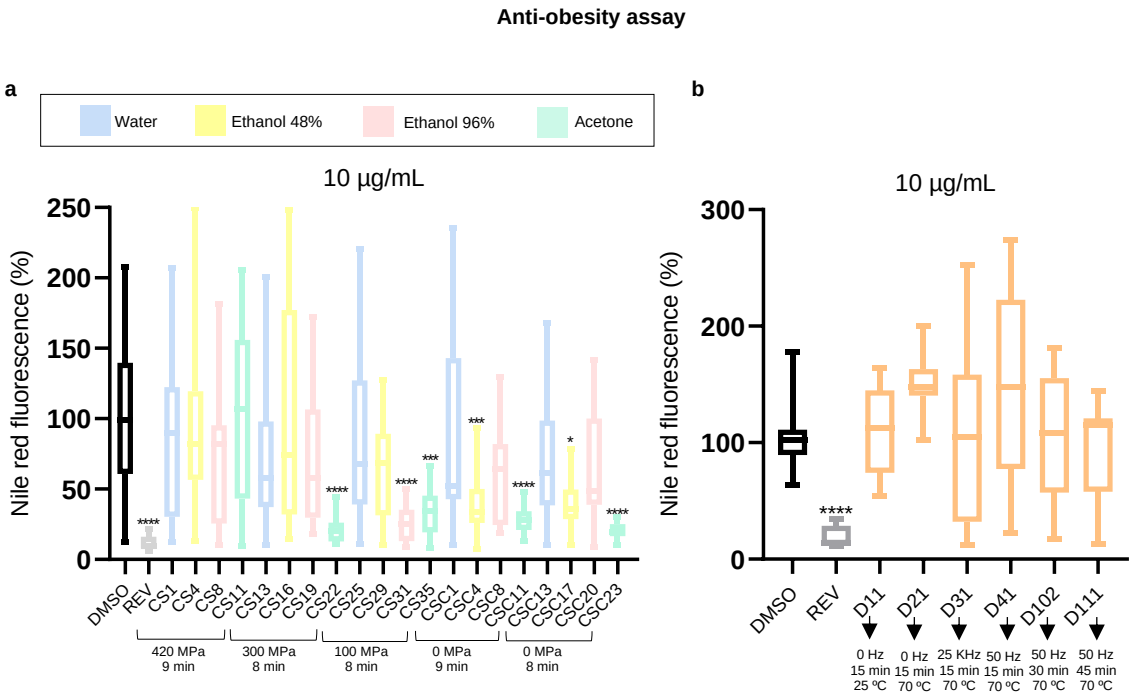

Figure 22 - Anti-obesity assay in zebrafish larvae stained with Nile red and exposed to 10 µg/mL of (**a**) HPP extracts; (**b**) ohmic extracts. Black represents DMSO control; grey represents REV control. The data have been derived from three independent assays and shown as box-and-whisker plots (5–95 percentiles). Statistical differences compared to DMSO control are indicated by asterisks. Asterisks highlight significant altered Nile red fluorescence percentage, indicating change in lipid content (**** = *p-value* ≤ 0.0001; *** = *p-value* ≤ 0.001; ** = *p-value* ≤ 0.01; * = *p-value* ≤ 0.05).

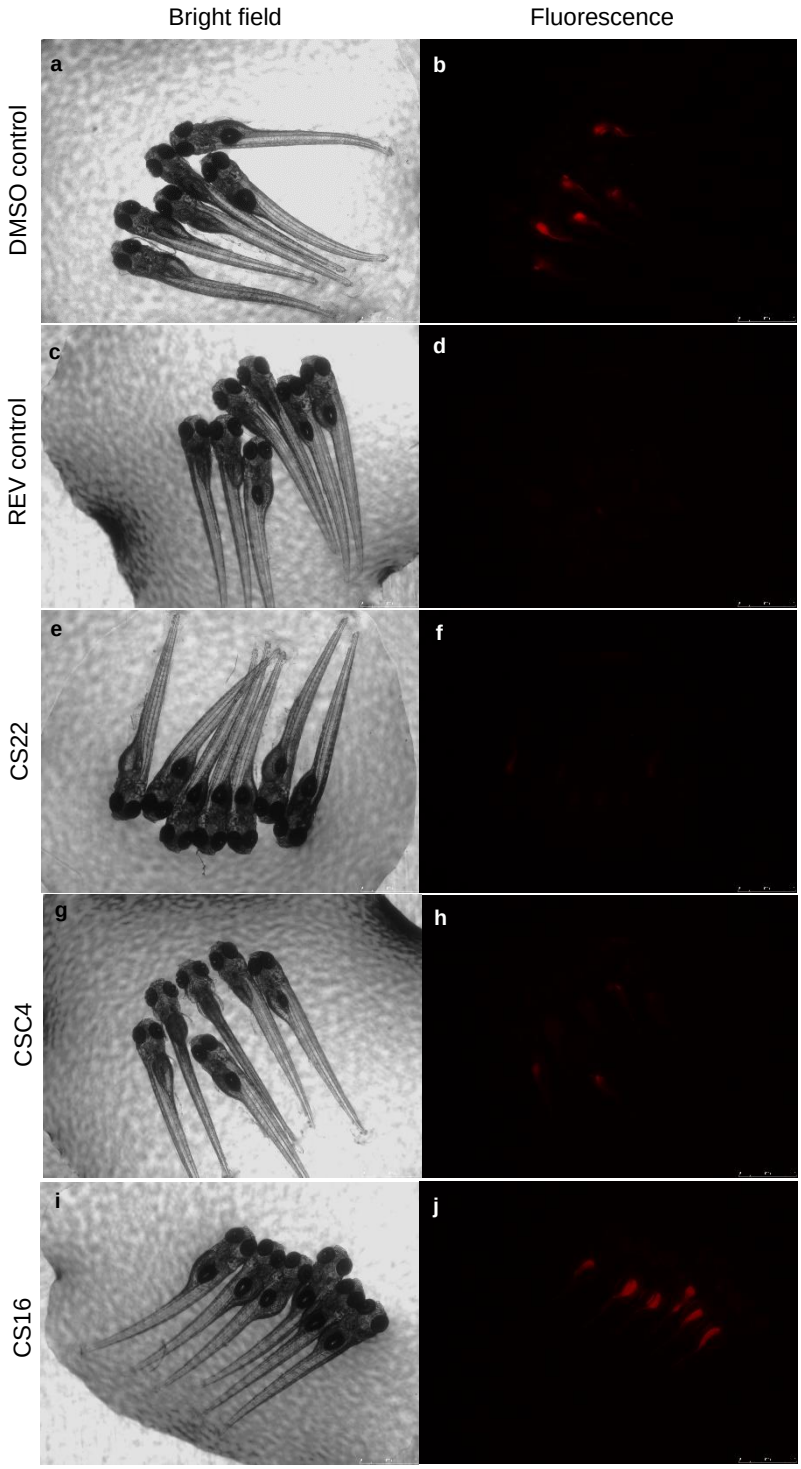

Figure 23 – Representative fluorescent images from the anti-obesity assay in zebrafish larvae exposed to 10 µg/mL of HPP extracts and Nile red to stain the lipids. (**a**) bright field image of DMSO control; (**b**) fluorescent image of DMSO control; (**c**) bright field image of REV control; (**d**) fluorescent image of REV control; (**e**) bright field image of CS22 exposure; (**f**) fluorescent image of CS22 exposure; (**g**) bright field image of CSC4 exposure; (**h**) fluorescent image of CSC4 exposure; (**i**) bright field image of CS16 exposure; (**j**) fluorescent image of CS16 exposure. (**f** and **h**) represent extracts with anti-obesogenic activity, able to decrease the fluorescence of the Nile red. (**j**) represents extracts without anti-obesogenic activity, unable to reduce Nile red fluorescence.

4.4 *In vivo* screening of *C. vulgaris* extracts for anti-diabetes activity in zebrafish larvae

The anti-diabetic effects of the extracts were evaluated by exposing zebrafish larvae to 10 µg/mL of extracts followed by fluorescent-tagged glucose probe 2-NBDG for

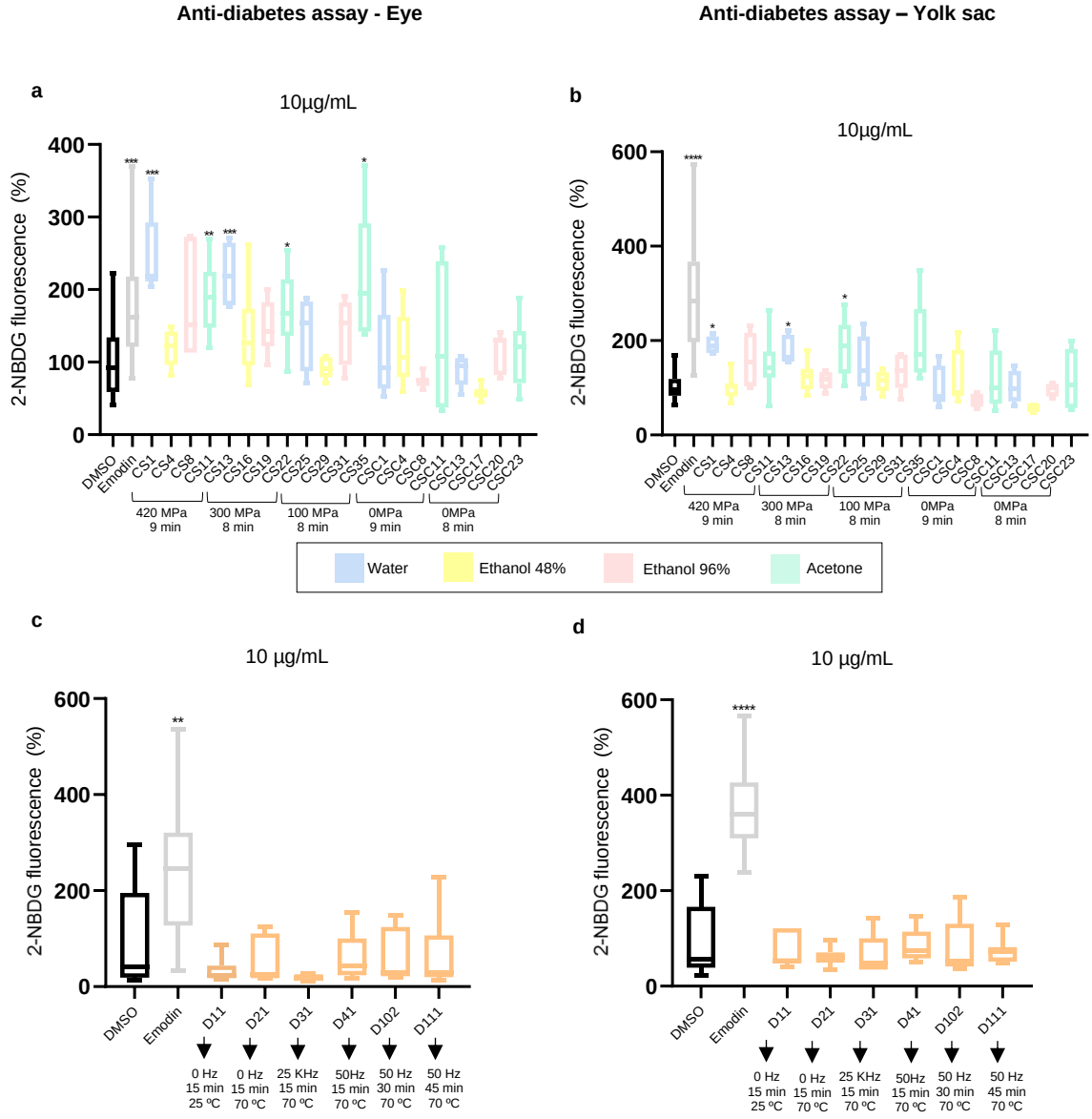

Figure 24 - Anti-diabetes assay in zebrafish larvae exposed 10 µg/mL of (**a** and **b**) HPP extracts; (**c** and **d**) ohmic extracts. (**a** and **c**) Represent 2-NBDG quantification in the eye; (**b** and **d) r**epresent 2-NBDG quantification in the yolk sac. Black represents DMSO control; grey represents emodin control. The data have been derived from two independent assays (n=8-10) and shown as box-and-whisker plots (5–95 percentiles). Statistical differences compared to DMSO control are indicated by asterisks. Asterisks highlight significant altered 2-NBDG fluorescence percentage, indicating change in glucose uptake (****=*p-value* ≤ 0.0001; *** = *p-value* ≤ 0.001; ** = *p-value* ≤ 0.01; * = *p-value* ≤ 0.05).

measurement of spatiotemporal glucose flux in the eye and yolk sac. HPP extractions (**Figure 24a** and **Figure 24b**) revealed significant activity for water extracts CS1 (420 MPa) and CS13 (300 MPa), consistent in eye and yolk sac measurements. However, such activity was not present in other pressure extractions with water or by water extraction alone. Also, for acetone extracts CS11 (420 MPa), CS22 (300 MPa) and CS35 (100 MPa) in the eye, an increased glucose uptake was observed, not present in acetone extractions without pressure. The fluorescent images allowed to visualise that the fluorescence emitted by 2-NBDG in CS22 (**Figure 25f**) and CS13 (**Figure25h**) exposures was somewhere between the DMSO control (**Figure 25b**) and the positive control emodin (**Figure 25d**), a compound known to increase glucose uptake. These two extracts exhibited significant activities in both eye and yolk sac, contrary to **Figure 22h**, that represented the non-active extracts in the anti-diabetes assay. The zebrafish exposed to extracts with no anti-diabetic effects, like CS29, had a very low fluorescence emission.

For ohmic extraction (**Figure24c** and **Figure 24d**), no significant results were obtained.

The extracts were evaluated for toxicity by lethality or malformations in zebrafish larvae, which were not verified.

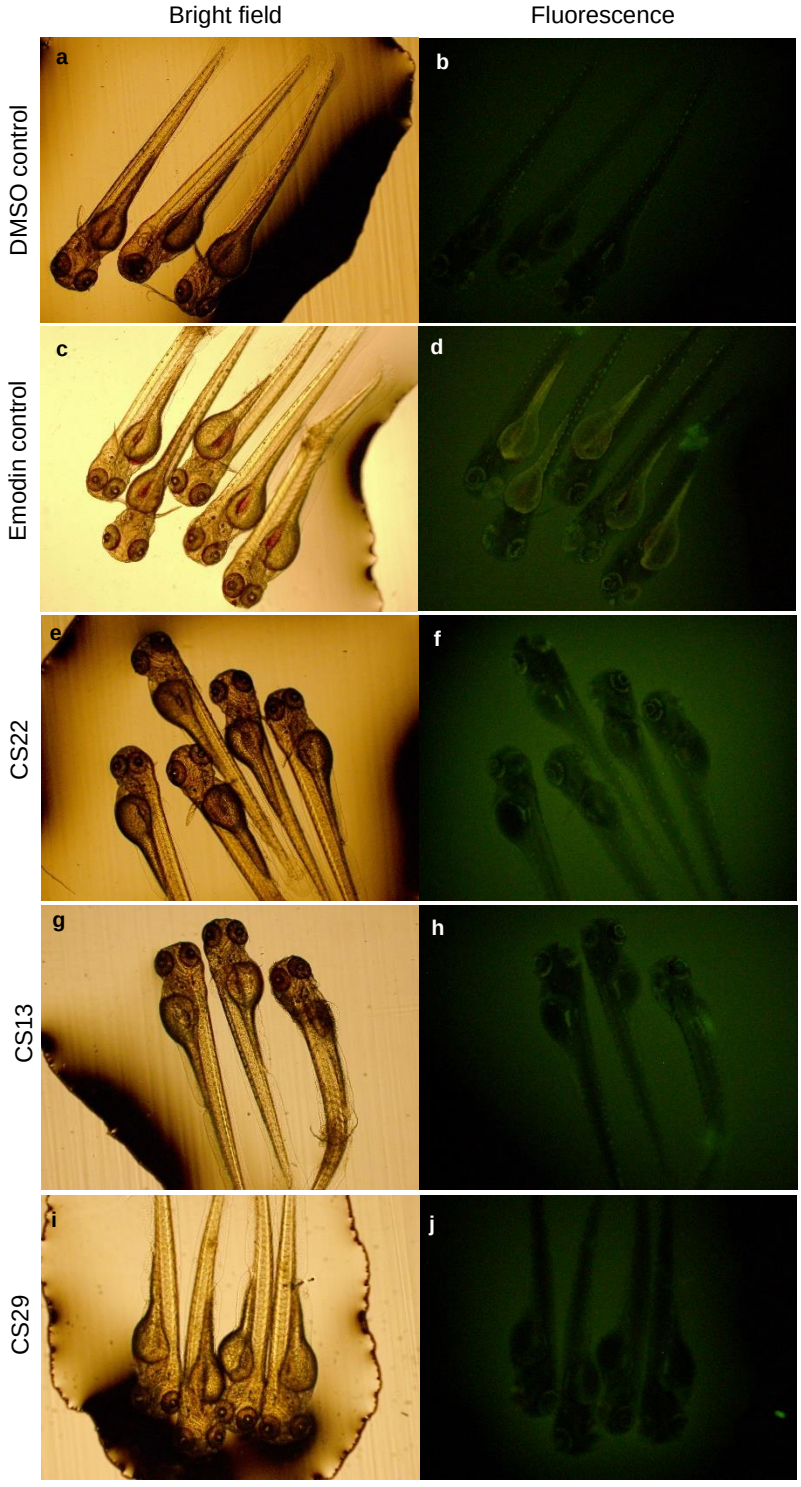

Figure 25 - Representative fluorescent images from the anti-diabetes assay in zebrafish larvae exposed to 10 µg/mL of HPP extracts and fluorescent-tagged glucose probe 2-NBDG for measurement of glucose flux. (**a**) bright field image of DMSO control; (**b**) fluorescent image of DMSO control; (**c**) bright field image of emodin control; (**d**) fluorescent image of emodin control; (**e**) bright field image of CS22 exposure; (**f**) fluorescent image of CS22 exposure; (**g**) bright field image of CS13 exposure; (**h**) fluorescent image of CS13 exposure; (**i**) bright field image of CS29 exposure; (**j**) fluorescent image of CS29 exposure. (**f** and **h**) represent extracts with anti-diabetic activity, able to increase the fluorescence emitted by 2-NBDG. (**j**) represents extracts without anti-diabetic activity, unable the fluorescence emitted by 2-NBDG.

4.5 Metabolite profiling

The acetone extracts were chosen for the bioactivity-based molecular networking of the LC-MS/MS data, based on their anti-steatosis activity. Those extracted at high pressures (CS11, CS22 and CS35) showed a very significant lipid-lowering activity, contrary to those extracted without pressure (CSC11 and CSC23), which did not significantly reduce the lipid content of the cells, based on the quantitative imaging approach on cells. The molecular network (**Figure 26**) enabled the visualization of the metabolites present in each extract by different colours, their precursor mass, and putative identifications. The comparison of metabolites in active or non-active extracts identified 33 nodes in clusters, which were unique to active extracts. Only 2 of these 33 nodes had already an identification by the GNPS database. Further tools were used for mass peak identifications, including the Dereplicator, the Dereplicator+ and the MoINetEnhancer, all included in the GNPS platform. For the ones that remained unidentified after the application of GNPS tools, another search was conducted in two public mass spectrometry databases: NPA and DNP. All 12 putative identifications are shown in **Table 4**.

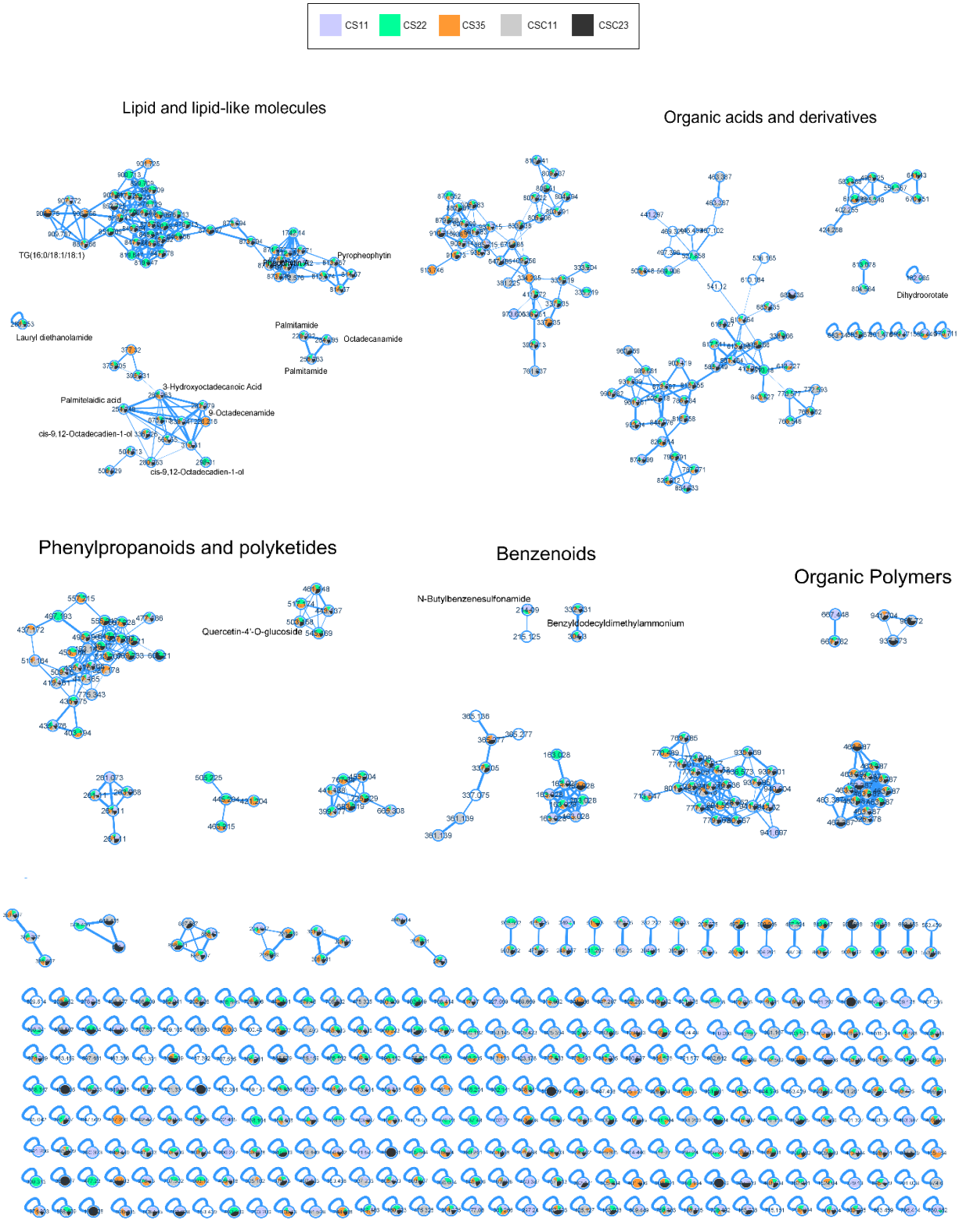

Figure 26 - Bioactivity-guided molecular network using LC-MS/MS and bioactivity data. The pie chart within the nodes illustrates the distribution of each mass peak of the six chosen *C. vulgaris* extracts, with its corresponding colour: purple represents CS11; green represents CS22; orange represents CS35; grey represents CSC11; black represents CSC23; and precursor mass indicated in the middle. In addition, some GNPS identified compounds are shown on the clusters. The network was an output of Cytoscape software.

Table 4 - Putative identification of unique compounds in active extracts from anti-steatosis assay through GNPS tools, DNP, and NPA. Identifications were based on the MS2 fragmentation on GNPS and on m/z values +/− 0.002 against the databases DNP and NPA. Possible matches were only considered if the calculated mass error was lower than 5 ppm. 12 out of 33 compounds present in the active extracts in anti-steatosis had a putative identification in database. H, hydrogen; ppm, parts per million.

Percursor mass	Percursor mass - H	Retention time Mean	Acurate mass in database	Calculation of ppm	Compound Name	Superclass	Database	Shared picks
441.297	440.28917	761.9892	440.288	1.2	N^2-(15,16-Dihydroxy-9,12-octadecadienoyl)glutamine	Organic acids and derivatives	DNP	
871.572		900.4600	871.572		Pheophytin A	Tetrapyrroles and derivatives	GNPS	11
913.746		897.9360	913.746		TG(20:2n6/18:4(6Z,9Z,12Z,15Z)/20:4(8Z,11Z,14Z,17Z))	Lipids and lipid-like molecules	DereplicatorPlus	
973.606		738.9555	973.606		Mycosubtilin B	Lipopeptide	Dereplicator	
497.193	496.18517	338.0935	496.184	1.2	Pumiloside Derivative: 7-Deoxy or 7-Deoxy, 3-epimer	Alkaloids and derivatives	DNP	
			496.186	-2.4	Punaglandin 3 **OR** 7Z-Isomer-Punaglandin 3	Alkaloids and derivatives		
			496.184	1.2	Correantoside Derivative: 5,6-Didehydro, N-de-Me	Alkaloids and derivatives		
453.186	452.17817	299.8028	452.179	-2.9	Nα-Glutamylaspartic acid; Derivate: L-L-form, N-Benzyloxycarbonyl, Asp-di-Et ester	Organic acids and derivatives	DNP	
557.215	556.20717	329.37573	556.205	2.6	Macrolidine	Alkaloids and derivatives	DNP	
			556.207	-0.6	Punaglandin 1	Lipids and lipid-like molecules		
			556.205	2.6	Strictosidinic acid; Derivate: 5-Oxo, 3,6-didehydro, N4-Me, Me ester	Alkaloids and derivatives		
403.194	402.18617	258.2643	402.186	- 0.2	Ambiguine G nitrile	Alkaloids and derivatives	DNP	
804.567		792.9667	804.568		Tolybyssidin A	Organic acids and derivatives	Dereplicator	
941.697		793.0630	941.704		TG(18:3(6Z,9Z,12Z)/20:2n6/20:4(8Z,11Z,14Z,17Z))	Lipids and lipid-like molecules	Dereplicator Plus	
377.32	376.31217	730.6500	376.313	-2.2	Ergosta-3,5,7,9(11),22-pentaene **OR** variant: (22E,24R)-form	Lipids and lipid-like molecules	DNP	
			376.313	-2.2	24,25-Dinor-1,3,5(10),9(11)-arborinatetraene **OR** 24,25-Dinor-1,3,5(10),12-oleanatetraene **OR** 24,25-Dinor-1,3,5(10),12-ursatetraene	Lipids and lipid-like molecules		
226.216	225.20817	606.7227	225.209	-4.8	Dendrobates Alkaloid 225	Alkaloids and derivatives	DNP	
			225.209	-4.8	2-Amino-4,6-tetradecadien-3-ol OR 2-Amino-4,13-tetradecadien-3-ol **OR** 2-Amino-5,7-tetradecadien-3-ol **OR** 2-Amino-5,13-tetradecadien-3-ol **OR** 2-Amino-11,13-tetradecadien-3-ol	Alkaloids and derivatives		
			225.209	-4.8	Plumerinine	Alkaloids and derivatives		
			226.216		9-Octadecenamide	Lipids and lipid-like molecules	GNPS	7
421.204	420.19617	45.9769	420.196	-1.5	Ambiguine K isonitrile	Alkaloids and derivatives	DNP	
505.225	504.21717	300.5751	504.214	4.7	Zizhine G	Lipids and lipid-like molecules	NPA	
569.906	568.89817	1054.3000						
527.858	526.85017	1057.0559						
613.48	612.47217	804.6976						
819.647	818.63917	933.2745						
900.713	899.70517	977.7615						
899.709	898.70117	976.4843						
334.235	333.22717	563.2828						
936.734	935.72617	877.0818						
936.573	935.56517	759.8644						
713.547	712.53917	878.2084						
770.489	769.48117	755.6320						
163.028	162.02017	567.5653						
517.174	516.16617	453.4395						
463.215	462.20717	258.43826						
445.204	444.19617	305.4263						
648.435	647.42717	697.4994						
249.11	248.10217	503.5141						
304.261	303.25317	716.6502						
667.448	666.44017	699.4050						

4.6 Western blot

CS11 (420 MPa) and CS22 (300 MPa) with anti-steatosis activity were also chosen for additional analysis. Western blots were performed in order to uncover some mechanisms of action involved in the lipid reduction activity. For that, the expression of already described proteins implicated in adipogenesis and fatty acid synthesis was evaluated. C/EBPα (**Figure 27a**) and PRKA-β1(**Figure 27c**) showed lower expression levels after exposure to extracts, but only C/EBPα expression in cells exposed to CS22 had a significant reduction (*p-value* ≤ 0.05). The protein expression levels of PPAR-y and ACACα (phosphorylated and non-phosphorylated) were not altered by the exposure to selected extracts (**Figure 27b**, **Figure 27e**, **Figure 27f**, **Figure 27h** and **Figure27i**).

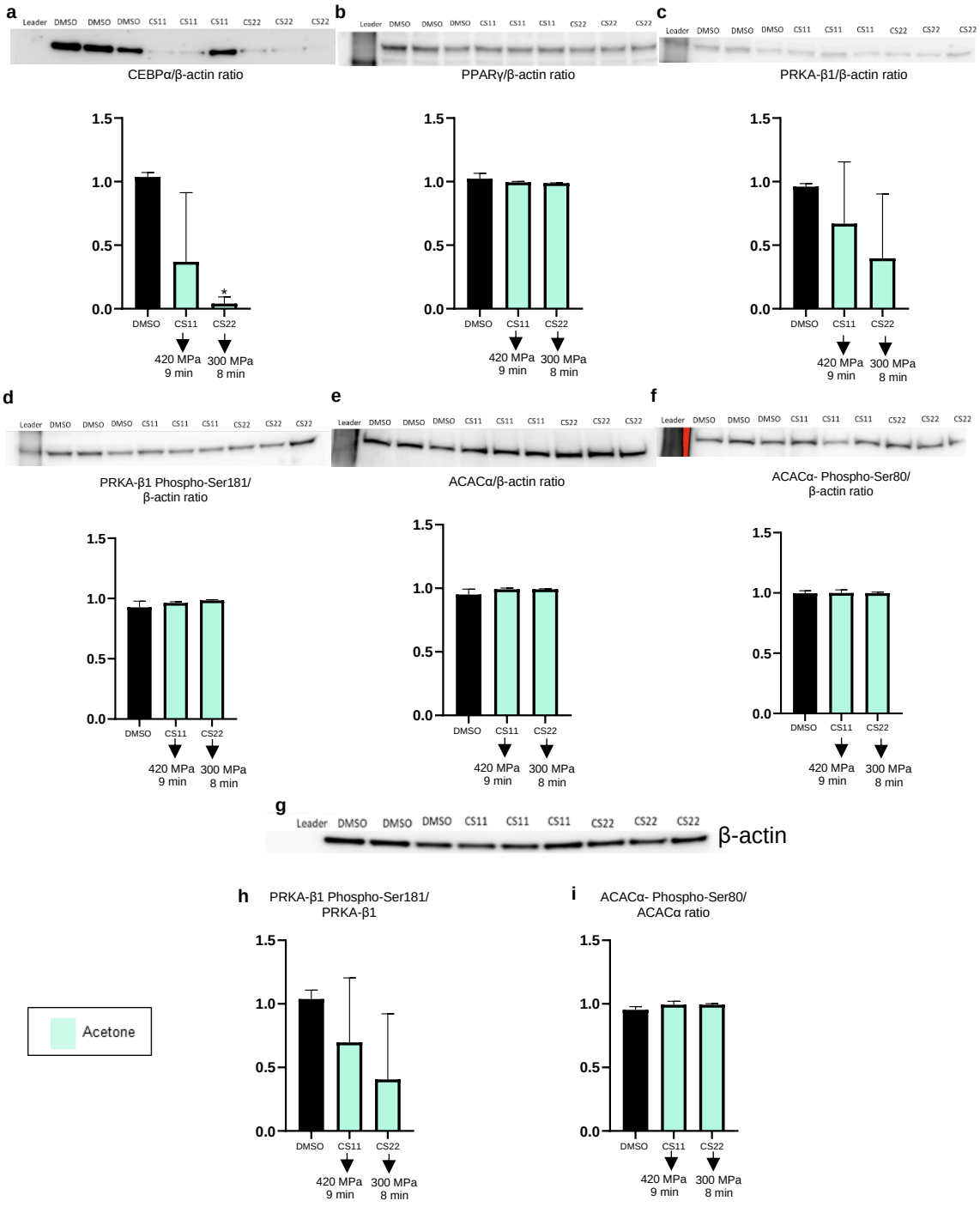

Figure 27 – Images of western blot membranes and respective quantification of the bands normalised by β-actin quantification. DMSO control, CS11 extract and CS22 extract samples were analysed in triplicates. (**a**) Western blot membrane of C/EBPα and corresponding quantification; (**b**) western blot membrane of PPARγ and corresponding quantification; (**c**) western blot membrane of PRKA-β1 and corresponding quantification; (**d**) western blot membrane of PRKA-β1 Phospho-Ser181 and corresponding quantification; (**e**) western blot membrane of ACACα and corresponding quantification; (**f**) western blot membrane of ACACα Phospho-Ser80 and corresponding quantification; (**g)** Representative image of β-actin western blot membrane used for loading control; (**h**) western blot quantification ratio between PRKA-β1 Phospho-Ser181 and PRKA-β1; (**i**) western blot quantification ratio between ACACα Phospho-Ser80 and ACACα. The quantification ratio is shown as column plots. Statistical differences compared to DMSO control are indicated by asterisks. Asterisks highlight significant altered band intensity, indicating change protein expression (* = *p-value* ≤ 0.05).

5. Discussion

Obesity has reached extremely worrying proportions. Twenty-four years have passed since its classification as a global epidemic by the World Health Organization, and even so, to date, there are only three approved drugs against this disease in Europe (Durrer Schutz et al., 2019). Thus, there has been a growing need to find new, safer and more efficient alternatives to this problem, and as a result, natural products have been discussed as potential targets for new therapies that can fill this gap (Arya et al., 2020). With the marine environment being the largest on the planet and a proven source of incredible biodiversity, attention has been turned to it. In fact, several marine species have already been described for their effect against obesity (Oliveira et al., 2018; Pan et al., 2018; Costa et al., 2019; Freitas et al., 2019; Hernández-Lepe et al., 2019; Kang et al., 2019). However, it is important to realize that one of the major setbacks in exploiting the natural compounds is their limitation to be chemically synthesized due to their structural complexity. Also, the majority of marine species are potentially unsustainable to cultivation due to being too expensive, too time-consuming to optimize, or lacking an environmentally sustainable procedure (Molinski et al., 2008). Furthermore, if the biomass is the subject of study to be consumed or applied in experimental stages in human trials for drug approval, it must be recognised and approved as subject to Novel Food Regulation in Europe or GRAS by the US FDA (García et al., 2017). Remarkably, the microalgae chosen for the present work, *C. vulgaris*, has all the characteristics to address these limitations. It is one of the best-established microalgae in the market, being produced hetero, auto or mixotrophically on industrial scales by several companies worldwide for many years (Sharma et al., 2012; Borowitzka, 2018a). Additionally, its biomass is also approved by law for human consumption due to its long history of safe use (García et al., 2017).

Taking this into account, the critical point for taking advantage of these inherent attributes of *C. vulgaris* is to find the best extraction conditions to obtain the valuable compounds produced since they are primarily stored intracellularly. Many extraction methods are suitable for obtaining microalgae compounds, and nowadays, traditional ones, such as extraction in Soxhlet apparatus, boiling, and distilling, have been outdated by novel technologies. Among these novel technologies are the ones studied in this work, the HPP extraction (Shouqin et al., 2004) and the ohmic extraction (Hasizah et al., 2018). By comparison with the older ones, these technologies allow a lower energy consumption along with shorter operation time because of the increased efficiency by

enhancing mass transfer rates, metabolite diffusion and cell permeability, thus creating a greener extraction method. These characteristics make it possible to scale the extraction to an industrial level because they contribute to higher extraction yields and fewer impurities on the final extract, along with the protection of degradation of more sensitive structures of compounds (Chemat et al., 2012; Michalak and Chojnacka, 2014; AE et al., 2016; Moreira et al., 2019). Specifically, ohmic extraction has as main advantages uniform heating, high energy efficiency (>90%), and low mechanical stress for biomass (Knirsch et al., 2010; Rodrigues et al., 2019), while HPP is characterized by higher extraction yield, lower extraction time and lower energy consumption (Jun, 2013; Chemat et al., 2020). However, in terms of drug industry applicability, the extraction methodology is more than just the yield or the efficiency obtained. It is essential to find the variables in the extraction procedure that allow extracting the most active compounds against the target in study. For instance, in HPP extraction, excessively high pressure may lead to disruption of the molecules, but, on the other hand, too low pressure may not be enough to extract them. And this logic is applicable for all variables in play, whether time, pressure, solvent, frequency, or temperature.

In this work, a screening approach was performed with 20 HPP extracts and 6 ohmic extracts, all obtained by project partners applying different extraction conditions. The screening was performed using diverse *in vivo* and *in vitro* models to detect the bioactivities of these extracts related to obesity and its comorbidities in order to discover the most suitable combination of extraction conditions.

The anti-steatosis assay was based on the importance of the liver in fatty acid metabolism. In obese patients, states of NAFLD are frequently observed (Polyzos et al., 2019), namely the less severe, which is steatosis. The applied model with HepG2 cells was already described in the literature (Gómez-Lechón et al., 2007; Cui et al., 2010), and some studies had used it successfully to demonstrate the effects of marine products against this disease. Zheng et al., 2018 used a synthetic agonist of a nuclear receptor that plays a vital role in hepatic *de novo* lipogenesis to stimulate an aggravated new synthesis and accumulation of triglycerides in HepG2 cells to investigate the influence of siphonaxanthin, a rare marine carotenoid, on hepatic lipogenesis. The aim was to investigate the potential of the natural products to prevent fat accumulation in the HepG2 cells, in other words, the potential to prevent hepatic steatosis and, consequently, more complex stages of NAFLD. As described in the literature, to determine the lipid content in the cells, the fluorescence emitted by the Nile red dye can be quantified, as it stains

neutral lipids. Yet, this quantification needed to be optimized. As cells grow heterogeneously distributed in the wells, a single measurement in the centre of the well ends up giving a somewhat random result, since it may be a point that is not representative of the well. Therefore, a technology that covered more than a single specific centred point was needed. A procedure named area scan enabled fluorescence measurement at multiple points in the well, allowing the coverage of a wider area. The area scan granted a less arbitrary fluorescence quantification, as the final results of each well became an average of multiple measurements. In the third approach, the fluorescence quantification in the procedure was replaced for a cell-by-cell direct measurement. Automated imaging in 96-well plates enabled to accurately identify the cells through image processing and quantify the lipid droplets in each cell per well. As a result, the total number of measurements obtained in each well increased enormously from point fluorescence to imaging. Therefore, a higher value of measurements in each well inevitably led to an increased precision in quantifications, because uncertainty decreased while the confidence in the estimate increased (Grimmett and Stirzaker, 2001).

From a more general observation of the plots, it is important to highlight that data obtained from point fluorescent had a higher dispersion, shown by a more considerable interquartile range and a consequent higher standard deviation, indicative of the data variation obtained between the three technical replicas (wells) of each assay. In contrast, the data obtained from the area scan shown precisely the opposite, lower data dispersion, with a smaller standard deviation. This is in line with what was explained above. As the total number of measurements increases in each well, so does precision of quantification and confidence, leading to a box-and-whisker plot with lower variability outside the upper and lower quartiles and smaller interquartile ranges. The observation of the data from the imaging process and its variability is a little more arduous to analyse. Hundreds of cells were evaluated with an enormous range of biological complexity. However, the extent of analysis per well is limited compared to the area scan, and some of the observed variation will come from this fact. Future works may evaluate the number of images per well to optimize the possible results and reduce variability.

Hence, the area scan and imaging seemed to be the two most adjusted quantification methodologies for this assay. Therefore, when deciding on the most promising extracts, area scan and imaging should be the ones to be taking into most consideration. However, choosing among these two quantification methodologies has more to be considered than only confidence and dispersion of the results. While imaging

allows for a more detailed cell-by-cell result and more options to investigate the assay output, it is also a much more time-consuming method to obtain results, which requires one hour to read an entire 96-well plate and more effort after to analyse and process the images so that the software recognises the object of study. Thus, both methodologies seemed to be validated in terms of quality, each having its own advantages and disadvantages that must be considered when opting for one of them to carry out the anti-steatosis assay. This issue did not seem to have been raised yet in the existing literature, and this fluorescence measurements optimization may consist of a new approach to this *in vitro* anti-steatosis assay.

By observing the results of those two methodologies, area scan and imaging, for the highest exposure concentration at 25 µg/mL, the HPP extracts extracted by acetone with pressure, CS11, CS22 and CS35, showed a strong inhibitory effect of excessive lipid accumulation on the HepG2 cell line. Furthermore, in the area scan, a correlation was even observed between the activity of the extracts and the pressure applied in the extraction, meaning that the higher the pressure applied, the more the extracts were able to decrease the lipid content of HepG2 cells with induced steatosis. Although this correlation pattern was not as evident in the imaging, there was still significant activity verified in the extracts extracted with pressure but not in the controls without it, indicating that some pressure was indeed necessary to extract the active compounds. In our work, the same procedure described in Costa et al., 2019 study was used, in which the model of HepG2 exposed to sodium oleate was applied to induce steatosis in the cells. Among the 263 analysed fractions obtained from 46 cyanobacterial strains, they found, through this model, 17 with promising lipid lowering activity a concentration of 10 µg/ml.

Furthermore, some effective natural products were described against NAFLD. For example, 1500 mg of cinnamon in capsules were given to 25 patients with NAFLD for 12 weeks, along with advice on implementing a balanced diet and physical activity. This ingestion decreased insulin resistance index, fasting blood glucose, total cholesterol, triglycerides, and abnormal liver enzymes profiles, compared to the placebo (n=25) group, showing that cinnamon supplementation can be an adjuvant therapeutic option for NAFLD (Askari et al., 2014). Another similar short-term supplementation with 1000 mg of curcumin to diagnosed NAFLD patients was performed for 8 weeks, along with the lifestyle and dietary advice. In this study, ultrasonographic findings revealed a 75% improvement in curcumin supplementation patients. The hepatic transaminase levels were also significantly reduced at the end of the trial, compared to the control

group (Panahi et al., 2017). Additionally, a 12-week supplement of 320 mg of purified anthocyanin extracted from *Vaccinium myrtillus* and *Ribesnigrum* improved indicators of liver injury and clinical evolution in NAFLD patients. The evaluated biomarkers, alanine aminotransferase, cytokeratin-18 M30 fragment, and myeloperoxidase, exhibited significant decreases in the anthocyanin supplementation group compared to the control, linked it to the improvement of NAFLD characteristics (Zhang et al., 2015). Another study with natural products that revealed significant decreases in hepatic aminotransferase levels in patients with NAFLD was a 12-week 500 mg green tea extract supplementation (Pezeshki et al., 2015).

The microalgae *C. vulgaris* was also the subject of these kinds of trials in patients with NAFLD. In three similar studies carried out over 2-3 months, patients received 1 g supplementation of the microalgae in one study (Chitsaz et al., 2016) and 1.2 mg in the other two (Panahi et al., 2012; Ebrahimi-Mameghani et al., 2014). Among these three trials, two measurements significantly decreased in patients who received supplementation with *C. vulgaris*, the enzyme alanine aminotransferase present in the liver, a biochemical marker of liver injury, and the serum triglyceride levels. In complement to supplementation trials with *Chlorella* biomass, *in vitro* assays can help to identify the responsible compounds for such bioactivities or molecular modes of action. This is particularly true nowadays, where human *in vitro* models have been developed, and coculture models (Barbero-Becerra et al., 2015) and 3D models (Kozyra et al., 2018) are already described. Moreover, other microalgae species are not recognised and accepted for human consumption and therefore cannot be subjected to human trials. That is the main reason why many microalgae studies have only been published in animal models (Kumar et al., 2015; Mayer et al., 2021). Nevertheless, it was possible to infer that the clinical trials and the *in vitro* anti-steatosis assays carried out in this study, point to the fact that the microalgae *C. vulgaris* seems to have a lipid-lowering effect that can be an effective treatment in NAFLD. Even more, the established optimisation in the fluorescent quantification of the anti-steatosis HepG2 cell line model was a useful starting point for supporting *in vitro* models to study the potential of a variety of marine species.

In the anti-obesity assay, the ability of extracts to reduce the neutral lipid content was assessed. The lipid-lowering activity was also observed in the exposure to acetone extracts of HPP extraction. The CS22 and CS35 extracts even showed significant reductions in both assays. The main difference was that in the anti-steatosis assay, the higher extraction pressure increased the activity, while in zebrafish assay the pressure

was not essential. In fact, acetone controls were equally efficient in lipid-lowering activity and the high pressure eliminated the bioactivity, probably by degrading the responsible metabolites.

This fat metabolism assay with zebrafish larvae was initially described by Jones et al., 2008 and had already been successfully applied in the past in studies carried out with cyanobacterial fractions (Costa et al., 2019) and with known and novel chlorophyll derivatives isolated from *Nodosilinea sp.* and *Cyanobium sp.* with anti-obesity activity (Freitas et al., 2019). As for the effect of *C. vulgaris* on lipid metabolism, 6-week-old male Wistar rats were fed with normal diets supplemented with 0, 5 or 10% *C. vulgaris,* and high-fat diets, also with 0, 5 or 10% *C. vulgaris* supplementation, in its powder form (Lee et al., 2008). After 9 weeks, serum total lipids and liver triglycerides concentration in 5 and 10% supplemented groups were significantly lower than in the 0% high fat diet group. In addition, a significantly higher total faecal lipid, triglycerides, and total cholesterol excretions were also verified in 5% and 10% *C. vulgaris* groups compared to 0% in normal and high fat diet groups. Thus, the authors concluded that *C. vulgaris* effectively prevented high fat levels in the body, probably due to modulation of lipid metabolism and increased faecal excretion of lipid. However, responsible compounds were not described yet.

Obesity is usually regarded as a chronic inflammation, an inflammatory state that lasts for a long time, characterized by the existence of macrophages and by the secretion of inflammatory cytokines, usually from the adipose tissue (Stępień et al., 2014). This state, in turn, is thought to lead to the development of other comorbidities such as T2DM (Saltiel and Olefsky, 2017). Moreover, it is essential to assess the ability of the extracts to reduce inflammation since it is a known state in obese individuals, which has tremendous implications in the development of the disease.

In our results, all extracts with ethanol 96% and acetone had anti-inflammatory activity, regardless of the applied pressure in HPP. In concordance, the anti-inflammatory effect of *C. vulgaris* was already described in the same model of LPS-induced inflammation in RAW264.7 cells with *C. vulgaris* fractions from an extraction made by ultrasounds with 80% ethanol (Sibi and Rabina, 2016). In that study, the anti-inflammatory activity was confirmed by the decrease of nitric acid production and adipokines like PGE2, TNF-α and IL-6.

Another study, performed with lipid extracts, extracted by homogenizing the biomass with dichloromethane: methanol 2: 1 (v/v), from auto and heterotrophic *C.*

vulgaris, showed 85% and 86% anti-inflammatory effects, respectively, by cyclooxygenase 2 inhibitory screening assay (Couto et al., 2021). However, these results were obtained with a 200x higher exposure concentration (5000 µg/ml) than the highest concentration used in the present work (25 µg/ml). Even so, the results obtained by HPP extracts with 96% ethanol and acetone showed anti-inflammatory effects of that order.

Additionally, and since *C. vulgaris* is approved for human consumption, another study investigated a beneficial immunostimulatory effect of this microalgae on healthy people. The subjects consumed 5 g of *C. vulgaris* (97% purity) for 8 weeks, which led to an increment of the activity of natural killer cells and the production of cytokines (Kwak et al., 2012). Thus, *C. vulgaris* appears to have an important and quite significant anti-inflammatory effect, but also a very interesting immunostimulatory effect.

Although the compounds responsible for these activities have not yet been identified in *C. vulgaris*, a study in *Chlorella ellipsoidea* using the same model with RAW764.7 LPS-stimulated showed that its major carotenoid, violaxanthin, had anti-inflammatory activity (Soontornchaiboon et al., 2012). Violaxanthin considerably inhibited the NO production in a dose-dependent way, with its maximum effect at 60 µM exposure. The other inflammatory mediator measured was prostaglandin E2, which was also significantly inhibited, with the higher effect observed at 60 µM exposure. The purified violaxanthin mechanism of action was assessed by quantitative real-time polymerase chain reaction, western blot, and electrophoretic-mobility shift assay. The authors suggested that violaxanthin activity may be based on inhibition of the NF-κB pathways. As this microalgae belongs to the same genus as *C. vulgaris*, this may be a mechanism of action shared by both, however further studies will be needed to demonstrate it.

T2DM is a disease characterized by the inability of tissues to capture glucose by entering a state of insulin resistance (Xu et al., 2003). Thus, the discovery of compounds capable of increasing glucose uptake is highly relevant to fight this comorbidity of obesity. The model developed in zebrafish by Lee et al., 2013 was used in this project to study the glucose flux, and it only required zebrafish larvae with 3 days of development after fertilization. In addition to the low growth time, another advantage arises from this model. Since the number of eggs produced by this species is very high, it is possible to screen many compounds or extracts for each reproduction performed.

Accordingly, the anti-diabetes assay was based on the fluorescent quantification of 2-NBDG, a fluorescent-tagged glucose probe with GLUTs as substrates, thus illustrating the glucose uptake. The quantification was performed in both eye and yolk

sac, as its expression at this stage of larval development has already been described (Tseng et al., 2009). Exposure of zebrafish larvae to 10 µg/mL of the HPP extracts led to a significant increase in glucose uptake exhibited in the higher pressure acetone extracts exposure, CS11 (420 MPa), CS22 (300 MPa) and CS35 (100 MPa), although the CS22 was the only one that demonstrated significant activity in both eye and yolk sac quantification. This activity associated with the extraction combination of high pressure and acetone as solvent was also verified in the anti-steatosis assay. Surprisingly, extracts extracted with water at higher pressures showed their only promising activity in this assay, which was confirmed in both eye and yolk sac quantifications. The potential of *C. vulgaris* to prevent insulin resistance had already been demonstrated in high-fat diet obese mice (Vecina et al., 2014). This was assessed by the increased glucose and insulin tolerance, verified by the improved insulin signalling pathway at its main target tissues, liver, skeletal muscle and adipose tissue. Previously to this study, Kim and Lee, 2009 reported the differences observed between Wistar rats with normal diets and high-fat diets, both with 0, 5 or 10% supplementation with *C. vulgaris* biomass for 9 weeks. They assessed that serum leptin concentration, a protein associated with insulin resistance, was significantly lower in rats fed with both normal and high-fat diets supplemented with 10% *C. vulgaris* than with the non-supplemented normal and high-fat diet. Additionally, the fasting glucose concentration and homeostasis model assessment of insulin resistance were also significantly lower in a high-fat diet group supplemented with 10% *C. vulgaris* compared to the non-supplemented high-fat diet group. Interestingly, a significantly higher expression of the glutamate transporter 4 protein was also observed between those two groups, which may explain the mechanism of action of *C. vulgaris* in the prevention of insulin resistance. Furthermore, the GLUT4 translocation was also shown to be altered in another study where the effects of the combination of *Chlorella* intake and aerobic exercise training in type 2 diabetic rats were evaluated (Horii et al., 2019). Although the species of *Chlorella* was not discriminated, a 0.5% intake in normal diet combined with aerobic exercise training significantly decreased fasting blood glucose, insulin levels and increased the insulin sensitivity index. They suggested that, as the molecular mechanism of *Chlorella* intake-induced activation of muscle protein kinase B and GLUT4 signalling may be similar to aerobic exercise training, the combination of both could activate muscle phosphatidylinositol-3 kinase, protein kinase B, and GLUT4 signalling, leading to further improvement in glycemic control.

In general, the bioactivities shown in these four assays had already been associated with the consumption of *C. vulgaris*. Nevertheless, the studies were carried out by supplementation of the diet with its biomass. To the best of our knowledge, this work is the first to investigate the impact of methodologies of extraction towards obesity and associated comorbidities and to putatively identify those compounds. The bioactivity exhibited by the acetone extracts on anti-steatosis activity was chosen to create the molecular networking of the LC-MS/MS data.

This first approach compared the metabolite profile of CS11, CS22 and CS35 (active extracts) against CSC11 and CSC23 (non-active extracts), based on the anti-steatosis assay at 25ug/mL exposure measured by imaging. The comparison between these two groups should reveal the unique metabolites, meaning the compounds that were only present in the active extracts. A bioinformatics approach, using GNPS for the creation of the networks, and dereplication in mass spectrometry databases, should lead to some putative identification of such unique compounds. Among these, it was possible to highlight N^2-(15,16-Dihydroxy-9,12-octadecadienoyl)glutamine, a glutamine derivative, which was only present in CS11 extract. Glutamine levels in human adipose tissue had previously been inversely correlated with fat mass and inflammation (Petrus et al., 2020). Additionally, an altered expression of glutamine-metabolizing genes in adipose tissue was verified in obesity. This recent study also concluded that glutamine levels appear to be proof of the link between obesity and inflammation. Furthermore, another study proved that oral glutamine supplementation in Wistar rats on a high-fat diet caused them to gain much less weight than those fed a high-fat diet without supplementation, and in obese humans caused a reduced waist circumference (Abboud et al., 2019).

As for the compound pheophytin a, a mixture of pheophytin a and b extracted from *Allophylus cominia Sw*. decreased the lipid accumulation in 3T3-L1 when added from the first day of the initiation of the adipocyte differentiation process (Semaan et al., 2018).

These two putatively identified compounds seem to be related by knowledge from the scientific literature to the decrease of some characteristics of obesity. Even so, all identifications must be rigorously reviewed against the existing literature, and future work needs to be developed with these isolated compounds to confirm their identifications (e.g., comparison of MS/MS fragments). For the other 19 peaks that did not have a match in mass spec databases, it could mean that they may represent novel compounds. This result was in accordance with previous studies, where promising effects of extracts or

fractions were observed on intestinal lipid absorption by cyanobacteria (Bellver et al., 2021), on the reduction of lipids by seagrass (Mabrouk et al., 2020), by cyanobacteria (Costa et al., 2019) or by actinobacteria (Santos et al., 2019), where the responsible metabolites await their identification in future works.

As for a more detailed analysis of the mechanisms of action of CS11 and CS22, a major change in protein expression was observed for C/EBPα of HepG2 fat overloaded cells exposed to CS22 extract. C/EBPα and the PPAR-γ are the transcription factors responsible for the differentiation of preadipocytes into mature adipocytes (Tariq et al., 2013). Although these exert a positive feedback mechanism in each other, it was demonstrated that in wild-type C/EBPα and in C/EBPα null mutant cells, the ectopic expression of PPAR-γ was sufficient to activate the genetic machinery involved in adipogenesis. However, it was found that the C/EBPα (-/-) cells expressed lower amounts of fatty acid synthase, adipsin, and genes involved in adipogenesis than the C/EBPα (+/+) cells. Additionally, the C/EBPα (-/-) cells accumulated smaller lipid droplets within the cytoplasm (Wu et al., 1999). These findings are, in fact, in agreement with the results obtained. Here, a decrease in the expression of C/EBPα in cells exposed to CS22 and CS11 extract was observed, which may imply that the compounds present in these extracts have the C/EBPα regulation as a target, that might have consequences on the amount of lipid droplets accumulated in the cytoplasm of the HepG2 cell. Moreover, the importance of the C/EBPα transcription factor is notorious since it also has a crucial role in regulating human fat mass and obesity-associated gene, also known as FTO Alpha-Ketoglutarate Dependent Dioxygenase. This FTO gene has a proven contribution to human obesity (Dina et al., 2007; Church et al., 2009; Fischer et al., 2009), and it has been suggested that C/EBPα works as its positive regulator, binding to the FTO promoter, activating the gene transcription (Ren et al., 2014). Even more interesting, this so-called obesity gene was also described in mice, and C/EBPα is responsible for its transcriptional activation as well (Hwang et al., 1996).

These findings all together constitute a new perspective on the study of the microalgae *C. vulgaris* for its application in the research of new compounds for the pharmaceutical industry, as well as for its targeted extraction to obtain biomass applicable in several areas of nutraceuticals.

6. Conclusions

20 HPP extracts and 6 ohmic extracts from heterotrophic grown *C. vulgaris* were screened through *in vitro* and *in vivo* bioassays to assess their potential against obesity and associated comorbidities. From the results acquired by the four bioassays performed, it was possible to infer that HPP extraction was more suitable to obtain active compounds against these diseases than ohmic extraction. HPP extracts with acetone as solvent revealed significant activities in all four bioassays. In the anti-steatosis assay, the combination with pressure was necessary to reveal the activity in the extracts, and the best results were achieved with 420 and 300 MPa. In contrast, acetone extracts that had lipid reducing effects in the anti-obesity assay, pressure was not essential, and eliminated bioactivity in the highest pressure group of 420 MPa. In the anti-diabetes assay, acetone extracts with pressure processing increased glucose uptake, as well as aqueous extracts with high pressure. Concerning the anti-inflammatory assay, all acetone and ethanol 96% extracts showed an almost total reduction of inflammation, independent of the high pressure processing.

The active acetone extracts (CS11, CS22 and CS35) were compared to non-active acetone extracts (CSC11 and CSC23) by molecular networking of the LC-MS/MS data and revealed the presence of 33 nodes that were unique to active extracts on the anti-steatosis assay. Among them, two putatively identified compounds had already some reported characteristics associated with obesity, the N^2-(15,16-Dihydroxy-9,12-octadecadienoyl)glutamine and the pheophytin a. Additionally, 19 non-identified mass peaks may also be responsible for the observed bioactivities and could represent novel molecules.

The involvement of known protein targets for the CS22 extract activity was uncovered by the western blot technique. The expression level of C/EBPα, one of the transcription factors responsible for the differentiation of preadipocytes into mature adipocytes, was significantly lower in cells exposed to CS22.

All these findings allowed us to unveil the enormous potential of *C. vulgaris* grown under heterotrophic conditions to fight the obesity epidemic. Future work should be developed in order to understand the mechanisms of action of all the extracts that showed promising effects, as well as the isolation and identification of the compounds behind that activity.

7. References

Abboud KY, Reis SK, Martelli ME, Zordão OP, Tannihão F, de Souza AZZ, Assalin HB, Guadagnini D, Rocha GZ, Saad MJA, et al (2019) Oral glutamine supplementation reduces obesity, pro-inflammatory markers, and improves insulin sensitivity in DIO wistar rats and reduces waist circumference in overweight and obese humans. Nutrients **11**: 536

Abdelaal M, le Roux CW, Docherty NG (2017) Morbidity and mortality associated with obesity. Ann Transl Med **5**: 1–12

Abdelmalek MF, Diehl AM (2007) Nonalcoholic Fatty Liver Disease as a Complication of Insulin Resistance. Med Clin North Am **91**: 1125–1149

Abood S, Veisaga ML, López LA, Barbieri MA (2018) Dehydroleucodine inhibits mitotic clonal expansion during adipogenesis through cell cycle arrest. Phyther Res **32**: 1583–1592

AE K, Singh A, NC S, JP P, Prakash O, TP S (2016) Novel Eco-Friendly Techniques for Extraction of Food Based Lipophilic Compounds from Biological Materials. Nat Prod Chem Res **4**: 5

Aguirre V, Uchida T, Yenush L, Davis R, White MF (2000) The c-Jun NH2-terminal kinase promotes insulin resistance during association with insulin receptor substrate-1 and phosphorylation of Ser307. J Biol Chem **275**: 9047–9054

Agwa OK, Ogugbue CJ, Williams EE (2017) Field Evidence of Chlorella vulgaris Potentials as a Biofertilizer for Hibiscus esculentus. Int J Agric Res **12**: 181–189

Ahmad MT, Shariff M, Md. Yusoff F, Goh YM, Banerjee S (2020) Applications of microalga Chlorella vulgaris in aquaculture. Rev Aquac **12**: 328–346

Alhattab M, Kermanshahi-Pour A, Brooks MSL (2019) Microalgae disruption techniques for product recovery: influence of cell wall composition. J Appl Phycol **31**: 61–88

Altmann KH (2017) Drugs from the oceans: Marine natural products as leads for drug discovery. Chim Int J Chem **71**: 646–651

Alves-Bezerra M, Cohen DE (2019) Triglyceride metabolism in the liver. Compr Physiol **8**: 1–8

Arner P, Bernard S, Appelsved L, Fu KY, Andersson DP, Salehpour M, Thorell A, Rydén M, Spalding KL (2019) Adipose lipid turnover and long-term changes in body weight. Nat Med **25**: 1385–1389

Arner P, Bernard S, Salehpour M, Possnert G, Liebl J, Steier P, Buchholz BA, Eriksson M, Arner E, Hauner H, et al (2011) Dynamics of human adipose lipid turnover in health and metabolic disease. Nature **478**: 110–113

Arya A, Nahar L, Khan HU, Sarker SD (2020) Anti-obesity natural products. *In* SD Sarker, L Nahar, eds, Annu. Rep. Med. Chem., 1st ed. Academic Press, pp 411–

433

Askari F, Rashidkhani B, Hekmatdoost A (2014) Cinnamon may have therapeutic benefits on lipid profile, liver enzymes, insulin resistance, and high-sensitivity C-reactive protein in nonalcoholic fatty liver disease patients. Nutr Res **34**: 143–148

Atanasov AG, Zotchev SB, Dirsch VM, Orhan IE, Banach M, Rollinger JM, Barreca D, Weckwerth W, Bauer R, Bayer EA, et al (2021) Natural products in drug discovery: advances and opportunities. Nat Rev Drug Discov **20**: 200–216

Barbero-Becerra VJ, Giraudi PJ, Chávez-Tapia NC, Uribe M, Tiribelli C, Rosso N (2015) The interplay between hepatic stellate cells and hepatocytes in an in vitro model of NASH. Toxicol Vitr **29**: 1753–1758

Bardou M, Barkun AN, Martel M (2013) Obesity and colorectal cancer. Gut **62**: 933–947

Barkia I, Saari N, Manning SR (2019) Microalgae for high-value products towards human health and nutrition. Mar Drugs **17**: 304

Bellver M, Lemos S, Sanchez BA, Vasconcelos V, Urbatzka R (2021) Inhibition of Intestinal Lipid Absorption by Cyanobacterial Strains in Zebrafish Larvae. Mar Drugs **19**: 161

Bentham J, Di Cesare M, Bilano V, Bixby H, Zhou B, Stevens GA, Riley LM, Taddei C, Hajifathalian K, Lu Y, et al (2017) Worldwide trends in body-mass index, underweight, overweight, and obesity from 1975 to 2016: a pooled analysis of 2416 population-based measurement studies in 128·9 million children, adolescents, and adults. Lancet **390**: 2627–2642

Bettina Mittendorfer (2013) Origins of metabolic complications in obesity: adipose tissue and free fatty acid trafficking. Curr Opin Clin Nutr Metab Care **14**: 535–541

Beutler JA (2009) Natural Products as a Foundation for Drug Discovery. Curr Protoc Pharmacol **46**: 9.11.1-9.11.21

Beyerinck MW (1890) Culturversuche mit Zoochlorellen, Lichenengonidien und anderen niederen Algen. Bot. Zeitung. pp 725–786

BioTek (2021) Gen5 Software Features for Detection. https://www.biotek.com/products/software-robotics-software/gen5-software-features-for-imaging-microscopy/ (Accessed 10/08/2021)

Blunt JW, Copp BR, Keyzers RA, Munro MHG, Prinsep MR (2015) Marine natural products. Nat Prod Rep **32**: 116–211

Boland LL, Folsom AR, Rosamond WD (2002) Hyperinsulinemia, dyslipidemia, and obesity as risk factors for hospitalized gallbladder disease: A Prospective Study. Ann Epidemiol **12**: 131–140

Borowitzka MA (2018a) Biology of Microalgae. *In* IA Levine, J Fleurence, eds, Microalgae Heal. Dis. Prev. Elsevier, London, pp 23–72

Borowitzka MA (2018b) Microalgae in medicine and human health: A historical perspective. *In* IA Levine, J Fleurence, eds, Microalgae Heal. Dis. Prev. Academic Press, pp 195–210

Borowitzka MA (1995) Microalgae as sources of pharmaceuticals and other biologically active compounds. J Appl Phycol **7**: 3–15

Bouchard C (2021) Genetics of Obesity: What We Have Learned Over Decades of Research. Obesity **29**: 802–820

Briggs JC (1995) Species diversity: Land and sea. *In* JC Briggs, ed, Dev. Palaeontol. Stratigr. pp 371–389

Broeder MJ Den, Kopylova VA, Kamminga LM, Legler J (2015) Zebrafish as a Model to Study the Role of Peroxisome Proliferating-Activated Receptors in Adipogenesis and Obesity. PPAR Res **2015**: 358029

Bumandalai O, Tserennadmid R (2019) Effect of chlorella vulgaris as a biofertilizer on germination of tomato and cucumber seeds. Int J Aquat Biol **7**: 95–99

Burhans MS, Hagman DK, Kuzma JN, Schmidt KA, Kratz M (2019) Contribution of adipose tissue inflammation to the development of type 2 diabetes mellitus. Compr Physiol **9**: 1–58

Caporgno MP, Mathys A (2018) Trends in Microalgae Incorporation Into Innovative Food Products With Potential Health Benefits. Front Nutr **5**: 58

Carten JD, Farber SA (2009) A new model system swims into focus: Using the zebrafish to visualize intestinal lipid metabolism in vivo. Clin Lipidol **4**: 501–515

Chadt A, Scherneck S, Joost H-G, Al-Hasani H (2018) Molecular links between Obesity and Diabetes: "Diabesity." Endotext [Internet], https://www.ncbi.nlm.nih.gov/books/NBK279051/ (Accessed 29/07/2021)

Chait A, den Hartigh LJ (2020) Adipose Tissue Distribution, Inflammation and Its Metabolic Consequences, Including Diabetes and Cardiovascular Disease. Front Cardiovasc Med **7**: 1–41

Chan TYK (2009) Potential risks associated with the use of herbal anti-obesity products. Drug Saf **32**: 453–456

Chemat F, Abert Vian M, Fabiano-Tixier AS, Nutrizio M, Režek Jambrak A, Munekata PES, Lorenzo JM, Barba FJ, Binello A, Cravotto G (2020) A review of sustainable and intensified techniques for extraction of food and natural products. Green Chem **22**: 2325–2353

Chemat F, Vian MA, Cravotto G (2012) Green Extraction of Natural Products : Concept and Principles. Int J Mol Sci **13**: 8615–8627

Cheung BMY, Cheung TT, Samaranayake NR (2013) Safety of antiobesity drugs. Ther Adv Drug Saf **4**: 171–181

Chin YX, Mi Y, Cao WX, Lim PE, Xue CH, Tang QJ (2019) A pilot study on anti-obesity

mechanisms of Kappaphycus alvarezii: The role of native κ-carrageenan and the leftover sans-carrageenan fraction. Nutrients **11**: 1133

Chitsaz M, Mozaffari-Khosravi H, Salman-Roghani H, Zavar-Reza J, Lotfi M (2016) Effect of Chlorella vulgaris vs. Spirulina supplementation on lipid profile and liver function in patients with nonalcoholic fatty liver disease: a randomized controlled trial. Int J Probiotics Prebiotics **11**: 127–136

Choe SS, Huh JY, Hwang IJ, Kim JI, Kim JB (2016) Adipose tissue remodeling: Its role in energy metabolism and metabolic disorders. Front Endocrinol (Lausanne) **7**: 1–16

Chu CY, Chen CF, Rajendran RS, Shen CN, Chen TH, Yen CC, Chuang CK, Lin DS, Hsiao C Der (2012) Overexpression of Akt1 enhances adipogenesis and leads to lipoma formation in zebrafish. PLoS One **7**: e36474

Church C, Lee S, Bagg EAL, McTaggart JS, Deacon R, Gerken T, Lee A, Moir L, Mecinović J, Quwailid MM, et al (2009) A mouse model for the metabolic effects of the human fat mass and obesity associated FTO gene. PLoS Genet **5**: e1000599

Clarke SD, Nakmura MT (2004) Fatty acid synthesis and its regulation. *In* WJ Lennarz, MD Lane, eds, Encycl. Biol. Chem. Elsevier, pp 99–103

Colman E (2007) Dinitrophenol and obesity: An early twentieth-century regulatory dilemma. Regul Toxicol Pharmacol **48**: 115–117

Colon-Gonzalez F, Kim GW, Lin JE, Valentino MA, Waldman SA (2013) Obesity pharmacotherapy: What is next? Mol Aspects Med **34**: 71–83

Coneski PN, Schoenfisch M (2012) Nitric oxide release: part III. Measurement and reporting. Chem Soc Rev **41**: 3753–3758

Costa M, Rosa F, Ribeiro T, Hernandez-Bautista R, Bonaldo M, Silva NG, Eiríksson F, Thorsteinsdóttir M, Ussar S, Urbatzka R (2019) Identification of cyanobacterial strains with potential for the treatment of obesity-related co-morbidities by bioactivity, toxicity evaluation and metabolite profiling. Mar Drugs **17**: 280

Couto D, Melo T, Conde TA, Costa M, Silva J, Domingues MRM, Domingues P (2021) Chemoplasticity of the polar lipid profile of the microalgae Chlorella vulgaris grown under heterotrophic and autotrophic conditions. Algal Res **53**: 102128

Cowley MA, Brown WA, Considine R V. (2016) Obesity: The Problem and Its Management. *In* JL Jameson, LJ De Groot, DM de Kretser, LC Giudice, AB Grossman, S Melmed, JT Potts, GC Weir, eds, Endocrinol. Adult Pediatr., Seventh. Elsevier Inc., pp 468–478

Cui W, Chen SL, Hu KQ (2010) Quantification and mechanisms of oleic acid-induced steatosis in HepG2 cells. Am J Transl Res **2**: 95–104

Daneschvar HL, Aronson MD, Smetana GW (2016) FDA-Approved Anti-Obesity Drugs in the United States. Am J Med **129**: 879–879

Daniele G, Guardado Mendoza R, Winnier D, Fiorentino T V., Pengou Z, Cornell J,

Andreozzi F, Jenkinson C, Cersosimo E, Federici M, Tripathy D, Folli F (2014) The inflammatory status score including IL-6, TNF-α, osteopontin, fractalkine, MCP-1 and adiponectin underlies whole-body insulin resistance and hyperglycemia in type 2 diabetes mellitus. Acta Diabetol **51**: 123–131

Daousi C, Casson IF, Gill G V., MacFarlane IA, Wilding JPH, Pinkney JH (2006) Prevalence of obesity in type 2 diabetes in secondary care: Association with cardiovascular risk factors. Postgrad Med J **82**: 280–284

DeFronzo RA, Ferrannini E, Groop L, Henry RR, Herman WH, Holst JJ, Hu FB, Kahn CR, Raz I, Shulman GI, Simonson DC, Testa MA, Weiss R (2015) Type 2 diabetes mellitus. Nat Rev Dis Prim **1**: 1–22

Deniz I, García-Vaquero M, Imamoglu E (2017) Trends in red biotechnology: Microalgae for pharmaceutical applications. *In* C Gonzalez-Fernandez, R Muñoz, eds, Microalgae-Based Biofuels Bioprod. From Feed. Cultiv. to End-Products. Woodhead Publishing, pp 429–460

Després JP (2007) Cardiovascular disease under the influence of excess visceral fat. Crit Pathw Cardiol **6**: 51–59

Dharuri H, 't Hoen PAC, van Klinken JB, Henneman P, Laros JFJ, Lips MA, el Bouazzaoui F, van Ommen GJB, Janssen I, van Ramshorst B, et al (2014) Downregulation of the acetyl-CoA metabolic network in adipose tissue of obese diabetic individuals and recovery after weight loss. Diabetologia **57**: 2384–2392

Dictionary of Natural Products (2021) Dictionary of Natural Products. https://dnp.chemnetbase.com/faces/chemical/ChemicalSearch.xhtml (Accessed 15/08/2021)

Dina C, Meyre D, Gallina S, Durand E, Körner A, Jacobson P, Carlsson LMS, Kiess W, Vatin V, Lecoeur C, et al (2007) Variation in FTO contributes to childhood obesity and severe adult obesity. Nat Genet **39**: 724–726

Ding Y, Wang L, Im S, Hwang O, Kim HS, Kang MC, Lee SH (2019) Anti-obesity effect of diphlorethohydroxycarmalol isolated from brown alga ishige okamurae in high-fat diet-induced obese mice. Mar Drugs **17**: 637

Diniz AFA, De Oliveira Claudino BF, Duvirgens MV, Da Silva Souza PP, Ferreira PB, Júnior FFL, Alves AF, Da Silva BA (2021) Spirulina platensis Consumption Prevents Obesity and Improves the Deleterious Effects on Intestinal Reactivity in Rats Fed a Hypercaloric Diet. Oxid Med Cell Longev **2021**: 3260789

Donnelly KL, Smith CI, Schwarzenberg SJ, Jessurun J, Boldt MD, Parks EJ (2005) Sources of fatty acids stored in liver and secreted via lipoproteins in patients with nonalcoholic fatty liver disease. J Clin Invest **115**: 1343–1351

Dooley K, Zon LI (2000) Zebrafish: A model system for the study of human disease. Curr Opin Genet Dev **10**: 252–256

Drira R, Chen S, Sakamoto K (2011) Oleuropein and hydroxytyrosol inhibit adipocyte differentiation in 3 T3-L1 cells. Life Sci **89**: 708–716

Durrer Schutz D, Busetto L, Dicker D, Farpour-Lambert N, Pryke R, Toplak H, Widmer D, Yumuk V, Schutz Y (2019) European Practical and Patient-Centred Guidelines for Adult Obesity Management in Primary Care. Obes Facts **12**: 40–66

Dvir I, Moppes D vam, Arad S (Malis) (2021) Foodomics: To Discover the Health Potential of Microalgae. *In* A Cifuentes, ed, Compr. Foodomics. Elsevier, pp 658–671

Dwyer JT, Allison DB, Coates PM (2005) Dietary supplements in weight reduction. J Am Diet Assoc **105**: 80–86

Ebrahimi-Mameghani M, Aliashrafi S, Javadzadeh Y, AsghariJafarabadi M (2014) The Effect of Chlorella vulgaris Supplementation on Liver En-zymes, Serum Glucose and Lipid Profile in Patients with Non-Alcoholic Fatty Liver Disease. Heal Promot Perspect **4**: 107–115

Egmond HP van (2004) Natural toxins: Risks, regulations and the analytical situation in Europe. Anal Bioanal Chem **378**: 1152–1160

Ellulu MS, Patimah I, Khaza'ai H, Rahmat A, Abed Y (2017) Obesity & inflammation: The linking mechanism & the complications. Arch Med Sci **13**: 851–863

Elo B, Villano CM, Govorko D, White LA (2007) Larval zebrafish as a model for glucose metabolism: Expression of phosphoenolpyruvate carboxykinase as a marker for exposure to anti-diabetic compounds. J Mol Endocrinol **38**: 433–440

European Medicines Agency Science Medicines Health (2013) Qsiva phentermine / topiramate. https://www.ema.europa.eu/en/medicines/human/EPAR/qsiva#overview-section (Accessed 24/08/2021)

Faheed FA, Fattah Z abd-el (2008) Effect of Chlorella vulgaris as Bio-fertilizer on Growth Parameters and Metabolic Aspects of Lettuce Plant. J Agric Soc Sci **4**: 165–169

Fischer J, Koch L, Emmerling C, Vierkotten J, Peters T, Brüning JC, Rüther U (2009) Inactivation of the Fto gene protects from obesity. Nature **458**: 894–898

Fleming A (1945) Sir Alexander Fleming - Nobel Lecture: Penicillin. Nov. Price

Fontaine KR, Redden DT, Wang C, Westfall AO, Allison DB (2003) Years of life lost due to obesity. JAMA **289**: 187–193

Foretz M, Even PC, Viollet B (2018) AMPK activation reduces hepatic lipid content by increasing fat oxidation in vivo. Int J Mol Sci **19**: 2826

Fowler SD, Greenspan P (1985) Application of Nile red, a fluorescent hydrophobic probe, for the detection of neutral lipid deposits in tissue sections: Comparison with oil red O. J Histochem Cytochem **33**: 833–836

Fradique Ḿonica, Batista AP, Nunes MC, Gouveia L, Bandarra NM, Raymundo A (2010) Incorporation of Chlorella vulgaris and Spirulina maxima biomass in pasta products. Part 1: Preparation and evaluation. J Sci Food Agric **90**: 1656–1664

Freedland SJ, Aronson WJ (2004) Examining the Relationship Prostate Cancer. Rev Urol **6**: 73–81

Freitas S, Silva NG, Sousa ML, Ribeiro T, Rosa F, Leão PN, Vasconcelos V, Reis MA, Urbatzka R (2019) Chlorophyll derivatives from marine cyanobacteria with lipid-reducing activities. Mar Drugs **17**: 229

Gaborit B, Abdesselam I, Kober F, Jacquier A, Ronsin O, Emungania O, Lesavre N, Alessi MC, Martin JC, Bernard M, Dutour A (2015) Ectopic fat storage in the pancreas using 1 H-MRS: Importance of diabetic status and modulation with bariatric surgery-induced weight loss. Int J Obes **39**: 480–487

García JL, de Vicente M, Galán B (2017) Microalgae, old sustainable food and fashion nutraceuticals. Microb Biotechnol **10**: 1017–1024

Gille A, Stojnic B, Derwenskus F, Trautmann A, Schmid-staiger U, Posten C, Briviba K, Palou A, Bonet ML, Ribot J (2019) A Lipophilic Fucoxanthin-Rich Phaeodactylum. Nutrients **11**: 796

Gitau MM, Farkas A, Balla B, Ördög V, Futó Z, Maróti G (2021) Strain-specific biostimulant effects of Chlorella and Chlamydomonas green microalgae on medicago truncatula. Plants **10**: 1060

Gómez-Lechón MJ, Donato MT, Martínez-Romero A, Jiménez N, Castell JV, O'Connor JE (2007) A human hepatocellular in vitro model to investigate steatosis. Chem Biol Interact **165**: 106–116

Greenspan P, Mayer EP, Fowler SD (1985) Nile red: A selective fluorescent stain for intracellular lipid droplets. J Cell Biol **100**: 965–973

Greenway FL, Fujioka K, Plodkowski RA, Mudaliar S, Guttadauria M, Erickson J, Kim DD, Dunayevich E (2010) Effect of naltrexone plus bupropion on weight loss in overweight and obese adults (COR-I): A multicentre, randomised, double-blind, placebo-controlled, phase 3 trial. Lancet **376**: 595–605

Grimmett G, Stirzaker D (2001) Laws of large numbers. Probab. Random Process., Third. Oxford University Press, pp 325–328

Guiry GM (2021) AlgaeBase. Chlorella vulgaris Beijerinck 1890, https://www.algaebase.org/ (Accessed 10/07/2021)

Guo B, Liu B, Wei H, Cheng KW, Chen F (2019) Extract of the Microalga Nitzschia laevis Prevents High-Fat-Diet-Induced Obesity in Mice by Modulating the Composition of Gut Microbiota. Mol Nutr Food Res **63**: e1800808

Halberstein RA (2005) Medicinal plants: Historical and cross-cultural usage patterns. Ann Epidemiol **15**: 686–699

Hall KD, Kahan S (2018) Maintenance of Lost Weight and Long-Term Management of Obesity. Med Clin North Am **102**: 183–197

Hardie DG (2004) The AMP-activated protein kinase pathway - New players upstream and downstream. J Cell Sci **117**: 5479–5487

Harvey AL, Edrada-Ebel R, Quinn RJ (2015) The re-emergence of natural products for drug discovery in the genomics era. Nat Rev Drug Discov **14**: 111–129

Hasizah A, Mahendradatta M, Laga A, Metusalach M, Supratomo, Waris A, Salengke S (2018) A novel ohmic-based technology for seaweed processing. Int Food Res J **25**: 1341–1348

Haththotuwa RN, Wijeyaratne CN, Senarath U (2020) Worldwide epidemic of obesity. *In* TA Mahmood, S Arulkumaran, FA Chervenak, eds, Obes. Obstet. Elsevier, pp 3–8

Henness S, Perry CM (2006) Orlistat A Review of its Use in the Management of Obesity. Drugs **66**: 1625–1656

Heo MG, Choung SY (2018) Anti-obesity effects of Spirulina maxima in high fat diet induced obese rats via the activation of AMPK pathway and SIRT1. Food Funct **9**: 4906–4915

Hernández-Lepe MA, Wall-Medrano A, López-Díaz JA, Juárez-Oropeza MA, Luqueño-Bocardo OI, Hernández-Torres RP, Ramos-Jiménez A (2019) Hypolipidemic Effect of Arthrospira (Spirulina) maxima Supplementation and a Systematic Physical Exercise Program in Overweight and Obese Men : A Double-Blind, Randomized, and Crossover Controlled Trial. Mar Drugs **17**: 270

Hitoe S, Shimoda H (2017) Seaweed Fucoxanthin Supplementation Improves Obesity Parameters in Mild Obese Japanese Subjects. Funct Foods Heal Dis **7**: 246

Horii N, Hasegawa N, Fujie S, Uchida M, Iemitsu K, Inoue K, Iemitsu M (2019) Effect of combination of chlorella intake and aerobic exercise training on glycemic control in type 2 diabetic rats. Nutrition **63**–**64**: 45–50

Hsu CC, Lai CY, Lin CY, Yeh KY, Her GM (2018) MicroRNA-27b depletion enhances endotrophic and intravascular lipid accumulation and induces adipocyte hyperplasia in zebrafish. Int J Mol Sci **19**: 93

Hwang CS, Mandrup S, MacDougald OA, Geiman DE, Lane MD (1996) Transcriptional activation of the mouse obese (ob) gene by CCAAT/enhancer binding protein α. Proc Natl Acad Sci U S A **93**: 873–877

John P Konhilas YL (2015) AMP-Activated Protein Kinase Signalling in Cancer and Cardiac Hypertrophy. Cardiovasc Pharmacol Open Access **4**: 154

Jones KS, Alimov AP, Rilo HL, Jandacek RJ, Woollett LA, Penberthy WT (2008) A high throughput live transparent animal bioassay to identify non-toxic small molecules or genes that regulate vertebrate fat metabolism for obesity drug development. Nutr Metab **5**: 23

Jun X (2013) High-Pressure Processing as Emergent Technology for the Extraction of Bioactive Ingredients From Plant Materials. Crit Rev Food Sci Nutr **53**: 837–852

Jurczyk A, Roy N, Bajwa R, Gut P, Lipson K, Yang C, Covassin L, Racki WJ, Rossini AA, Phillips N, et al (2011) Dynamic glucoregulation and mammalian-like responses to metabolic and developmental disruption in zebrafish. Gen Comp

Endocrinol **170**: 334–345

Kahn BB, Flier JS (2000) Obesity and insulin resistance. J Clin Invest **106**: 473–481

Kahn SE, Hull RL, Utzschneider KM (2006) Mechanisms linking obesity to insulin resistance and type 2 diabetes. Nature **444**: 840–846

Kang JG, Park CY (2012) Anti-obesity drugs: A review about their effects and safety. Diabetes Metab J **36**: 13–25

Kang MC, Ding Y, Kim HS, Jeon YJ, Lee SH (2019) Inhibition of adipogenesis by diphlorethohydroxycarmalol (DPHC) through AMPK activation in adipocytes. Mar Drugs **17**: 44

Karastergiou K, Mohamed-Ali V (2010) The autocrine and paracrine roles of adipokines. Mol Cell Endocrinol **318**: 69–78

Karbalamahdi A, Abedi B, Fatolahi H, Pazoki A (2019) Effect of Aerobic Training and C. vulgaris Intake on Lipid Profile and Leptin in Obese Women. Hormozgan Med J **23**: e91436

Kearney J (1999) Physical inactivity , sedentary lifestyle and obesity in the European Union. Int J Obes **23**: 1192–1201

Kelly T, Yang W, Chen C, Reynolds K, He J (2008) Global burden of obesity in 2005 and projections to 2030. Int J Obes **32**: 1431–1437

Kershaw EE, Flier JS (2004) Adipose tissue as an endocrine organ. J Clin Endocrinol Metab **89**: 2548–2556

Kessner D, Chambers M, Burke R, Agus D, Mallick P (2008) ProteoWizard: open source software for rapid proteomics toolsdevelopment. Bioinformatic Appl note **24**: 2534–2536

Khan MAB, Hashim MJ, King JK, Govender RD, Mustafa H, Kaabi J Al (2020) Epidemiology of Type 2 diabetes - Global burden of disease and forecasted trends. J Epidemiol Glob Health **10**: 107–111

Kim CW, Addy C, Kusunoki J, Anderson NN, Deja S, Fu X, Burgess SC, Li C, Chakravarthy M, Previs S, et al (2017) Acetyl CoA Carboxylase Inhibition Reduces Hepatic Steatosis but Elevates Plasma Triglycerides in Mice and Humans: A Bedside to Bench Investigation. Cell Metab **26**: 394–406

Kim HJ, Yoon BK, Park H, Seok JW, Choi H, Yu JH, Choi Y, Song SJ, Kim A, Kim JW (2016) Caffeine inhibits adipogenesis through modulation of mitotic clonal expansion and the AKT/GSK3 pathway in 3T3-L1 adipocytes. BMB Rep **49**: 111–115

Kim MK, Lee HS (2009) Effect of Chlorella vulgaris on glucose metabolism in wistar rats fed high fat diet. J Med Food **12**: 1029–1037

Kim S hee, Park HS, Lee M su, Cho YJ, Kim YS, Hwang JT, Sung MJ, Kim MS, Kwon DY (2008) Vitisin A inhibits adipocyte differentiation through cell cycle arrest in 3T3-

L1 cells. Biochem Biophys Res Commun **372**: 108–113

Kim WH, Lee J, Jung DW, Williams DR (2012) Visualizing sweetness: Increasingly diverse applications for fluorescent-tagged glucose bioprobes and their recent structural modifications. Sensors **12**: 5005–5027

Kimmel CB, Ballard WW, Kimmel SR, Ullmann B, Schilling TF (1995) Stages of embryonic development of the zebrafish. Dev Dyn **203**: 253–310

Knirsch MC, Alves dos Santos C, Martins de Oliveira Soares Vicente AA, Vessoni Penna TC (2010) Ohmic heating - a review. Trends Food Sci Technol **21**: 436–441

Koch A, Brandenburger S, Türpe S, Birringer M (2014) The Need for a Legal Distinction of Nutraceuticals. Food Nutr Sci **5**: 905–913

Koo SY, Hwang J, Yang S, Um J, Hong KW (2019) Anti-Obesity Effect of Standardized Extract of Microalga Phaeodactylum tricornutum. Mar Drugs **17**: 311

Koyande AK, Chew KW, Rambabu K, Tao Y, Chu DT, Show PL (2019) Microalgae: A potential alternative to health supplementation for humans. Food Sci Hum Wellness **8**: 16–24

Kozyra M, Johansson I, Nordling Å, Ullah S, Lauschke VM, Ingelman-Sundberg M (2018) Human hepatic 3D spheroids as a model for steatosis and insulin resistance. Sci Rep **8**: 14297

Kruger NJ (1996) The Bradford Method for Protein Quantitation. *In* JM Walker, ed, Methods m Mol. Biol. Humana Press, pp 9–15

Kumar SA, Magnusson M, Ward LC, Paul NA, Brown L (2015) A green algae mixture of Scenedesmus and Schroederiella attenuates obesity-linked metabolic syndrome in rats. Nutrients **7**: 2771–2787

Kwak JH, Baek SH, Woo Y, Han JK, Kim BG, Kim OY, Lee JH (2012) Beneficial immunostimulatory effect of short-term Chlorella supplementation: Enhancement of Natural Killer cell activity and early inflammatory response (Randomized, double-blinded, placebo-controlled trial). Nutr J **11**: 53

Lachance PA, Das YT (2007) Nutraceuticals. *In* JB Taylor, DJ Triggle, eds, Compr. Med. Chem. II. Elsevier, pp 449–461

Lai CS, Chen YY, Lee PS, Kalyanam N, Ho CT, Liou WS, Yu RC, Pan MH (2016) Bisdemethoxycurcumin Inhibits Adipogenesis in 3T3-L1 Preadipocytes and Suppresses Obesity in High-Fat Diet-Fed C57BL/6 Mice. J Agric Food Chem **64**: 821–830

Landgraf K, Schuster S, Meusel A, Garten A, Riemer T, Schleinitz D, Kiess W, Körner A (2017) Short-term overfeeding of zebrafish with normal or high-fat diet as a model for the development of metabolically healthy versus unhealthy obesity. BMC Physiol **17**: 4

Lane MD (2013) Adipogenesis. *In* WJ Lennars, MD Lane, eds, Encycl. Biol. Chem. II, Second. Academic Press, pp 52–56

Lee HG, Lu YA, Li X, Hyun JM, Kim HS, Lee JJ, Kim TH, Kim HM, Kang MC, Jeon YJ (2020) Anti-obesity effects of Grateloupia elliptica, a red seaweed, in mice with high-fat diet-induced obesity via suppression of adipogenic factors in white adipose tissue and increased thermogenic factors in brown adipose tissue. Nutrients **12**: 1–15

Lee HS, Park HJ, Kim MK (2008) Effect of Chlorella vulgaris on lipid metabolism in Wistar rats fed high fat diet. Nutr Res Pract **2**: 204

Lee J-E, Schmidt H, Lai B, Ge K (2019) Transcriptional and Epigenomic Regulation of Adipogenesis. Mol Cell Biol **39**: 1–20

Lee J, Jung DW, Kim WH, Um JI, Yim SH, Oh WK, Williams DR (2013) Development of a highly visual, simple, and rapid test for the discovery of novel insulin mimetics in living vertebrates. ACS Chem Biol **8**: 1803–1814

Lekehal M, Pessayre D, Lereau JM, Moulis C, Fourasté I, Fau D (1996) Hepatotoxicity of the herbal medicine germander: Metabolic activation of its furano diterpenoids by cytochrome P450 3A depletes cytoskeleton- associated protein thiols and forms plasma membrane blebs in rat hepatocytes. Hepatology **24**: 212–218

Lim SL, Chu WL, Phang SM (2010) Use of Chlorella vulgaris for bioremediation of textile wastewater. Bioresour Technol **101**: 7314–7322

Longo M, Zatterale F, Naderi J, Parrillo L, Formisano P, Raciti GA, Beguinot F, Miele C (2019) Adipose tissue dysfunction as determinant of obesity-associated metabolic complications. Int J Mol Sci **20**: 2358

Luo L, Liu M (2016) Adipose tissue in control of metabolism. J Endocrinol **231**: R77–R99

Lyu C, Chen T, Qiang B, Liu N, Wang H, Zhang L, Liu Z (2021) CMNPD: A comprehensive marine natural products database towards facilitating drug discovery from the ocean. Nucleic Acids Res **49**: D509–D515

Mabrouk SB, Reis M, Maria L, Ribeiro T, Almeida JR, Pereira S, Antunes J, Rosa F, Vasconcelos V, Achour L, et al (2020) The Marine Seagrass Halophila stipulacea as a Source of Bioactive Metabolites against Obesity and Biofouling. Mar Drugs **18**: 88

Maliwat GCF, Velasquez SF, Buluran SMD, Tayamen MM, Ragaza JA (2021) Growth and immune response of pond-reared giant freshwater prawn Macrobrachium rosenbergii post larvae fed diets containing Chlorella vulgaris. Aquac Fish **6**: 465–470

Mao G, Shi K, Zhang C, Li J, Chen S, Wang P (2020) Biodiesel Fuel from Chlorella vulgaris and Effects of Its Low-Level Blends on the Performance, Emissions, and Combustion Characteristics of a Nonroad Diesel Engine. J Energy Eng **146**: 04020016

Masojídek J, Torzillo G (2008) Mass Cultivation of Freshwater Microalgae. *In* J Sven Erik Jørgensen, Brian D. FathMasojídek, G Torzillo, eds, Encycl. Ecol. Academic Press, pp 2226–2235

Mayer C, Richard L, Côme M, Ulmann L, Nazih H, Chénais B, Ouguerram K, Mimouni V (2021) The marine microalga, Tisochrysis lutea, protects against metabolic disorders associated with metabolic syndrome and obesity. Nutrients **13**: 1–18

Meerloo J van, Kaspers GJL, Cloos J (2011) Cell Sensitivity Assays: The MTT Assay Johan. *In* I Cree, ed, Methods Mol. Biol. Humana Press, pp 237–245

Meyers JR (2018) Zebrafish: Development of a Vertebrate Model Organism. Curr Protoc Essent Lab Tech **16**: e19

Michalak I, Chojnacka K (2014) Algal extracts : Technology and advances. Eng Life Sci **14**: 581–591

Moini J, Ahangari R, Miller C, Samsam M (2020) What is obesity? *In* J Moini, R Ahangari, C Miller, M Samsam, eds, Glob. Heal. Complicat. Obes. Elsevier, pp 1–16

Molinski TF, Dalisay DS, Lievens SL, Saludes JP (2008) Drug development from marine natural products. Nat Rev Drug Discov Discov **8**: 69–85

Moore SC, Patel A V., Matthews CE, Berrington de Gonzalez A, Park Y, Katki HA, Linet MS, Weiderpass E, Visvanathan K, Helzlsouer KJ, et al (2012) Leisure Time Physical Activity of Moderate to Vigorous Intensity and Mortality: A Large Pooled Cohort Analysis. PLoS Med **9**: 1–14

Mora C, Tittensor DP, Adl S, Simpson AGB, Worm B (2011) How many species are there on earth and in the ocean? PLoS Biol **9**: 1–8

Moreira SA, Alexandre EMC, Pintado M, Saraiva JA (2019) Effect of emergent non-thermal extraction technologies on bioactive individual compounds profile from different plant materials. Food Res Int **115**: 177–190

Mourelle ML, Gómez CP, Legido JL (2017) The potential use of marine microalgae and cyanobacteria in cosmetics and thalassotherapy. Cosmetics **4**: 46

Mubashar M, Naveed M, Mustafa A, Ashraf S, Baig KS, Alamri S, Siddiqui MH, Zabochnicka-świątek M, Szota M, Kalaji HM (2020) Experimental investigation of chlorella vulgaris and enterobacter sp. Mn17 for decolorization and removal of heavy metals from textile wastewater. Water **12**: 3034

Mueller M, Jungbauer A (2009) Culinary plants, herbs and spices - A rich source of PPARγ ligands. Food Chem **117**: 660–667

Nakamura K, Fuster JJ, Walsh K (2014) Adipokines: A link between obesity and cardiovascular disease. J Cardiol **63**: 250–259

Nassir F, Rector RS, Hammoud GM, Ibdah JA (2015) Pathogenesis and prevention of hepatic steatosis. Gastroenterol Hepatol **11**: 167–175

NCBI (2021) ACACA acetyl-CoA carboxylase alpha [Homo sapiens (human)]. Natl. Cent. Biotechnol. Inf., https://www.ncbi.nlm.nih.gov/gene/31 (Accessed 17/08/2021)

Newman DJ, Cragg GM (2020) Natural Products as Sources of New Drugs over the Nearly Four Decades from 01/1981 to 09/2019. J Nat Prod **83**: 770–803

Ng ACT, Delgado V, Borlaug BA, Bax JJ (2021) Diabesity: the combined burden of obesity and diabetes on heart disease and the role of imaging. Nat Rev Cardiol **18**: 291–304

Nicoletti M (2012) Nutraceuticals and botanicals: Overview and perspectives. Int J Food Sci Nutr **63**: 2–6

Oka T, Nishimura Y, Zang L, Hirano M, Shimada Y, Wang Z, Umemoto N, Kuroyanagi J, Nishimura N, Tanaka T (2010) Diet-induced obesity in zebrafish shares common pathophysiological pathways with mammalian obesity. BMC Physiol **10**: 21

Oliveira RM, Câmara RBG, Monte JFS, Viana RLS, Melo KRT, Queiroz MF, Filgueira LGA, Oyama LM, Rocha HAO (2018) Commercial fucoidans from fucus vesiculosus can be grouped into antiadipogenic and adipogenic agents. Mar Drugs **16**: 193

Onstad MA, Schmandt RE, Lu KH (2016) Addressing the role of obesity in endometrial cancer risk, prevention, and treatment. J Clin Oncol **34**: 4225–4230

Paliwal C, Mitra M, Bhayani K, Bharadwaj SVV, Ghosh T, Dubey S, Mishra S (2017) Abiotic stresses as tools for metabolites in microalgae. Bioresour Technol **244**, **Part**: 1216–1226

Pan H, Fu C, Huang L, Jiang Y, Deng X, Guo J, Su Z (2018) Anti-obesity effect of chitosan oligosaccharide capsules (coscs) in obese rats by ameliorating leptin resistance and adipogenesis. Mar Drugs **16**: 198

Panahi Y, Ghamarchehreh ME, Beiraghdar F, Zare M, Jalalian HR, Sahebkar A (2012) Investigation of the effects of Chlorella vulgaris supplementation in patients with non-alcoholic fatty liver disease: A randomized clinical trial. Hepatogastroenterology **59**: 2099–2103

Panahi Y, Kianpour P, Mohtashami R, Jafari R, Simental-Mendía LE, Sahebkar A (2017) Efficacy and Safety of Phytosomal Curcumin in Non-Alcoholic Fatty Liver Disease: A Randomized Controlled Trial. Drug Res (Stuttg) **67**: 244–251

Pardal D, Caro M, Tueros I, Barranco A, Navarro V (2014) Resveratrol and piceid metabolites and their fat-reduction effects in zebrafish larvae. Zebrafish **11**: 32–40

Park J, Um JI, Jo A, Lee J, Jung DW, Williams DR, Park SB (2014) Impact of molecular charge on GLUT-specific cellular uptake of glucose bioprobes and in vivo application of the glucose bioprobe, GB2-Cy3. Chem Commun **50**: 9251–9254

Park JH, Moon JH, Kim HJ, Kong MH, Oh YH (2020) Sedentary Lifestyle : Overview of Updated Evidence of Potential Health Risks. Korean J Fam Med **41**: 365–373

Park UH, Jeong HS, Jo EY, Park T, Yoon SK, Kim EJ, Jeong JC, Um SJ (2012) Piperine, a component of black pepper, inhibits adipogenesis by antagonizing PPARγ activity in 3T3-L1 cells. J Agric Food Chem **60**: 3853–3860

Petrus P, Lecoutre S, Dollet L, Wiel C, Sulen A, Gao H, Tavira B, Laurencikiene J, Rooyackers O, Checa A, et al (2020) Glutamine Links Obesity to Inflammation in Human White Adipose Tissue. Cell Metab **31**: 375–390

Pezeshki A, Safi S, Feizi A, Askari G, Karami F (2015) The effect of green tea extract supplementation on liver enzymes in patients with nonalcoholic fatty liver disease. Int J Prev Med. **6**: 131

Pillitteri JL, Shiffman S, Rohay JM, Harkins AM, Burton SL, Wadden TA (2008) Use of dietary supplements for weight loss in the united states: Results of a national survey. Obesity **16**: 790–796

Pittler MH, Abbot NC, Harkness EF, Ernst E (1999) Randomized, double-blind trial of chitosan for body weight reduction. Eur J Clin Nutr **53**: 379–381

Pittler MH, Ernst E (2001) Guar gum for body weight reduction: Meta-analysis of randomized trials. Am J Med **110**: 724–730

Polyzos SA, Kountouras J, Mantzoros CS (2019) Obesity and nonalcoholic fatty liver disease: From pathophysiology to therapeutics. Metab Clin Exp **92**: 82–97

Powell A, Teichtahl AJ, Wluka AE, Cicuttini FM (2005) Obesity: A preventable risk factor for large joint osteoarthritis which may act through biomechanical factors. Br J Sports Med **39**: 4–5

Powell EE, Wong VWS, Rinella M (2021) Non-alcoholic fatty liver disease. Lancet **397**: 2212–2224

Pruvost J, Van Vooren G, Le Gouic B, Couzinet-Mossion A, Legrand J (2011) Systematic investigation of biomass and lipid productivity by microalgae in photobioreactors for biodiesel application. Bioresour Technol **102**: 150–158

Ramirez-Llodra E, Brandt A, Danovaro R, De Mol B, Escobar E, German CR, Levin LA, Martinez Arbizu P, Menot L, Buhl-Mortensen P, et al (2010) Deep, diverse and definitely different: Unique attributes of the world's largest ecosystem. Biogeosciences **7**: 2851–2899

Rasband W. (1997) ImageJ. U. S. Natl. Institutes Heal. Bethesda, https://imagej.nih.gov/ij/, 1997-2018 (Accessed 03/09/2021)

Reena Mehra, Redline S (2008) Sleep apnea: A proinflammatory disorder that coaggregates with obesity. J Allergy Clin Immunol **121**: 1096–1102

Ren W, Guo J, Jiang F, Lu J, Ding Y, Li A, Liang X, Jia W (2014) CCAAT/enhancer-binding protein α is a crucial regulator of human fat mass and obesity associated gene transcription and expression. Biomed Res Int **2014**: 406909

Rico M, González AG, Santana-Casiano M, González-Dávila M, Pérez-Almeida N, Tangil MS de (2017) Production of Primary and Secondary Metabolites Using Algae. *In* B Tripathi, D Kumar, eds, Prospect. Challenges Algal Biotechnol. Springer, Singapore, pp 311–326

Rodrigues RM, Genisheva Z, Rocha CMR, Teixeira JA, Vicente AA, Pereira RN

(2019) Ohmic heating for preservation, transformation, and extraction. *In* F Chemat, E Vorobiev, eds, Green Food Process. Tech. Academic Press, pp 159–191

Ruiz-Ojeda FJ, Rupérez AI, Gomez-Llorente C, Gil A, Aguilera CM (2016) Cell models and their application for studying adipogenic differentiation in relation to obesity: A review. Int J Mol Sci **17**: 1040

Rumin J, Nicolau E, de Oliveira RG, Fuentes-Grünewald C, Flynn KJ, Picot L (2020) A bibliometric analysis of microalgae research in the world, Europe, and the European Atlantic area. Mar Drugs **18**: 79

Safi C, Zebib B, Merah O, Pontalier PY, Vaca-Garcia C (2014) Morphology, composition, production, processing and applications of Chlorella vulgaris: A review. Renew Sustain Energy Rev **35**: 265–278

Sakanoi Y, Shuang E, Yamamoto K, Ota T, Seki K, Imai M, Ota R, Asayama Y, Nakashima A, Suzuki K, et al (2018) Simultaneous intake of Euglena gracilis and vegetables synergistically exerts an anti-inflammatory effect and attenuates visceral fat accumulation by affecting gut microbiota in mice. Nutrients **10**: 1417

Saltiel AR, Olefsky JM (2017) Inflammatory mechanisms linking obesity and metabolic disease. J Clin Invest **127**: 1–4

Samadi M, Shirvani H, Shafeie AA (2020) Effect of Chlorella vulgaris supplementation with eccentric exercise on serum interleukin 6 and insulin resistance in overweight men. Sport Sci Health **16**: 543–549

Sanayei M, Izadi A, Hajizadeh-sharafabad F, Amirsasan R, Kaviani M, Barzegar A (2021a) Chlorella vulgaris in combination with high intensity interval training in overweight and obese women: a randomized double-blind clinical trial. J Diabetes Metab Disord **20**: 781–792

Sanayei M, Kalejahi P, Mahinkazemi M, Fathifar Z, Barzegar A (2021b) The effect of Chlorella vulgaris on obesity related metabolic disorders: a systematic review of randomized controlled trials. J. Complement. Integr. Med.

Santen JA van, Jacob GG, Singh AL, Aniebok V, Balunas MJ, Bunsko D, Neto FC, Castañ O-Espriu L, Chang C, Clark TN, et al (2019) The Natural Products Atlas: An Open Access Knowledge Base for Microbial Natural Products Discovery. ACS Cent Sci **5**: 1824–1833

Santos JD, Vitorino I, Cruz M De, Díaz C, Cautain B, Annang F, Pérez-moreno G, Martinez IG, Tormo JR, Martín JM, et al (2019) Bioactivities and Extract Dereplication of Actinomycetales Isolated From Marine Sponges. Front Microbiol **10**: 727

Sarine Markossian, Grossman A, Brimacombe K, Arkin M, Auld D, Austin CP, Baell J, Chung TDY, Coussen NP, L J, et al (2012) The Assay Guidance Manual [Internet]. https://www.ncbi.nlm.nih.gov/books/NBK53196/ (Accessed 30/07/2021)

Satapathy SK, Kuwajima V, Nadelson J, Atiq O, Sanyal AJ (2015) Drug-induced fatty liver disease: An overview of pathogenesis and management. Ann Hepatol **14**: 774–776

Sathasivam R, Radhakrishnan R, Hashem A, Abd_Allah EF (2019) Microalgae metabolites: A rich source for food and medicine. Saudi J Biol Sci **26**: 709–722

Sattar N, Gill JMR (2014) Type 2 diabetes as a disease of ectopic fat? BMC Med **12**: 1–6

Schelbert KB (2009) Comorbidities of Obesity. Prim Care - Clin Off Pract **36**: 271–285

Schneider CA, Rasband WS, Eliceiri KW (2012) NIH Image to ImageJ: 25 years of image analysis. Nat Methods **9**: 671–675

Semaan DG, Igoli JO, Young L, Gray AI, Rowan EG, Marrero E (2018) In vitro anti-diabetic effect of flavonoids and pheophytins from Allophylus cominia Sw. on the glucose uptake assays by HepG2, L6, 3T3-L1 and fat accumulation in 3T3-L1 adipocytes. J Ethnopharmacol **216**: 8–17

Seo YJ, Kim KJ, Choi J, Koh EJ, Lee BY (2018) Spirulina maxima extract reduces obesity through suppression of adipogenesis and activation of browning in 3T3-L1 cells and high-fat diet-induced obese mice. Nutrients **10**: 712

Shannon P, Markiel A, Ozier O, Baliga NS, Wang JT, Ramage D, Amin N, Schwikowski B, Ideker T (2003) Cytoscape: A Software Environment for Integrated Models. Genome Res **13**: 2498–2504

Sharma R, Singh GP, Sharma VK (2012) Effects of Culture Conditions on Growth and Biochemical Profile of Chlorella. Jounal Plant Pathol Microbiol **3**: 131

Shouqin Z, Junjie Z, Changzhen W (2004) Novel high pressure extraction technology. Int J Pharm **278**: 471–474

Shultz MD (2019) Two Decades under the Influence of the Rule of Five and the Changing Properties of Approved Oral Drugs. J Med Chem **62**: 1701–1714

Sibi G, Rabina S (2016) Inhibition of Pro-inflammatory mediators and cytokines by Chlorella Vulgaris extracts. Pharmacognosy Res **8**: 118–122

Soontornchaiboon W, Joo SS, Kim SM (2012) Anti-inflammatory effects of violaxanthin isolated from microalga Chlorella ellipsoidea in RAW 264.7 macrophages. Biol Pharm Bull **35**: 1137–1144

Spolaore P, Joannis-Cassan C, Duran E, Isambert A (2006) Commercial applications of microalgae. J Biosci Bioeng **101**: 87–96

Srivastava G, Apovian CM (2018) Current pharmacotherapy for obesity. Nat Rev Endocrinol **14**: 12–24

Stępień M, Stępień A, Wlazeł RN, Paradowski M, Banach M, Rysz J (2014) Obesity indices and inflammatory markers in obese non-diabetic normo- and hypertensive patients : a comparative pilot study. Lipids Health Dis **13**: 29

Stuehr DJ, Marletta MA (1985) Mammalian nitrate biosynthesis: Mouse macrophages produce nitrite and nitrate in response to Escherichia coli lipopolysaccharide. Proc Natl Acad Sci U S A **82**: 7738–7742

Sugimoto R, Ishibashi-Ohgo N, Atsuji K, Miwa Y, Iwata O, Nakashima A, Suzuki K (2018) Euglena extract suppresses adipocyte-differentiation in human adipose-derived stem cells. PLoS One **13**: e0192404

Swinburn BA, Kraak VI, Allender S, Atkins VJ, Baker PI, Bogard JR, Brinsden H, Calvillo A, De Schutter O, Devarajan R, et al (2019) The Global Syndemic of Obesity, Undernutrition, and Climate Change: The Lancet Commission report. Lancet **393**: 791–846

Swinburn BA, Sacks G, Hall KD, Mcpherson K, Finegood DT, Moodie ML, Gortmaker SL (2011) The global obesity pandemic : shaped by global drivers and local environments. Lancet **378**: 804–814

Szulinska M, Gibas-Dorna M, Miller-Kasprzak E, Suliburska J, Miczke A, Walczak-Gałezewska M, Stelmach-Mardas M, Walkowiak J, Bogdanski P (2017) Spirulina maxima improves insulin sensitivity, lipid profile, and total antioxidant status in obese patients with well-treated hypertension: a randomized double-blind placebo-controlled study. Eur Rev Med Pharmacol Sci **21**: 2473–2481

Tabassum N, Tai H, Jung DW, Williams DR (2015) Fishing for Nature's Hits: Establishment of the Zebrafish as a Model for Screening Antidiabetic Natural Products. Evidence-based Complement Altern Med **2015**: 287847

Tak YJ, Lee SY (2021) Long-Term Efficacy and Safety of Anti-Obesity Treatment: Where Do We Stand? Curr Obes Rep **10**: 14–30

Tapia-Martinez J, Hernández-Cruz K, Franco-Colín M, Mateo-Cid LE, Mendoza-Gonzalez C, Blas-Valdivia V, Cano-Europa E (2019) Safety evaluation and antiobesogenic effect of Sargassum liebmannii J. Agardh (Fucales: Phaeophyceae) in rodents. J Appl Phycol **31**: 2597–2607

Tariq A, Hochfeld WE, Myburgh R, Pepper MS (2013) Adipocyte and adipogenesis. Eur J Cell Biol **92**: 229–236

Tehrani Z, Lin S (2011) Endocrine pancreas development in zebrafish. Cell Cycle **10**: 3466–3472

Télessy IG (2019) Nutraceuticals. *In* RB Singh, RR Watson, T Takahashi, eds, Role Funct. Food Secur. Glob. Heal. Academic Press, pp 409–421

The European Union Parliament and the Council of the European (2015) Regulation (EU) 2015/2283 of the European Parliament and of the Council of 25 November 2015 on novel foods, amending Regulation (EU) No 1169/2011 of the European Parliament and of the Council and repealing Regulation (EC) No 258/97 of the European Parliam. 1–22

The Global Goals for Sustainable Development (2015) The Global Goals for Sustainable Development. https://www.globalgoals.org/ (Accessed 18/07/2021)

The World Obesity Federation (World Obesity) (2019) Global Obesity Observatory. World Obes. Fed., https://data.worldobesity.org/ (Accessed 01/08/2021)

Tilinca MC, Tiuca RA, Burlacu A, Varga A (2021) A 2021 update on the use of

liraglutide in the modern treatment of 'diabesity': A narrative review. Medicina (B Aires) **57**: 1–11

Tiong I, Ru K, Sung YY, Jusoh M, Abdul ME, Nagappan T (2020) Chlorella vulgaris : a perspective on its potential for combining high biomass with high value bioproducts. Appl Phycol **1**: 2–11

Tseng YC, Chen RD, Lee JR, Liu ST, Lee SJ, Hwang PP (2009) Specific expression and regulation of glucose transporters in zebrafish ionocytes. Am J Physiol - Regul Integr Comp Physiol **297**: 275–291

Tung YC, Hsieh PH, Pan MH, Ho CT (2017) Cellular models for the evaluation of the antiobesity effect of selected phytochemicals from food and herbs. J Food Drug Anal **25**: 100–110

Tworoger SS, Eliassen AH, Kelesidis T, Colditz GA, Willett WC, Mantzoros CS, Hankinson SE (2007) Plasma adiponectin concentrations and risk of incident breast cancer. J Clin Endocrinol Metab **92**: 1510–1516

U.S. Food and Drug Administration (1997) Substances Generally Recognized as Safe. **62**: 18938–18964

Ulloa PE, Iturra P, Neira R, Araneda C (2011) Zebrafish as a model organism for nutrition and growth: Towards comparative studies of nutritional genomics applied to aquacultured fishes. Rev Fish Biol Fish **21**: 649–666

Um J, Lee J, Jung D-W, Williams D (2015) Sugars that Glow in the Dark: Fluorescent Tagged Glucose Bioprobes and their Facilitation of the Drug Discovery Process. Curr Med Chem **22**: 1793–1807

Urbatzka R, Freitas S, Palmeira A, Almeida T, Moreira J, Azevedo C, Afonso C, Correia-da-Silva M, Sousa E, Pinto M, et al (2018) Lipid reducing activity and toxicity profiles of a library of polyphenol derivatives. Eur J Med Chem **151**: 272–284

Vargas R, Vásquez IC (2017) Effects of overfeeding and high-fat diet on cardiosomatic parameters and cardiac structures in young and adult zebrafish. Fish Physiol Biochem **43**: 1761–1773

Vecina JF, Oliveira AG, Araujo TG, Baggio SR, Torello CO, Saad MJA, Queiroz MLDS (2014) Chlorella modulates insulin signaling pathway and prevents high-fat diet-induced insulin resistance in mice. Life Sci **95**: 45–52

van de Venter M, Didloff J, Reddy S, Swanepoel B, Govender S, Dambuza NS, Williams S, Koekemoer TC, Venables L (2021) Wild-type zebrafish (Danio rerio) larvae as a vertebrate model for diabetes and comorbidities: A review. Animals **11**: 54

Vichai V, Kirtikara K (2006) Sulforhodamine B colorimetric assay for cytotoxicity screening. Nat Protoc **1**: 1112–1116

Vidhu V. Thaker (2017) Genetic and Epigenetic Causes Of Obesity. Adolesc Med State Art Rev **28**: 379–405

Viegas C, Gonçalves M, Soares L, Mendes B (2016) Bioremediation of Agro-industrial Effluents Using Chlorella Microalgae. Technol. Innov. CyberPhysical Syst. Springer, pp 127–134

Wallace KN, Pack M (2003) Unique and conserved aspects of gut development in zebrafish. Dev Biol **255**: 12–29

Wang M, Carver JJ, Phelan V V., Sanchez LM, Garg N, Peng Y, Nguyen DD (2016) Sharing and community curation of mass spectrometry data with Global Natural Products Social Molecular Networking. Nat Biotechnol **34**: 828–837

Weisberg SP, McCann D, Desai M, Rosenbaum M, Leibel RL, Ferrante AW (2003) Obesity is associated with macrophage accumulation in adipose tissue. J Clin Invest **112**: 1796–1808

Weyer C, Funahashi T, Tanaka S, Hotta K, Matsuzawa Y, Pratley RE, Tataranni PA (2001) Hypoadiponectinemia in obesity and type 2 diabetes: Close association with insulin resistance and hyperinsulinemia. J Clin Endocrinol Metab **86**: 1930–1935

WHO (2021) Obesity and overweight. World Heal. Organ., https://www.who.int/ (Accessed 08/07/2021)

WHO Consultation on Obesity (1999: Geneva Switzerland) & World Health Organization (2000) Obesity : preventing and managing the global epidemic.

Wilcox G (2005) Insulin and insulin resistance. Clin Biochem Rev **88**: 19–39

Williams DM, Nawaz A, Evans M (2020) Drug Therapy in Obesity: A Review of Current and Emerging Treatments. Diabetes Ther **11**: 1199–1216

Woods A, Cheung PCF, Smith FC, Davison MD, Scott J, Beri RK, Carling D (1996) Characterization of AMP-activated protein kinase B and γ subunits Assembly of the heterotrimeric complex in vitro. J Biol Chem **271**: 10282–10290

Wright SM, Aronne LJ (2012) Causes of obesity. Abdom Radiol **37**: 730–732

Wu Z, Rosen ED, Brun R, Hauser S, Adelmant G, Troy AE, McKeon C, Darlington GJ, Spiegelman BM (1999) Cross-regulation of C/EBPα and PPARγ controls the transcriptional pathway of adipogenesis and insulin sensitivity. Mol Cell **3**: 151–158

Xu H, Barnes GT, Yang Q, Tan G, Yang D, Chou CJ, Sole J, Nichols A, Ross JS, Tartaglia LA, et al (2003) Chronic inflammation in fat plays a crucial role in the development of obesity-related insulin resistance. J Clin Invest **112**: 1821–1830

Xue J, Ding W, Liu Y (2010) Anti-diabetic effects of emodin involved in the activation of PPARγ on high-fat diet-fed and low dose of streptozotocin-induced diabetic mice. Fitoterapia **81**: 173–177

Yang Z, Yin J, Wang Y, Wang J, Xia B, Li T, Yang X, Hu S, Ji C, Guo S (2019) The fucoidan A3 from the seaweed Ascophyllum nodosum enhances RCT-related genes expression in hyperlipidemic C57BL/6J mice. Int J Biol Macromol **134**: 759–769

Yasin NMN, Shalaby SM (2013) Quality Characteristics of Croissant Stuffed with Imitation Processed Cheese Containing Microalgae *Chlorella vulgaris* Biomass. World J Dairy Food Sci **8**: 58–66

Younossi ZM, Golabi P, de Avila L, Paik JM, Srishord M, Fukui N, Qiu Y, Burns L, Afendy A, Nader F (2019) The global epidemiology of NAFLD and NASH in patients with type 2 diabetes: A systematic review and meta-analysis. J Hepatol **71**: 793–801

Yousefi R, Mottaghi A, Saidpour A (2018) Spirulina platensis effectively ameliorates anthropometric measurements and obesity-related metabolic disorders in obese or overweight healthy individuals: A randomized controlled trial. Complement Ther Med **40**: 106–112

Zang L, Maddison LA, Chen W (2018) Zebrafish as a model for obesity and diabetes. Front Cell Dev Biol **6**: 91

Zeinalian R, Farhangi MA, Shariat A, Saghafi-Asl M (2017) The effects of Spirulina Platensis on anthropometric indices, appetite, lipid profile and serum vascular endothelial growth factor (VEGF) in obese individuals: A randomized double blinded placebo controlled trial. BMC Complement Altern Med **17**: 225

Zhang PW, Chen FX, Li D, Ling WH, Guo HH (2015) A CONSORT-Compliant, Randomized, Double-Blind, Placebo-Controlled Pilot Trial of Purified Anthocyanin in Patients with Nonalcoholic Fatty Liver Disease. Medicine (Baltimore). **94**: e758

Zhao B, Cui Y, Fan X, Qi P, Liu C, Zhou X, Zhang X (2019) Anti-obesity effects of Spirulina platensis protein hydrolysate by modulating brain-liver axis in high-fat diet fed mice. PLoS One. **14**: e0218543.

Zheng J, Li Z, Manabe Y, Kim M, Goto T, Kawada T (2018) Siphonaxanthin , a Carotenoid From Green Algae , Inhibits Lipogenesis in Hepatocytes via the Suppression of Liver X Receptor α Activity. Lipids **53**: 41–52

Zhou Z, Xu MJ, Gao B (2016) Hepatocytes: A key cell type for innate immunity. Cell Mol Immunol **13**: 301–315

Zorena K, Jachimowicz-Duda O, Ślęzak D, Robakowska M, Mrugacz M (2020) Adipokines and obesity. Potential link to metabolic disorders and chronic complications. Int J Mol Sci **21**: 3570

8. Supplementary data

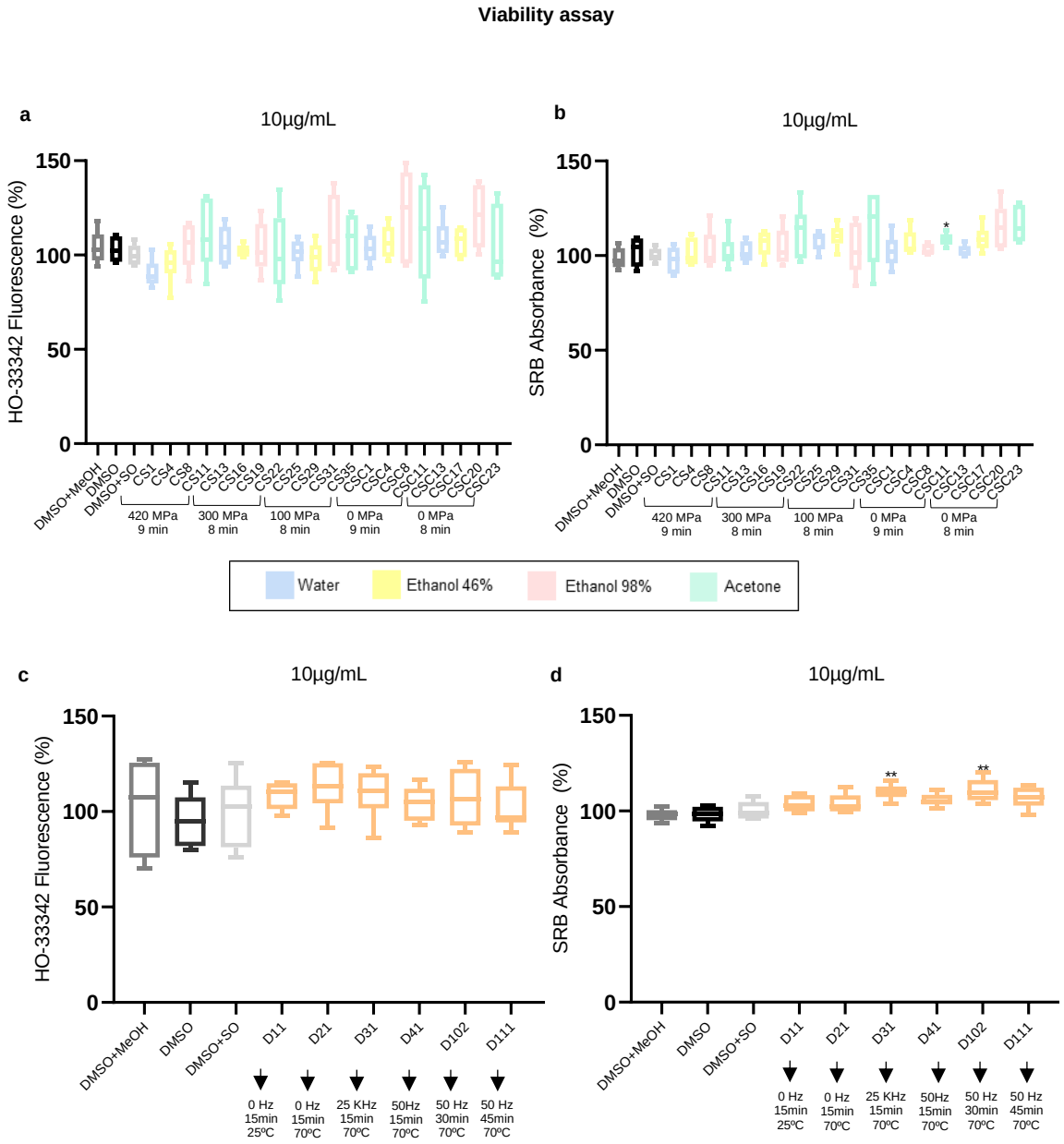

Supplementary Figure 1 - HepG2 cell viability for anti-steatosis assay assessed by (**a** and **c**) HO-33342 fluorescence reading and (**b** and **d**) SRB method. (**a** and **b**) Refer to 10 µg/mL exposure to HPP extracts; (**c** and **d**) refer to 10 µg/mL exposure to ohmic extracts. Dark grey represents DMSO+MeOH control; black represents DMSO control; light grey represents DMSO+SO control. The data have been derived from two independent assays and shown as box-and-whisker plots (5–95 percentiles) as percentage considering 100% the DMSO+SO control. Statistical differences compared to DMSO+SO control are indicated by asterisks (** = *p-value* ≤ 0.01; * = *p-value* ≤ 0.05).

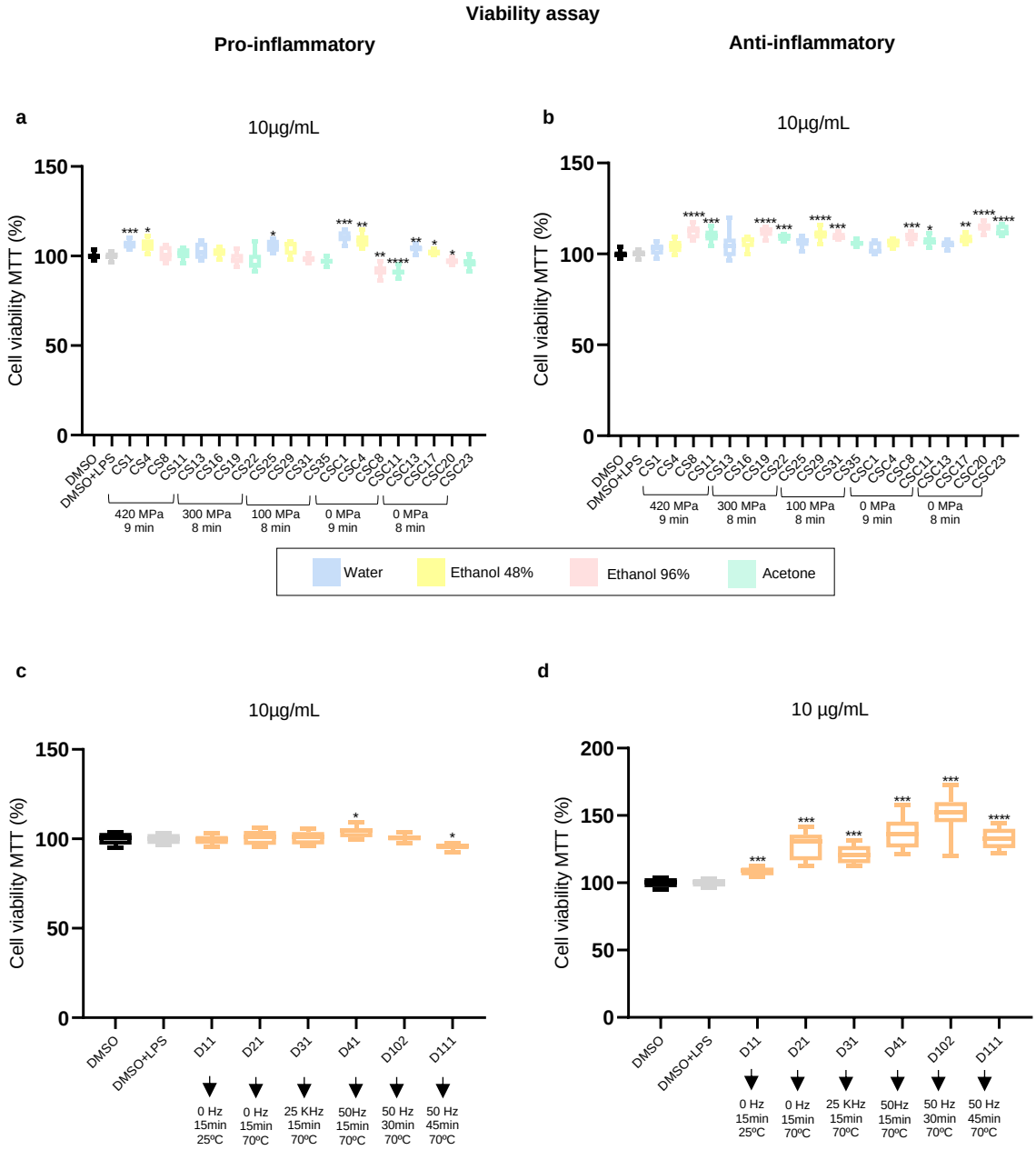

Supplementary Figure 2 - Cell viability MTT assay in RAW264.7 cell line of (**a**) pro-inflammatory assay with HPP extracts 10 µg/mL exposure; (**b**) anti-inflammatory assay with HPP extracts 10 µg/mL exposure; (**c**) pro-inflammatory assay with ohmic extracts 10 µg/mL exposure; (**d**) anti-inflammatory assay with ohmic extracts 10 µg/mL exposure. Black represents DMSO control; grey represents DMSO+LPS control. The data have been derived from two independent assays and shown as box-and-whisker plots (5–95 percentiles) as percentage considering 100% the DMSO control. Statistical differences compared to DMSO+LPS control are indicated by asterisks (****=*p-value* ≤ 0.0001; *** = *p-value* ≤ 0.001; ** = *p-value* ≤ 0.01; * = *p-value* ≤ 0.05).